

Aptamer-modified particles for biotechnological and analytical applications

Von der Naturwissenschaftlichen Fakultät
der Gottfried Wilhelm Leibniz Universität Hannover
zur Erlangung des Grades
Doktorin der Naturwissenschaften
-Dr. rer. nat.-
genehmigte Dissertation von

Master-Chem. Guohong Zhu
geboren am 30.11.1976, in Shanghai, China

Referent: Prof. Dr. Thomas Scheper
Korreferentin: Prof. Dr. Ursula Rinas

Tag der Promotion: 20. August 2013

Declaration

This dissertation was done between February 2010 and January 2013 in the institute for technical chemistry, Gottfried Wilhelm Leibniz University Hannover, in the group of Prof. Dr. Thomas Scheper and in the division of Dr. Frank Stahl.

I declare hereby, that this dissertation is self drafted, except indicated resources there are no other documents, which were used. This work has not been used as a master, diplom or similar examination paper.

Hannover, 01.02.2013

Acknowledgements

First, I would like to thank Prof. Dr. Thomas Scheper who generously accepted me to work in his group on this interesting topic and his willingness to be my first examinant.

Secondly, I want to thank Prof. Dr. Ursula Rinas for her willingness to be my second examinant.

Third, I want to thank Prof. Dr. Andreas Kirschning who has provided me with professional knowledge during the period of my master's study and his willingness to be my third examinant.

I would like to thank Dr. Frank Stahl for allowing me to do my dissertation in his working group and his enormous supporting during the period of my doctor's study.

My sincere thanks also go to my adviser Dr. Johanna-Gabriela Walter for her professional knowledge, timely feedback and solutions.

I also received efficient help in daily laboratory work from Martin Pähler and Martina Weiss.

Along with them, my thanks to Dr. Sascha Beutel and Angelika Behnsen, they have provided the management of project funds.

Finally, other laboratory colleagues created a pleasant and supporting working environment. I want to extend my sincere thanks to them as well.

Zusammenfassung

In biotechnologischen Verfahren, einschließlich der Affinitätsseparation und der Analyse, werden hoch selektive und affine Liganden benötigt. Aufgrund ihrer Bindungseigenschaften ermöglichen Aptamere die Aufreinigung und Detektion sowohl von Proteinen, als auch von kleinen Molekülen. Die herkömmlichen Methoden zur affinitätsbasierten Proteinaufreinigung verwenden überwiegend Antikörper als Liganden. Eine sehr konkurrenzfähige Alternative stellt die Anwendung von aptamermodifizierten Partikeln dar. Aptamere sind einzelsträngige DNA- oder RNA-Oligonukleotide, die in der Lage sind, verschiedene Arten von Molekülen zu binden. Verglichen mit Antikörpern verfügen Aptamere zwar über ähnliche Spezifitäten und Affinitäten, weisen aber eine höhere Stabilität auf.

Der Hauptteil der vorliegenden Arbeit untersucht das Potential und die Effektivität von Aptameren hinsichtlich der Reinigung von Proteinen und kleinen Molekülen. Für die Untersuchungen wurden his-getaggte Proteine, Antikörper und kleine Moleküle (Theophyllin, Malathion) verwendet. Zur Entwicklung der Aufreinigungsstrategien wurden Magnetpartikel als festes Trägermaterial für die Immobilisierung der Aptamer genutzt.

Ausgehend von einem bereits bestehenden Protokoll wurde die Reinigung his-getaggtter Proteine über aptamermodifizierte Magnetpartikel optimiert. Nach der Optimierung wurde das Protokoll erfolgreich auf weitere Aptamere, die gegen humane Antikörper, Theophyllin und Malathion gerichtet sind, übertragen und angepasst. Um eine maßstabsgetreue Vergrößerung der entwickelten Aufreinigungsstrategien zu ermöglichen, wurde die Methode zudem auf weitere chromatographische Trägermaterialien übertragen. Aptamermodifizierte Sepharose und CIM[®] DISK wurden erfolgreich zur Reinigung des humanen F_c Fragments eingesetzt. Um humanes IgG aufzureinigen wurde das Aptamer zusätzlich mit einem integrierten Spacer versehen und auf Sepharose immobilisiert.

Ein weiterer Teil dieser Arbeit dient der Entwicklung von neuen Methoden zur Proteindetektion unter Verwendung aptamermodifizierter Quantenpunkte. Die Nachweistauglichkeit von Aptameren wurde durch den Einsatz von aptamermodifizierten Quantenpunkten mit der Reverse Phase Protein Microarray Methode untersucht. Dieses Experiment zeigte eine hohe Spezifität der Aptamere.

Key words: Aptamer, affinitätsbasierte Separation, Aufreinigung, Oberflächen

Abstract

High selective and affine ligands are required in biotechnological techniques, including affinity separation and analysis. Because of their binding properties, aptamers can be used to purify and detect proteins, as well as small molecules. The conventional methods for affinity-based purification of proteins use primarily antibodies. A strongly competitive alternative is the application of aptamer-modified particles. Aptamers are single stranded DNA- or RNA- oligonucleotides that are able to bind different kinds of molecules. Compared with antibodies, aptamers exhibit similar specificities and affinities, but higher stability.

The main part of this work intends to examine the capability and effectiveness of aptamers to purify proteins and small molecules. His-tagged proteins, antibodies and small molecules (theophylline, malathion) were employed for the testing. Magnetic beads were used as solid support for the immobilization of aptamers during the development of the purification strategies.

Based on an existing protocol, the purification of his-tagged proteins via aptamer-modified magnetic beads was optimized. After optimization, the protocol was successfully transferred and adapted to other aptamers directed against human antibodies, theophylline and malathion. In order to enable a scale-up of the developed purification strategy, the method was transferred to other chromatographic supports. Aptamer-modified sepharose and CIM[®] DISK were successfully used to purify human F_c fragment. In order to purify human IgG, aptamer with integrated spacer was employed and immobilized on sepharose.

Another part of this work provides the development of new methods for the detection of proteins by using aptamer-modified quantum dots. The applicability of aptamers for detection of proteins was examined by using lab-made aptamer-modified quantum dots in a reverse phase protein microarray. This experiment exhibited high specificities of aptamers.

Key words: aptamer, affinity separation, purification, surfaces

1	Introduction and Task.....	10
2	Theory.....	12
2.1	Origin of aptamer-technology.....	12
2.2	Structures of aptamers.....	13
2.3	Binding mechanisms of aptamers.....	15
2.4	Selection of aptamers.....	16
2.4.1	Conventional SELEX procedure.....	16
2.4.2	MonoLEX.....	17
2.4.3	FluMag-SELEX.....	17
2.5	Advantages of aptamers over antibodies.....	18
2.6	Applications of aptamers.....	19
2.7	Application of aptamers in affinity separations.....	20
2.7.1	Separations of small molecules via specific aptamer-target-recognition.....	20
2.7.2	Separations of small molecules via enantioselective properties of aptamers.....	20
2.7.3	Separations of small molecules via non-specific aptamer-target-recognition.....	21
2.7.4	Separations of proteins via specific aptamer-target-recognition.....	21
2.7.5	Separations of proteins via non-specific aptamer-target-recognition.....	22
2.8	Application of aptamers in downstream processes.....	23
2.8.1	Immobilization of aptamers.....	23
2.8.2	Binding of aptamers with their targets.....	24
2.8.3	Eluting of targets from aptamer-modified matrixs.....	25
2.8.4	Regeneration and storage of aptamer-modified matrixs.....	26
2.8.5	Current limitations and future prospects for aptamer-based downstream processes.....	27
3	Results and discussion.....	29
3.1	Aptamer-based purification of his-tagged proteins.....	29
3.1.1	Immobilization of aptamers on amino-modified magnetic beads.....	30
3.1.2	Capping of amino-modified magnetic beads.....	35
3.1.3	Immobilization of aptamers on carboxyl-modified magnetic beads.....	35
3.1.3.1	Comparison of aptamer functionalities between aptamer 6H7 and 6H5 utilizing carboxyl-modified beads.....	40
3.1.3.2	Comparison of aptamer functionalities by using different types of beads.....	43
3.1.4	Aptamer-based automatic purification utilizing a robot.....	45
3.1.5	Aptamer-based purification of his-tagged HLA utilizing carboxyl-modified magnetic beads.....	46
3.1.6	Conventional IMAC-based downstream process by using his-select nickel magnetic agarose beads.....	47
3.1.7	Scal-up via binding of aptamers on NHS-modified sepharose.....	49
3.2	Aptamer-based purification of F _c fragment and IgGs.....	53
3.2.1	Immobilization of aptamers on magnetic beads.....	54
3.2.2	Optimization of aptamer activity and binding capacity.....	55
3.2.3	Aptamer-based purification of F _c fragment from FCS.....	59
3.2.4	Aptamer-based purification of human IgG from FCS.....	59
3.2.5	Conventional protein A-based downstream process.....	60
3.2.6	Scale-up via binding of aptamers on NHS-modified sepharose and methyl-carboxyl-modified CIM [®] DISK.....	61
3.3	Aptamer-based purification and depleting of small molecules.....	68
3.3.1	Aptamer-based purification of theophylline.....	68
3.3.2	Aptamer-based depleting of malathion.....	78
3.4	Aptamer-based detection of proteins via quantum dots.....	81

4	Summary and outlook.....	83
4.1	Aptamer-based purification of his-tagged proteins.....	83
4.2	Aptamer-based purification of antibodies.....	84
4.3	Scale-up.....	85
4.4	Aptamer-based purification and depleting of small molecules.....	86
4.5	Aptamer-based detection of proteins	86
4.6	Outlook	88
5	Appendices	89
5.1	Materials	89
5.1.1	Chemicals	89
5.1.2	Buffers and solutions	90
5.1.3	Biomolecules	91
5.1.3.1	Aptamers	91
5.1.3.2	Antibodies	92
5.1.3.3	Proteins.....	92
5.1.3.4	Other materials	92
5.1.3.5	Protein sequences	92
5.1.4	Consumables.....	93
5.1.5	Equipments	93
5.1.6	Software.....	93
5.2	Methods.....	94
5.2.1	General methods.....	94
5.2.1.1	Determination of concentrations of immobilized aptamers as well as bound and eluted proteins via NanoDrop TM	94
5.2.1.2	Determination of concentrations of immobilized aptamers via propidium iodide (PI) assay	95
5.2.1.3	Determination of concentrations of bound and eluted proteins via Bradford assay	95
5.2.1.4	Determination of the amount of immobilized aptamers.....	96
5.2.1.5	Determination of the amount of bound and eluted proteins.....	96
5.2.1.6	Calculation of aptamer activity	97
5.2.1.7	Calculation of the elution efficiency	97
5.2.1.8	Dialysis.....	97
5.2.1.9	Buffer exchange by ultrafiltration	97
5.2.1.10	SDS-PAGE.....	98
5.2.2	Production of the target protein PFEI.....	99
5.2.2.1	His-Tag-Protein PFEI.....	99
5.2.3	Immobilization of aptamers on different solid supports.....	101
5.2.3.1	Immobilization of aptamers on magnetic beads.....	101
5.2.3.2	Immobilization of aptamers on NHS-modified sepharose.....	104
5.2.3.3	Immobilization of aptamers on methyl-carboxyl-modified CIM [®] DISK 104	
5.2.4	Aptamer-based downstream process for his-tagged proteins	105
5.2.4.1	Aptamer-based purification of PFEI	105
5.2.4.2	Aptamer-based purification of HLA	105
5.2.4.3	Aptamer-based automatic downstream process via KingFisher	105
5.2.5	Aptamer-based downstream process for antibodies	106
5.2.6	Aptamer-based downstream process for small molecules.....	107
5.2.6.1	Aptamer-based purification of theophylline	107
5.2.6.2	Aptamer-based purification of malathion	108
5.2.7	Conventional purification methods	108

5.2.7.1	Purification of lysate (PFEL) via his-select nickel magnetic agarose beads	108
5.2.7.2	Purification of antibodies via BioMag [®] Protein A.....	109
5.2.8	Aptamer-based detection of proteins via quantum dots	109
5.2.8.1	Immobilization of aptamers on ITK carboxyl-modified quantum dots	109
5.2.8.2	Detection of proteins via aptamer-modified quantum dots.....	110
5.3	Abbreviations.....	110
6	References	112
7	Resume	121
8	Publications and conference contributions	122

1 Introduction and Task

The efforts to look for new methods or to improve already-known methods to purify and detect proteins in biotechnological and analytical applications have never ceased. Because each cell is composed of a complex mixture of proteins in different compositions, it is difficult to purify an individual protein. However, the variation of sizes, charges and solubilities or affinities toward binding partners make it possible that proteins can be purified in different ways. Conventional methods for protein purification are for example gel filtration (GF), ion exchange chromatography (IEX), hydrophobic interaction chromatography (HIC) and affinity chromatography (AC). Based on these conventional methods, the application of different kinds of aptamer-modified particles becomes a strongly competitive alternative. In this context, aptamer-based high selective and specific affinity separations are advantageous. Aptamers are single stranded DNA or RNA oligonucleotides that are able to bind different kinds of molecules. Compared with previously developed affinity chromatography methods that are primarily based on antibodies, aptamers exhibit although similar specificities and affinities to their targets, yet higher stability to higher temperature and extreme pH values. Especially, they enable the purification of targets under mild conditions and can be denatured and renatured, which enables regeneration of aptamer-modified supports. Furthermore, aptamers can be selected *in vitro* via various SELEX (Systematic Evolution of Ligands by Exponential enrichment) processes based on their specificity and affinity recognition and binding properties with their targets. Once a new aptamer is selected, it is easy to be chemical synthesized, which reduces the cost of production.

Besides their applications in the downstream processes, aptamers can also be used to detect proteins. In order to detect proteins, the development of indirect optical methods is very important, for example for the staining of proteins. Fluorescence labelling is one of the most widely used methods for protein detection. Compared with normally used organic fluorophores or reporter proteins such as GFP (green fluorescent protein), the use of quantum dots, fluorescent semiconductor nanoparticles, in combination with aptamers, is a promising alternative to current methods. Due to the stability and modifiability of the quantum dots, as well as the quick and easy identification of aptamers against a variety of proteins, the application of aptamer-modified quantum dots will be investigated in this thesis.

The main part of this work intends to examine the capability and effectiveness of aptamers to purify proteins and small molecules. Three solid supports will be used for the aptamer immobilization: magnetic beads, sepharose and CIM[®] DISK (CIM[®] monolithic columns). His-tagged proteins [*Pseudomonas Fluorescens Esterase I* (PFEI), *human leukocyte antigen* (HLA)], antibodies [F_c fragment, human Immunoglobulin G (IgG)] and small active substances (theophyllin, malathion) are employed for the testing of aptamer functionalities. The study should conduct through a series of experiments with each next one performed based on the success of the previous one. Aptamer-modified magnetic beads against his-tagged protein PFEI will be first examined, followed by his-tagged protein HLA, antibodies (F_c fragment of human IgG, IgGs), and small molecules (theophylline and malathion). As the aptamer-based purification is till now solely realized in rather small-scale, the scale-up for future preparative scale will be done via aptamer-modified sepharose and CIM[®] monolithic columns. Finally, conventional chromatography methods, like the commonly used purification by using immobilized metal chelate affinity chromatography (IMAC) for his-tagged proteins and protein A for antibodies will be tested and compared with the developed aptamer-based methods. The second part of this work deals with the utilization of aptamers for the detection of their targets. Thereby lab-made aptamer-modified quantum dots (QD) will be examined in a reverse phase microarray.

2 Theory

Aptamers are short, stable single-stranded DNA or RNA oligonucleotides or peptide molecules that can bind with high affinity and specificity to different types of targets [1]. The word aptamer is derived from Latin *aptus* (= fitting) and Greek *meros* (= part). Natural aptamers exist in riboswitches [2]. Aptamers that consist of single-stranded DNA- or RNA- strands with a length of 25 to 80 nucleotides were classified as DNA or RNA aptamers. Aptamers that consist of amino acids and can interact with other protein inside cells were peptide aptamers [3, 4]. A lot of aptamers can bind to their targets with K_d (dissociation constant) in the range of 1 pM to 1 nM [5-7]. They can bind to metal ions [8, 9], vitamins [10], drugs [11-13], proteins [14, 15], nucleic acids [16-18], small organic compounds: for example organic dyes [19, 20], and even entire organisms like viruses [21, 22] and cells [23-26]. How aptamers recognize and interact with their targets depends on the nature of targets, the nucleotide sequences and three dimensional structures of the aptamers. Those tRNA, ribozymes, DNA binding proteins and DNAzymes are examples of how nucleic acids recognize proteins via molecular shape [27-31]. Aptamers can be selected *in vitro*. This *in vitro* selection technique is named as Systematic Evolution of Ligands by Exponential enrichment (SELEX) [1, 4, 32, 33]. With the SELEX method, aptamers are enriched from large pools of partially randomized oligonucleotides containing approximately 10^{15} different sequences. The selection process is initiated by incubation of the oligonucleotides with a target which is either coupled to a matrix (e.g., magnetic beads) [25, 34-39] or on a surface (e.g., cell surface) [40-45]. Subsequently, non-binding oligonucleotide molecules are washed away, and the bound molecules are recovered, amplified by PCR (Polymerase Chain Reaction) or RT-PCR (Real Time-Polymerase Chain Reaction) [46, 47], and then separated into single-stranded oligonucleotides again. These oligonucleotides are subjected to a subsequent SELEX cycle. Typically, aptamers with high affinity will be obtained through 10 to 15 SELEX cycles of selection and amplification. Several variations of the SELEX procedure and other techniques have been developed and successfully applied over the past years [33, 48].

2.1 Origin of aptamer-technology

The development of aptamer-technology could be traced back to the discovery of ribozymes. In 1989, Thomas Cech from University of Colorado and Sidney Altman from

Yale University were awarded with the Nobel Prize because they discovered that single-stranded RNA-molecules exhibiting enzymatic properties existed in the nature. The finding reveals that RNAs are not only carriers that deliver genetic information from DNAs to proteins, but also catalysts in chemical reactions like enzymes [49-52]. Therefore, this catalytically active RNA strands were termed ribozymes. Before the discovery of ribozymes, it was a common understanding that only proteins could act as enzymes. When ribozymes bind to specific substrates, their catalytic properties are activated. Following the discovery of ribozymes, in 1990, three research groups independently reported RNA aptamers for the first time. The group of Ellington and Szostak identified RNA molecules binding to organic dyes by *in vitro* selection. They introduced the term aptamer [1]. Another group of Tuerk and Gold reported that *in vitro*-selected RNA molecules could bind to the T4 DNA polymerase from bacteriophage [4]. The group of Robertson and Joyce worked with ribozymes and found that ribozymes changed their functionalities during the *in vitro* selection, which lead to DNA degradation [53]. Two years later, Ellington and Szostak discovered single-stranded DNAs, which showed higher stabilities than RNAs [54]. However, RNA aptamers can bind not only to the protein binding region, but in many cases to protein itself. Thus, RNA aptamers are capable to distinguish between various isoforms of a target. It seems that RNA aptamers are better suited to attach to a molecule, which is why many research groups still prefer to use RNA aptamers in their work although RNAs are not stable to nucleases [55], even though production of RNAs is expensive. In the last ten years, a variety of targets were tested to investigate aptamers' binding capacity [56-62].

2.2 Structures of aptamers

The recognition and binding of molecules (targets) by aptamers are mainly based on the special aptamers' three-dimensional structures [63]. They have two features: secondary and tertiary elements [64-67]. The secondary structures consist of hydrogen bonds between the complementary nucleotide bases and are influenced by the aptamers' nucleotide sequences [68]. Known forms of secondary structures include, for example, loops, mismatches or junctions (Figure 2.2 1) [69-73], and pseudoknots (Figure 2.2 2) [73, 74]. A pseudoknot is formed when bases outside of the stem-loop bind with bases within the loop, which in return forms a second stem-loop (Figure 2.2 2) [73].

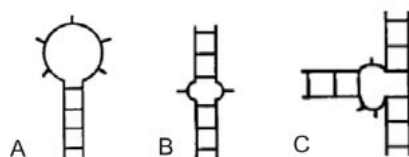


Figure 2.2 1: Different secondary structures of aptamers (A) stem-loop, (B) mismatch, (C) three-way junction [73].

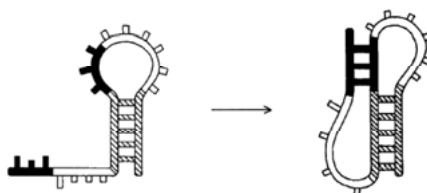


Figure 2.2 2: Schematic representation of the formation of a pseudoknot [73].

The complex tertiary structures are formed by interactions of existing secondary structure elements [69, 73]. Tinocco et al. (1999) observed that during the formation of tertiary structures, the secondary elements will normally not change, however, the stability of some area will decrease. For example, kissing-hairpins will be influenced and changed. The secondary and tertiary oligonucleotide structures can be stabilized through the interactions between various metal ions and the negatively charged sugar-phosphate backbone of the nucleotide [69, 70, 75-77]. For example, the reformation and stabilization of kissing-hairpins structures can be carried out via addition of magnesium ions. The secondary structures are “pre-folded”, they exist without the presence of metal ions, and the structures will not change in the presence of metal ions. In contrast, in some cases, tertiary structures are folded only in the presence of metal ions [69, 78]. Furthermore, monovalent ions such as K^+ and Na^+ promote the formation and stabilization of G-quadruplex structures [79]. The G-quadruplexes consist of four-stranded inter- or intramolecular structures, consisting of a square arrangement of guanine. G-quadruplexes can occur when aptamers have a high proportion of guanine [80]. One advantage of metal ion-independent structure formation is the possibility of a simple regeneration of the aptamer. By removal of the ions, for example divalent cations, with chelating reagents such as ethylenediaminetetraacetic acid (EDTA), the target molecule will be released from the aptamer. To investigate the possibilities of aptamer folding, an aptamer structure prediction is helpful. However, depending on the external conditions, for instance, buffer, temperature, ionic concentrations, pH-values, etc., various aptamer structures can coexist in equilibrium [69].

2.3 Binding mechanisms of aptamers

Through intra-molecular hybridization, aptamers can fold into particular molecular shapes. By various structural shapes, aptamers can recognize and bind their targets through hydrogen bonds, hydrophobic and electrostatic interactions, as well as van der Waals force, steric influence by aromatic stacking or, in most cases, a combination thereof [81]. In the simplest case of aptamer-target binding, aptamers have already folded correctly into their three dimensional structure in the absence of the target, and the target attaches to the pre-folded aptamer according to the "key-lock principle" (key-lock mechanism). However, aptamers form the final structures in most cases during the binding process. This binding mechanism is called induced-fit mechanism [82]. Induced-fit mechanism could be confirmed by various investigation methods for most known aptamer-target complexes: for instance, x-ray diffraction and NMR spectroscopy [69, 83-85]. Aptamer against theophylline gives a good example of induced-fit mechanism. As soon as the theophylline approaches to the aptamer, two internal-loop regions were formed. But in the presence of other methylxanthines (for example, caffeine, theobromine), which have similar structure like theophylline, corresponding aptamer 3D (three dimensional) structure is not formed [86].

Based on the classical key-lock and induced-fit mechanisms, more binding forms between aptamers and targets are conceivable. For example, RNA aptamer-protein-complexes were built through induced-fit from both sides [87-89]. In addition to the aptamer structure change, structures of proteins can also be changed during the binding to form a stable complex [87]. In conclusion, aptamers have different binding mechanisms, therefore the binding mechanism for each aptamer-target complex should be considered independently.

In most instances, binding domains of aptamers play an important role in the target binding. But in some cases the non-binding domains may interfere with the interaction between the aptamer and target and eventually prevent the binding domain from folding into the desired 3D conformation [90]. This may result in reduction or complete loss of the aptamer binding affinity. In order to stabilize the correct binding conformation of the aptamer, monovalent cations such as Na^+ and K^+ can be used as well as divalent ions such as Mg^{2+} , and Ca^{2+} . In some thrombin aptasensor studies, the effects of these cations were validated by addition of Na^+ or K^+ which could stabilize G-quadruplex structures and reduce nonspecific binding [91, 92]. However, Na^+ or K^+ is also able to interact with negatively

charged phosphate backbone of an aptamer and result in weak complexes at a higher cation concentration [92]. Thus, they may lead to the conformational changes of binding site and lessen the affinity of aptamers to their targets. Under such circumstances, suitable cation concentrations have to be used during binding, so that aptamers can bind their targets properly. Nevertheless, aptamers binding to their targets are generally performed in the buffer used during the selection of aptamers.

2.4 Selection of aptamers

The SELEX process was discovered by Tuerk [4] und Gold [1] independently at the beginning of 1990. This method is based on the specific recognition and binding of oligonucleotides to target molecules and enables the extraction of the most appropriate aptamer sequences against a variety of different molecules [93]. The conventional SELEX process and two variations of SELEX are presented below.

2.4.1 Conventional SELEX procedure

The steps of the conventional SELEX procedure are shown in figure 2.4 1. The target molecule is immobilized on a solid phase, usually an affinity column based on agarose or sepharose [1, 94]. The immobilized targets are incubated with a highly diverse oligonucleotide library (pool). The initially used oligonucleotide library consists of a multitude of different DNA or RNA sequences, which are produced entirely by chemical synthesis [95, 96]. The wide variety of DNA or RNA pools ensures that each individual, synthesized oligonucleotide molecule has a unique sequence. In practice, the diversity of sequences is limited from 10^{14} to 10^{15} [90, 97-99]. Those sequences which have no or only a small affinity to the target molecule are removed through several washing steps. The stronger binding sequences are then eluted, amplified by PCR and then the smaller pool of binders is introduced to another SELEX cycle. This procedure is repeated until there are only very strong binding sequences left in the oligonucleotide pool. Usually it takes about ten to fifteen cycles [90]. Afterwards, these acquired sequences are amplified and sequenced. Hereafter, the binding properties of these sequences are investigated with the help of target molecules. The duration of the entire process including the final cloning with sequencing is approximately two months [90]. Once the aptamer sequence is known, it can be produced relatively easily and cheap with chemical solid-phase synthesis.

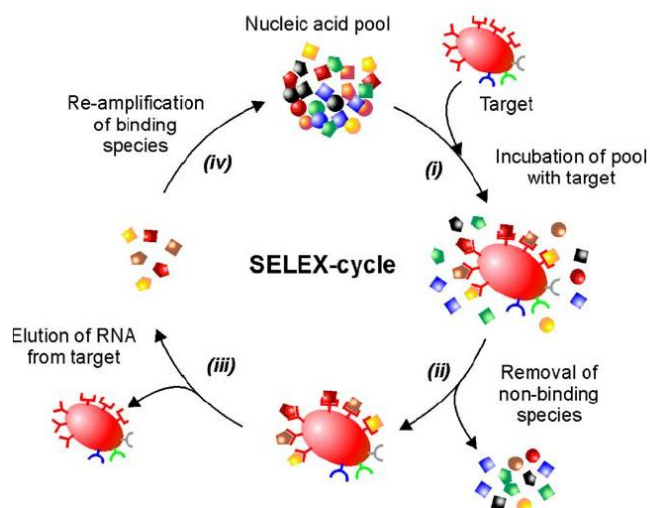


Figure 2.4 1: Schema of the *in vitro* SELEX process to obtain aptamers [100].

The SELEX process can be adjusted by selective variation to reach desired sequence with specific properties. For instance aptamers can be obtained with greatly increased specificity in a counter-SELEX. This specificity allows aptamers to distinguish very similar structures, such as enantiomers [101, 102].

2.4.2 MonoLEX

The MonoLEX procedure is a one-step selection process for the recovery of aptamer sequences by a single affinity chromatography step. The process starts with the incubation of the library with the target molecule, which is immobilized on an affinity column. Subsequently the non-binding sequences are removed by excessive washing steps. After subsequent physical segmentation of the affinity column, bound aptamers are removed via heat denaturation from the column slices. Finally, eluted aptamers are amplified via a single final PCR amplification step [103]. The aptamers against human F_c fragment, which were used in this study, were derived from a MonoLEX-process by the company AptaRes (Mittenwalde, Germany).

2.4.3 FluMag-SELEX

The FluMag-SELEX process differs from the conventional selection methods by the use of fluorescent dyes for the nucleic acid quantification [33, 104]. In this method, the target is coupled to magnetic particles (magnetic beads). Magnetic beads show several advantages.

First, they require few targets. Second, they enable automation. Third, the magnetic separation works fast, which increases the efficiency of the entire process. By fluorescent labeling of the bound aptamers after the first selection-cycle, the depletion of the non-binding oligonucleotides, and also the enrichment of target-specific aptamers can be monitored during the SELEX procedure. Upon completion of the selection process, the oligonucleotides can be synthesized without fluorescent dyes for further analysis and use.

2.5 Advantages of aptamers over antibodies

Although antibodies are able to bind their targets remarkably, aptamers show advantages in multiple aspects. First, the production of aptamers with *in vitro* selection is better than the production of antibodies with *in vivo* process, because the *in vivo* selection can only be done under physiological conditions. This restricts the application and function of antibodies. On the contrary, aptamers can be optimized under any conditions. Furthermore, under an *in vitro* process, the control over the production is very high. An investigator can recover aptamers that bind to a particular region of the target under specific binding conditions, such as salt concentration, pH-value and temperature. Second, the variation batches can be minimized. By isolation aptamers *in vitro*, an aptamer can be produced for any target molecule and can be synthesized rapidly, while each immunoassay must be optimized during each production by isolation antibodies *in vivo*. Third, given the fact that, the selection of antibody could last as long as 6 months, aptamers can be obtained in approximately two months. Fourth, the production of antibodies involves an immune response, while aptamers can be isolated by *in vitro* methods without immune response. Therefore, aptamers can be selected to recognize and bind a wide range of targets including toxic compounds and inherently non-immunogenic molecules that antibodies are hard to be raised against. Fifth, aptamers are more chemically stable over a wide range of temperature. They can be regenerated easily after denaturation. Their ability to renature from a denatured state provides very long shelf life. Sixth, aptamers are easy to be modified and labeled. Site-specific modification techniques are capable to attach various molecules such as biotin groups [105], thiol groups [106], and label molecules [107] at 3' or 5' end of aptamer without affecting the target binding site and can make one-to-one conjugate (aptamer to label) [108-110]. However, labels on antibodies can cause them to lose their affinity to their target molecules, because the labels occur at a random position of antibodies. Finally, as aptamers are 10-100 times smaller than antibodies, they are

expected to achieve higher immobilization density [90]. Table 2.5 1 shows the comparison of aptamers and antibodies [93, 111-113].

Table 2.5 1: Comparison of aptamers and antibodies as recognition molecules.

Field	Antibody	Aptamer
production	<i>in vivo</i> (animals or cell lines) limited in selection conditions	<i>in vitro</i> various selection parameters applicable
batch-to-batch variation	due to variations in the production, each immunoassay must be optimized	production via chemical synthesis, reproducible with little variations
selection period	more than 6 months	approximately two months
target	production against little immunogenic or toxic targets is very difficult	production is independent of the immunogenicity and toxicity targets
stability	risk of irreversible denaturation	reversible denaturation
modification	can not be modified during production	can be modified during production
labeling	occurs at a random position, lead to reduction or loss of binding affinity	can be defined to a desired position without affecting the binding affinity

2.6 Applications of aptamers

Because of relatively high stability and easy production, aptamers have received more and more attention within life science research and applications. Aptamers are playing their roles in ELISAs (enzyme-linked immuno sorbent assay) [114, 115], western blots [116], flow cytometry [117, 118] and microarrays [119-122] and may replace antibodies in all of the areas currently dominated by antibodies. Aptamers are also used in medical area for diagnosis, treatment of diseases and development of medications because of their low or non-immunogenic properties [100, 123, 124]. Similarly, as aptamers can be chemically modified, the pharmacokinetics can be improved through specific chemical modifications [100, 125]. Aptamers are recently reported in the application of aptasensors for detection of various substances, such as bio-molecules or toxins [126, 127]. A new interesting application is the purification of proteins [128]. For example, recombinant Ig-fusion protein with an L-selectin-tag was successfully purified from the supernatant of eukaryotic cell cultivations by using an aptamer affinity chromatography in 1999 [129].

2.7 Application of aptamers in affinity separations

As antibodies' competitors, aptamers have already successfully been used in the following applications: liquid chromatography (LC), capillary electro chromatography (CEC) [130], high-pressure liquid chromatography (HPLC) [131] and magnetic separations [36]. The core of all these applications is affinity separation (referred to review [132]).

2.7.1 Separations of small molecules via specific aptamer-target-recognition

In the approach of liquid chromatography, adenosine was successfully separated from related compounds like NAD (nicotinamide adenine dinucleotide), AMP (adenosine monophosphate), ADP (adenosine diphosphate) and ATP (adenosine triphosphate) via isocratic elution [133] by utilizing different affinities towards the aptamer. It was also reported that adenosine was successfully separated from complex biological samples via aptamer-modified solid matrix and mobile phase [134, 135]. An example of separation by utilizing capillary electro chromatography was reported by Clark et al. (2003). RNA aptamers against flavin mononucleotide (FMN) were immobilized on capillaries. The FMN could be separated from other molecules, which have no flavin moiety [136-138]. This experiment specifically showed the high stability of aptamers against organic solvents by using 50% acetonitrile [139]. In a striking example of specificity, aptamers against the theophylline (1, 3-dimethylxanthine) bind with 10,000-fold lower affinity to caffeine (1,3,7-trimethylxanthine) that differs from theophylline only by a single methyl group [48].

2.7.2 Separations of small molecules via enantioselective properties of aptamers

As aptamers are able to distinguish very similar structures, such as enantiomers, they have been successfully used to separate the enantiomers of adenosine [140] and arginine-vasopressin (AVP) [131]. Michaud et al. (2004) reported in his research that DNA aptamers could be selected against D-adenosine and L- tyrosine amide for the separation of respective enantiomers. The results showed D-adenosine had an average enantiomer selectivity and L-tyrosine amide an excellent enantiomer selectivity [141]. Later, Brumbt et al. (2005) used a D-RNA aptamer instead of aforementioned DNA aptamers directed against L-arginine. Unfortunately, the RNA aptamer was degraded very quickly via RNases. Although only natural D-oligonucleotides will be accepted as substrats by nucleases, it is not difficult to overcome the limitation of degradation. The L-RNA aptamer

which is the mirror image of the natural D-RNA aptamer was created. Thus the L-RNA against the mirror image of targets can replace the original D-RNA aptamer against the targets [55].

2.7.3 Separations of small molecules via non-specific aptamer-target-recognition

Separation can not only be performed with the target-specific recognition, but also via non-target-specific aptamers. Some small molecules like aromatic hydrocarbons can be separated via non-target-specific aptamers which contain G-quartets and related oligonucleotides. For example, DNA aptamers selected against thrombin can be used to separate benzoperylene and naphthalene [142]. Another example for separation of isomeric dipeptides by utilizing G-quadruplexes was reported by Charles et al. (2002) [143]. Moreover, G-quadruplexes have also been used for the separation of homodipeptides and alanyl dipeptides [144], fibrinogen peptides [145] and binary mixtures of amino acids [142]. Vo et al. (2006) acclaimed that some instable G-quartet structures are beneficial for the non-target-specific binding [145].

2.7.4 Separations of proteins via specific aptamer-target-recognition

A four-plane G-quartet DNA aptamer against bovine beta-lactoglobulin gives an example for target-specific separation of proteins. This DNA aptamer separated the variants A and B of lactoglobulin, although variants A and B differed only by 2 of their 162 amino acid residues [139]. Using the same method, via DNA oligonucleotides with G-quartet structures, alpha-, beta-, kappa-casein, alpha-lactoalbumin and beta-lactoglobulin from bovine milk proteins were successfully separated [146].

The application of aptamer-based protein purification was first discovered by Roming et al. (1999). A 36nt biotinylated DNA aptamer was immobilized on streptavidin-modified resin. As the aptamer recognized and bound to the lectin domain of human L-selectin, recombinant human L-selectin-Ig fusion protein with the extracellular lectin domain was successfully purified from a CHO (chinese hamster ovary) cell culture supernatants [129]. Moreover, Connor et al. (2006) used a DNA aptamer directed against thrombin to purify the target protein from human serum albumin. The target protein was eluted by DNase [147]. With the same elution strategy, *thyroid transcription factor 1* (TTF1) from complex proteinmixtures and bacterial lysates was purified utilizing aptamer [128]. Another

example reported by Oktem et al. (2007), DNA aptamers directed against *thermus aquaticus* DNA polymerase was immobilized on magnetic beads and were used to purify the target from bacterial lysates with a total of 93% purity and 89% recovery. This experiment was performed in a one-step purification procedure [39].

Recently, the use of DNA aptamers for the purification of his-tagged proteins was discovered [36]. Aptamers which were directed against his-tagged proteins were first immobilized on magnetic beads and then incubated with corresponding his-tagged proteins from crude *E. coli* lysates. With the help of 1M imidazole, the purified his-tagged proteins could be eluted. The effectiveness of purification is similar to the immobilized metal chelate chromatography [36].

In 2008, Miyakawa et al. reported to use RNA aptamers to purify IgG. An RNA aptamer was first selected directed against the F_c fragment of human IgG, and then used to purify IgG from serum. It was demonstrated that the optimized 23-nucleotide RNA aptamer bound only to the F_c fragment of human IgG, not to other species of IgGs, this is because that the 3D conformation of the recognition sites on the F_c domain differ significantly among different species of IgGs. Therefore, the high specificity of the aptamer can be used as a protein A alternative for affinity purification of human IgG. Compared to purification of IgG from CHO culture fluid with protein A, aptamer-based purification showed similar efficiencies [148].

Furthermore, aptamers can distinguish between closely related but non-identical members of a protein family, or between different functional or conformational states of the same protein. The separation of his-tagged proteins from *E. coli* lysates [36] and the separation of human IgG from the human sera, CHO culture fluid [148, 149] with the help of aptamer were referred for the aptamer-based downstream process in this study.

2.7.5 Separations of proteins via non-specific aptamer-target-recognition

In addition to non-target-specific aptamers' applications of separating small molecules, the G-quartets of aptamers can separate proteins as well. Several applications of aptamers in this field have been reported. Zhao et al. (2008) reported a successful purification of target protein from human serum and rat liver tissue lysate via DNA aptamers immobilized on a monolithic support. The DNA aptamer was selected directed against cytochrome C [150].

This monolithic support immobilized aptamer was also used for the purification of thrombin. The reason why this aptamer can be applied to both target molecules is that their G-quartet structure showed affinity to both targets [151]. Another example showed a G-quartet aptamer which was originally selected against thrombin was used to separate various species of albumins [152]. Since these non-target-specific separations are based on weak and non-specific interactions, their application is limited. Separation based on high affinity and specificity has a broader prospect [153].

2.8 Application of aptamers in downstream processes

Because aptamers exhibit high affinity and selectivity towards their corresponding targets, they can therefore act as affinity ligands for the binding and purification of corresponding targets. Based on current applications of aptamers in affinity separations described above, aptamer-based purifications are investigated in this study. The strategy of aptamer application in the downstream process will be divided as followings: (i) immobilization of aptamers, (ii) binding of aptamers with their targets, (iii) eluting of targets from aptamer-modified matrixs, (iv) regeneration and storage of aptamer-modified matrixs (referred to review [132]).

2.8.1 Immobilization of aptamers

In the downstream process, aptamers should be first immobilized on solid supports. As aptamers show a size range of approximately 13-26 kDa, it is possible that they are able to be immobilized in a higher density than antibodies, which are around 150 kDa. The high aptamer density on the solid support enhances the efficiency of support's utilization. Theoretically higher aptamer density can bind more targets. However, this could only work for small targets, because large targets require more space for themselves.

In order to immobilize selected aptamers on designated supports, generally noncovalent attachment or covalent immobilization is applied. A typical example of noncovalent binding is the attachment of biotinylated aptamers onto streptavidin coated chromatographic supports. The easy conduction of this immobilization procedure makes it a popular choice [55, 128, 129, 131, 133, 154-156]. However, this noncolvalent binding method shows limitations in comparison of covalent binding. The noncovalent binding between biothynlated aptamers and streptavidin depends on the ionic strength. Under a

low ionic strength condition, the aptamer-streptavidin-complex can undergo dissociation. For example, approximately 25% of bound aptamers are released from streptavidin at 30°C with a low ionic strength [157]. As streptavidin can undergo irreversible denaturation, which will result in a loss of aptamer and thus the binding capacity, the purification conditions are largely restricted for aptamers which immobilized via biotin-streptavidin interaction.

For most of the downstream processes, covalent binding between aptamers and supports is very important, because the covalent binding is stable, which can prevent the release of aptamers during the later elution of targets and thus facilitate the later regeneration of aptamer-modified supports. To achieve covalent immobilization, the previously selected aptamers and the surface of solid supports should be first chemically modified. Aptamer modified with functional groups can be easily done at desired position during their *in vitro* synthesis.

2.8.2 Binding of aptamers with their targets

The effectiveness of aptamers binding with their corresponding targets is determined by their specific three dimensional structures, aptamers are able to fold into their 3D structures either in the presence of the target or in the selection buffer without target. The factors, for example buffer composition, pH-value and temperature that affect the aptamers' correct folding must be carefully controlled in order to reach a good binding result. Usually, the buffer will be chosen for the binding of targets, which was used during the selection of the aptamer. Reported in multiple references is that a buffer composition can be modified and optimized as needed [140, 158]. A uniform buffer can also be chosen for different aptamers, which were selected in different buffers [159]. Even though choices for buffers are available, a few aptamers show dependence on the buffers containing cations, in which they could fold into their 3D conformation properly. It is known that cations like Mg^{2+} and Ca^{2+} are able to interact with negatively charged phosphate backbone of the aptamer, which improves the correct 3D folding of aptamers [130]. In addition to the buffer composition, the pH-value is also very important for the binding between aptamers and their targets because pH-variations may result in ionization. If the functional groups of the target, which directly interact with the aptamer's binding site, are protonated or deprotonated through the change of pH-values, the binding between targets and aptamers

will be interrupted. The same is true, if the bases of aptamers which are responsible for binding of the target are protonated or deprotonated, aptamer's folding will be interfered. Beside the buffer compositions and pH-value influences, temperature also plays an important role in the optimal binding of target. In general speaking, lower temperature results in higher affinity of aptamers to targets [130].

2.8.3 Eluting of targets from aptamer-modified matrixs

Since binding can be achieved through aptamer's 3D conformation, to recover the bound targets could be done by destroying the 3D conformation in the way to change buffer composition, pH-values, or temperature.

As many aptamers' correct folding rely on divalent ions, removing such divalent ions in the elution buffer and adding chelating agents can make aptamers no longer able to fold into their 3D structures and therefore release the bound targets. For example, adding EDTA to the elution buffer can chelate divalent ions to form a metal-EDTA chelate and destroy the 3D conformations of such divalent ions dependent aptamers.

Romig et al., reported that a L-selectin fusion protein was eluted from an aptamer-modified sepharose support via EDTA [129]. In addition to using EDTA, competitive molecules can be used for elution of the target. Since metal ions like Zn^{2+} and Ni^{2+} can coordinate to adenosine through N1 and N7, which can interfere with the binding between adenosine and aptamer, they were used as competitors for target elution [134]. It was reported recently, that imidazole could be utilized for the elution of his-tagged proteins from aptamer-modified magnetic beads [36].

Targets can also be eluted via changing the pH-value or heating the aptamer-target complex during elution steps. However, these methods only work for small molecules, not for proteins. Because most proteins denature under extreme pH values or degrade in heating.

The target can also be eluted by removal aptamers from the solid support. It was reported that an aptamer against hepatitis C virus (HCV) RNA polymerase was immobilized via a photo-cleavable Fmoc linker. Results of this experiment showed that the aptamer and the bound target were both eluted under the irradiation with UV [160, 161]. This method is not

suitable for efficient purification of proteins, because the purified proteins are contaminated with aptamers after elution. Furthermore, the aptamer-modified solid support is destroyed after single-use. For the same reason, the elution of targets utilizing nucleases destroys the immobilized aptamers [128]. However, this approach can be used in analytical applications.

Other elution-strategies are for example the utilization of detergents or urea, because they are able to destruct the correct folding of aptamers or targets. However, their incompatibility with the solid support or with the native state of the target limits the usage.

2.8.4 Regeneration and storage of aptamer-modified matrixs

Aptamers can be denatured and renatured. The regeneration process is relatively easy. It is known that heating can melt the secondary structures of aptamers, which can be used for denaturation. Usually, the aptamer renaturation can be performed by incubation of aptamer-modified support in the aptamer selection buffer. It was known RNA aptamers are not stable against nucleases, which results in a short-term stability and decreases the reusability of aptamer-modified supports. It was reported that the binding capacity for the target L-arginine was reduced to 65% in 8 days via enzymatic cleavage when using an RNA aptamer as an affinity ligand [55]. To avoid loss of binding capacity by enzymatic cleavage, nuclease resistant aptamers can be used, such as post-SELEX-modified aptamers [102]. Mirror images of the initial aptamer can be used for chiral separations to prevent aptamer degradation. Furthermore, DNA aptamers can also be successfully used for the purification of a target from a complex biological samples [36]. These DNA aptamers were immobilized on magnetic beads and displayed several successful protein purification and regeneration cycles [36]. It is also proved that DNA aptamer-modified magnetic beads can be stored in buffer at 4°C for up to 6 months [36]. Under various conditions, the stability of aptamer-modified columns can be improved. For example, an aptamer-modified column can be stored for several days in a solution of water and methanol (50%) with no influence on aptamer binding [140].

2.8.5 Current limitations and future prospects for aptamer-based downstream processes

The above sections revealed that several aptamers were successfully used in affinity separations. However, most of these aptamers which are suitable in affinity separations may not be available for the downstream process. This is because most aptamers were selected directed against their targets solely based on their specificity and affinity without considering possible elution conditions during the SELEX process. Therefore, elution strategies not compatible with the targets' native state were applied. For example, during SELEX process, heat denaturation was used for the elution of oligonucleotides from the targets. But in the downstream process, heating destroys targets which are sensible to high temperature, such as proteins. Thus, gentle denaturation methods need to be developed during the SELEX process which can consequently be used in the aptamer-based downstream process for temperature sensible targets. Several mild elution conditions will be investigated in the present work. By adding imidazole, his-tagged proteins can be eluted. Imidazole plays a role as competitive molecule in the elution process. Thereby heat-induced denaturation will be avoided. For the purification of antibodies, the elution strategy will be performed via removing divalent ions in the elution buffer and adding chelating agents EDTA to destroy aptamers' 3D conformation, so that antibodies can be gently eluted. In addition to these mild elution strategies for proteins, suitable elution methods for aptamer-based purifications of small molecules were also investigated. It was reported that aptamers against theophylline (1, 3-dimethylxanthine) binds with 10,000-fold lower affinity to caffeine (1,3,7-trimethylxanthine) that differs from theophylline only by a single methyl group [48]. In this thesis, several elution methods will be investigated to achieve the optimal theophylline elution efficiency. It was known that malathion is used as insecticide and acaricide. Because of its hazardous effects on human health and the ecosystems, in some cases, malathion is regarded as contamination. Therefore malathion was employed in this study as another small molecule for the investigation of aptamer-based downstream process, which is hoped to fulfill the possibility of removing or depletion contaminations utilizing aptamer.

Moreover, the reports published till now are only limited to laboratory-scale. In industrial applications, amounts of kilogram aptamers would be required. Aptamers are already used in the therapeutic field, for example, the first therapeutic application was approved for the treatment of age-related macular degeneration in 2004 [162]. The required large-scale

synthesis of oligonucleotides is especially accelerated by biopharmaceutical companies. Thus if aptamers can be produced in large-scale at low cost, aptamer-based downstream process will have more prospects in the near future. In this study, scale-up of aptamer-based purification strategies will be investigated. Because sepharose is commonly used as stationary phase in downstream processing, it will be employed for scale-up experiments. Moreover, considering that CIM[®] monolithic columns have big internal pores and the purification process by using CIM[®] DISK can be automated via FPLC, it will be employed as another solid support for aptamer-based large scale downstream process.

3 Results and discussion

Downstream process plays an important role in biotechnology. In this study aptamers were used to purify proteins and small molecules. The first part of this study conducted the purification of his-tagged *Pseudomonas Fluorescens Esterase I* (PFEI) from *E. coli* via immobilized aptamers on various solid supports like magnetic particles and *N*-Hydroxysuccinimide (NHS)-activated sepharose; generalized this purification method to another target protein, that is the aptamer 6H5-based purification of human leukocyte antigen (HLA) utilizing carboxyl-modified magnetic beads and NHS-activated sepharose; compared this aptamer-based method with the conventional purification method for his-tagged proteins by using his-select nickel magnetic agarose beads. Furthermore, in order to transfer the manual operations to the automatic control, an automatic purification process by using KingFischer was introduced and tested. In the second part of this study, an investigation was made for the downstream process of human F_c fragment and the whole IgG via immobilized aptamers on carboxyl-modified magnetic beads, NHS-modified sepharose and methylcarboxyl-modified CIM[®] DISK. Comparison was made between conventional purification method by utilizing protein A and aptamer-based method for antibodies. As the first two parts handle the purification of proteins, the third part of this study examines aptamer-based purification methods for small molecule targets like theophylline and malathion. The development of aptamer-modified purification strategies for small molecules may not only be useful for the purification of the respective targets, it may also provide new avenues to remove or deplete contaminations such as toxins. In addition to the application of purification, aptamers can also be used to detect proteins. In the last part of this study, aptamer-modified quantum dot 525 was tested for the applicability of protein detection.

3.1 Aptamer-based purification of his-tagged proteins

In a previous publication, anti-his-tag aptamers modified with amino linkers were first covalently immobilized on amino-modified magnetic beads and then incubated with his-tagged protein PFEI. This approach allowed the elution of the bound target protein utilizing imidazole [36]. Because this method required toxic cyanuric chloride and PFEI could bind unspecifically to the amino-modified magnetic beads. A new immobilization method was sought. Considering that 1-Ethyl-3-(3-dimethylaminopropyl) carbodiimid

(EDC) is a water soluble carbodiimide, it is generally used as a carboxyl activating agent for the coupling of primary amines to yield amide bonds and the resulting urea can be easily separated, an EDC-based immobilization strategy was developed by using carboxyl-modified magnetic beads in this study. Then, the process of aptamer-based purification of his-tagged proteins was applied to another target protein HLA in order to demonstrate the general applicability. Sepharose was introduced as solid support for scale-up of aptamer-based downstream process.

The target protein PFEI was produced in *E. coli* and purified via membrane adsorber-based IMAC. Purified PFEI was used to characterize the aptamer-modified supports with regard to aptamers' binding capacity to their targets. PFEI from crude *E. coli* lysates was used to investigate the purification efficiency by using aptamers. Another his-tagged protein HLA from cell culture media was used to test the general applicability of aptamer-based purification efficiency.

3.1.1 Immobilization of aptamers on amino-modified magnetic beads

A suitable solid support is required for the immobilization of aptamers. Solid supports should be coated with functional groups, which enable the covalent binding with amino-modified aptamers. Magnetic particles coated with affinity ligands become an efficient, alternative tool for a quick and easy extraction of biomolecules. Therefore magnetic particles coated with amino groups and carboxyl groups were investigated in this study. As in the previous publication, amino-modified aptamers were successfully immobilized on amino-modified magnetic beads via toxic cyanuric chloride. This method was first tested as the cornerstone of aptamer immobilization. BioMag[®] Amine magnetic beads consist of a suspension of magnetic iron oxide particles coated with primary amino groups, the amino groups allow covalent attachment of proteins or ligands with retention of biological activity.

In order to immobilize aptamers directed against his-tag on amino-modified magnetic beads, amino-modified aptamer 6H7 was first activated via the agent: cyanuric chloride (Fig. 3.1.1 1). This immobilization allowed the oriented binding of the aptamers to achieve high functionality [36, 122].

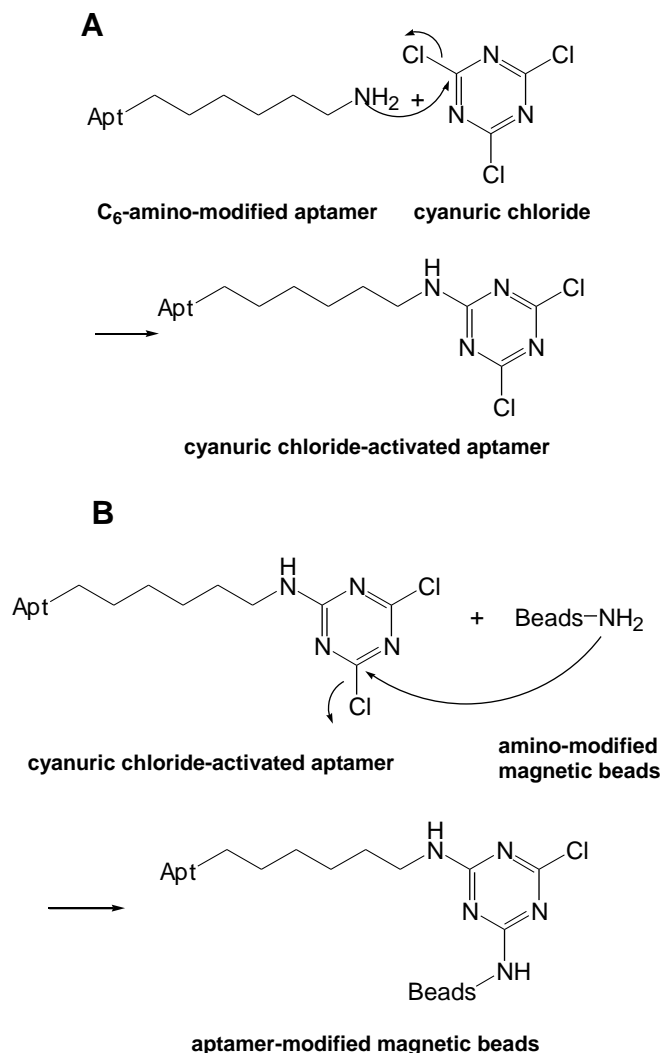


Figure 3.1.1 1: Immobilization of amino-modified aptamers to amino-modified magnetic beads via cyanuric chloride. (A) The amino-modified aptamer is activated via cyanuric chloride. (B) The activated aptamer is immobilized on amino-modified magnetic beads.

In order to investigate the functionalities of aptamers, which immobilized on amino-modified magnetic beads, via IMAC purified PFEI was utilized. Functionalities of aptamers can be interpreted via two key parameters: aptamer activity and elution efficiency. The aptamer binding activity (AA_{PFEI}) is defined as the percentage of the amount of bound PFEI divided by the amount of immobilized aptamer on the magnetic beads. The elution efficiency (EE_{PFEI}) is the percentage of the amount of eluted PFEI divided by the amount of bound PFEI. Using purified PFEI enables the determination of the amount of bound and eluted PFEI. To realize the binding between immobilized aptamers and PFEI, the correct 3D conformations of aptamers are crucial. Because aptamers can fold into their three dimensional structures correctly in the buffer, in which they were selected, before incubation PFEI with immobilized aptamers, PFEI was first transferred to the selection

buffer of corresponding aptamers. After incubation, the unspecifically bound PFEI was washed down via wash buffer, to avoid losing PFEI activity in the elution process, mild elution condition was used. According to the previous study from Koekpinar et al. [36] Imidazole was added to release the bound PFEI with more ease because of the competition between imidazole and histidine.

The amount of aptamer immobilized on the magnetic beads (D_{Apt}) was quantified as well as the amount of PFEI bound to the immobilized aptamer (Q_{PFEI}) and the amount of eluted PFEI (E_{PFEI}). The amount of immobilized aptamer 6H7 was calculated based on the Lambert-Beer equation by an extinction coefficient of $382 \text{ mM}^{-1} \text{ cm}^{-1}$ utilizing NanoDropTM 1000. The molecular weight of aptamer 6H7 is 12667 Da. The amount of bound and eluted PFEI was also calculated with the help of using NanoDropTM 1000. Due to the presence of imidazole in protein elution solutions, the determination of the absorbance of eluted PFEI by using NanoDropTM 1000 was disturbed. Therefore, dialysis was performed before the analysis to remove the contamination of imidazole from elution solutions of PFEI. Because some PFEI was losing during dialysis, another method of Bradford assay for the determination of the PFEI concentrations was carried out. Via Bradford assay, proteins could be detected colorimetrically via coomassie brilliant blue-staining. The increase of absorbance at 595 nm is the protein concentration in a solution. Bovine serum albumin (BSA) was used as reference in the concentration range of 0-200 $\mu\text{g/ml}$. [163]. Table 3.1.1 1 and Figure 3.1.1 2 show the results of the functionalities from aptamer 6H7 immobilized on amino-modified magnetic beads. Based on the publication from Kokpinar, that the amount of immobilized aptamer was saturated by applied aptamer concentration of 1500 $\mu\text{g/ml}$ and the amount of eluted PFEI was saturated by applied aptamer concentration of 1000 $\mu\text{g/ml}$ [36], the highest concentration of applied aptamer was chosen at 85 μM in this experiment, which is in accordance with 1070 $\mu\text{g/ml}$ for aptamer 6H5 and 1076 $\mu\text{g/ml}$ for aptamer 6H7. Since the functionalities of the aptamer may be weakened at high immobilization densities due to steric hindrance, the aptamer loading density was optimized by variation of aptamer concentrations (0, 25, 45 and 85 μM) during the coupling procedure, which resulted in no, low, medium and high aptamer loading. 0 μM aptamer was chosen as a negative control, which performed as non-aptamer-modified amino-magnetic beads.

Table 3.1.1 1: Characterization of aptamer 6H7 functionalities utilizing purified PFEI

c [μM] ^a	D_{Apt} ^b [pmol/mg beads]	Q_{PFEI} ^c [pmol/mg beads]	E_{PFEI} ^d [pmol/mg beads]	AA_{PFEI} ^e [%]	EE_{PFEI} ^f [%]
0		174 ± 7	69.4 ± 31		39.9 ± 48
25	491 ± 23	264 ± 4	256.3 ± 7	42.0 ± 6	97.1 ± 4
45	881 ± 25	259 ± 12	119.1 ± 5	29.4 ± 7	46.0 ± 9
85	1584 ± 20	183 ± 8	45.4 ± 1	11.6 ± 6	24.8 ± 7

^a applied aptamer concentrations during immobilization, ^b aptamer loading densities on amino-modified magnetic beads, ^c amount of bound PFEI (via IMAC purified) to immobilized aptamer, ^d amount of eluted PFEI, ^e aptamer activity ratio for PFEI ($Q_{\text{PFEI}}/D_{\text{Apt}}$), ^f elution efficiency ratio for PFEI ($E_{\text{PFEI}}/Q_{\text{PFEI}}$).

Table 3.1.1 1 shows the amount of immobilized aptamer 6H7 on the amino-modified magnetic beads, the amount of bound PFEI to immobilized aptamer 6H7, the amount of eluted PFEI and the calculated aptamer activity and PFEI elution efficiency achieved with different aptamer concentrations (0, 25, 45 and 85 μM). The data in table 3.1.1 1 displays that the aptamer concentration of 25 μM produced the highest aptamer activity and the best elution efficiency of PFEI. The amount of immobilized aptamer 6H7, the amount of bound PFEI and the amount of eluted PFEI under different aptamer concentrations are shown in the following graph (Fig.3.1.1 2).

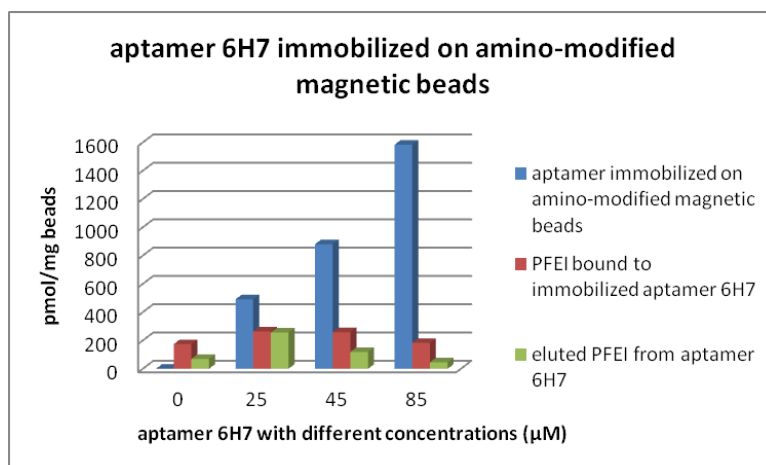
**Figure 3.1.1 2: Influence of different aptamer concentrations applied to amino-modified magnetic beads on the amount of immobilized aptamer 6H7, the amount of bound and eluted PFEI.**

Figure 3.1.1 2 shows that the amount of immobilized aptamers increased with the increment of applied aptamer concentration. The amount of bound and eluted PFEI reached maximum at aptamer concentration of 25 μM . At aptamer concentration of 0 μM ,

which means that no aptamers were applied to the amino-modified magnetic beads, an unexpected result occurred: PFEI bound directly to amino-modified magnetic beads. In order to replicate the result, PFEI from crude *E. coli* lysates was incubated with amino-modified magnetic beads without aptamer. Samples were applied to SDS PAGE gel (Fig. 3.1.1 3). At the elution fraction 1 (5), there was a clear band emerged at ca. 30 kDa (PFEI molecular weight), which was deeper and thicker than the band of the last wash fraction (4) -- a proof that PFEI bound unspecifically to the amino-modified beads. Considering the isoelectric point (PI) of PFEI is 11.562 (calculated with an online calculating editor www.isoelectric.ovh.org/files/calculate.php, based on amino acid sequences of PFEI [164]), under this condition, $PI > pH$ (7.5), PFEI act as cation. The explanation of a formed ionic interaction between PFEI and amino groups could be that the PFEI binding surface was negative charged and the beads binding site was positive charged which led to the binding of PFEI directly onto the amino-modified magnetic beads.

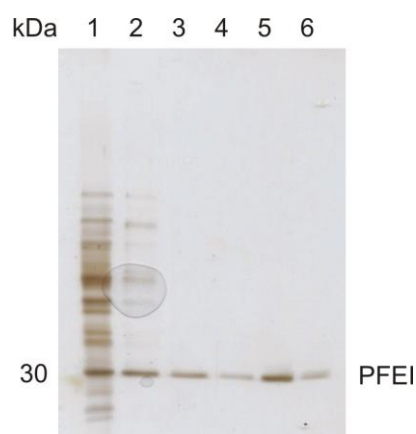


Figure 3.1.1 3: Negative control, binding of PFEI (from *E. coli* lysate) directly on amino-modified magnetic beads without aptamer. Following samples were applied: (1) supernatant of PFEI (from *E. coli* lysate) after incubation with amino-modified magnetic beads, (2-4) washing fractions, and (5-6) eluates.

To avoid the unspecific binding of PFEI directly onto the amino-modified magnetic beads, an EDC-based immobilization strategy was developed in this study. Capping was designed to transfer amino groups which coated on the magnetic beads to carboxyl groups. It was assumed that no ionic interaction between PFEI and carboxyl groups formed and thereby avoided the unspecific binding. To achieve the coupling between the capped beads and the amino-modified aptamers, EDC was used as coupling agent. Capped beads were first activated via EDC. This procedure will be discussed in the chapter 3.1.3. To modify the

amino-modified magnetic beads via capping shows a further advantage, that the using of toxic cyanuric chloride will be avoided.

3.1.2 Capping of amino-modified magnetic beads

Succinic anhydride was employed to cap the amino groups on the beads surface. The amino groups of the magnetic beads were converted to carboxyl groups with the help of dimethyl sulfoxide (DMSO) and bicarbonate. DMSO is a polar aprotic solvent that dissolves both polar and non-polar compounds and is miscible in a wide range of organic solvents as well as water. Utilizing DMSO in the capping procedure, reaction was promoted. Sodium bicarbonate was also added in the succinic anhydride solution to adjust the pH value, so that the amino groups on the beads surface could easily attach to the carbonyl groups of the succinic anhydride. Figure 3.1.2 1 shows the reaction of capping by using succinic anhydride.

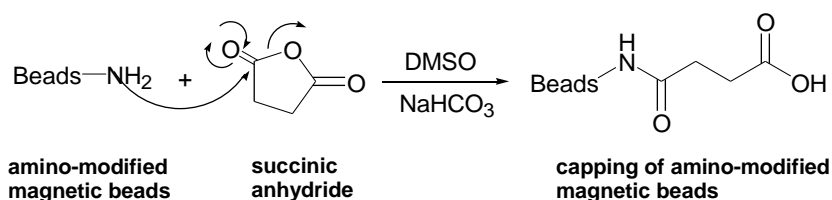


Figure 3.1.2 1: Reaction of amino-modified beads with succinic anhydride (capping).

The results showed that after capping of the amino-modified magnetic beads, amino-modified aptamer 6H7 was bound to the beads by using EDC. Comparatively, PFEI did not bind directly to the capped beads (data not shown). Capped beads, however, reduced the aptamer loading density on the surface, which resulted in low binding capacity to proteins. To explore alternative support materials, which perform the advantage of capped beads, but enhance aptamer loading capacities, the carboxyl-modified magnetic beads (BioMag[®] Carboxyl) were investigated for the aptamer-based downstream process.

3.1.3 Immobilization of aptamers on carboxyl-modified magnetic beads

It is mentioned above that EDC is generally used as a carboxyl activating agent for the coupling of primary amines. Moreover, EDC is often used in combination with *N*-Hydroxysuccinimide (NHS) to increase the coupling efficiency by creating a more reactive

ester product. Based on this theory, two methods for the immobilization of amino-modified aptamers on the carboxyl-modified magnetic beads were tested: the two-step coating procedure using EDC and NHS and the one-step coating procedure by using EDC. (The two-step and the one-step couplings were performed according to the protocol for Dynabeads[®] M-270 Carboxylic Acid with slight modifications.

<http://www.invitrogen.com/site/us/en/home/References/protocols/proteins-expression-isolation-and-analysis/protein-isolation-protocol/m-270-carboxylic-acid.html#prot2>). Via SDS PAGE (gel not shown) and calculation with the help of NanoDrop[™] 1000 spectrophotometer (data not shown), the two-step coating procedure showed poorer aptamer binding to carboxyl-modified magnetic beads than the one-step coating. Presumably the active ester was hydrolyzed before the primary amino groups of aptamers reached the active center of ester. The used two-step coating protocol needed to be modified during the aptamer immobilization. Thus the one-step coating procedure was used in the following experiments. In the one-step coating process, EDC was used as coupling agent. The EDC coupling chemistry is shown in Fig. 3.1.3 1.

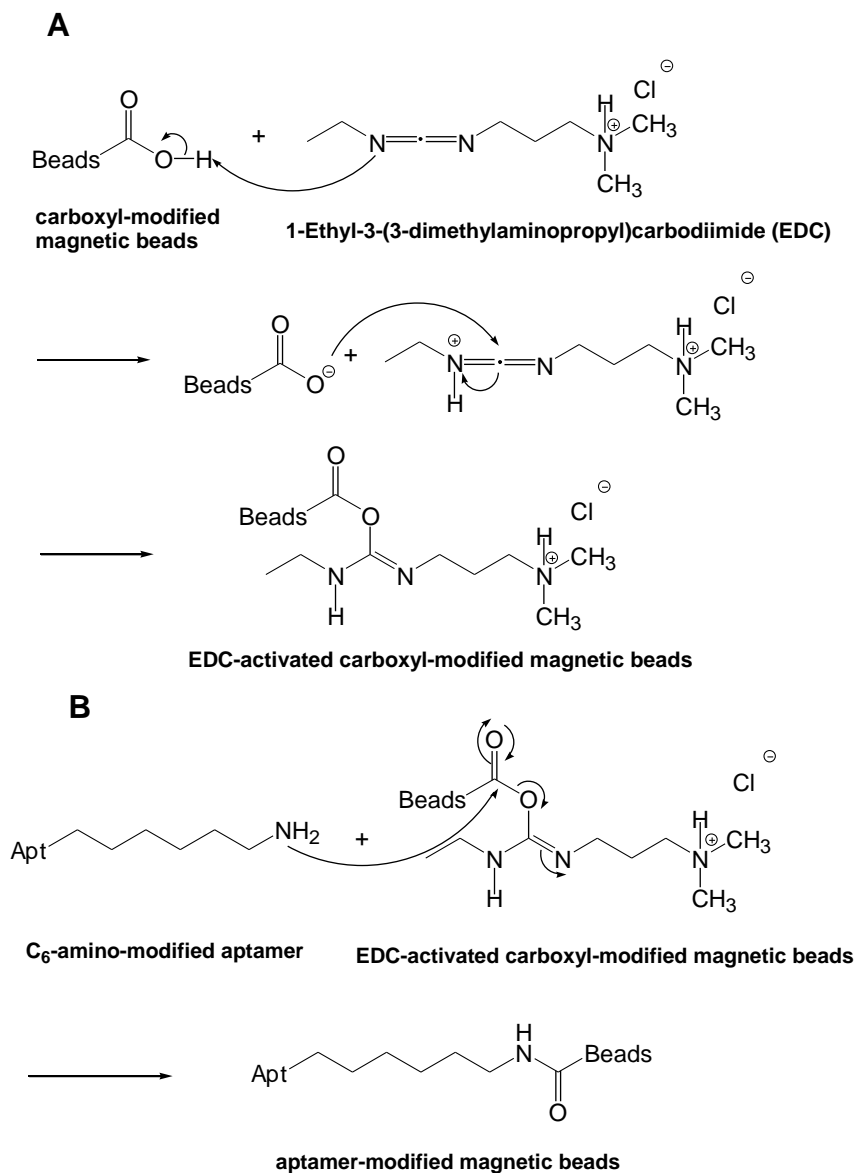


Figure 3.1.3 1: Immobilization of amino-modified aptamers to carboxyl-modified magnetic beads via EDC. (A) The carboxyl-modified magnetic beads are activated via EDC. (B) The amino-modified aptamer is immobilized on EDC-activated magnetic beads.

It was assumed that lower applied aptamer concentrations could reduce the aptamer loading density on the surface of solid supports, which resulting in low binding capacity to targets, and higher applied aptamer concentrations could interfere the aptamer folding capacity to their 3D conformation, which resulting in low aptamer activity. To optimize the performance of aptamer-modified carboxyl beads, different concentrations of aptamer 6H7 (0, 25, 50, 100 μ M) were applied to carboxyl-modified magnetic beads during the EDC-mediated coupling. 0 μ M aptamer was chosen as a negative control. Via IMAC purified PFEI was used to characterize the functionalities of aptamer-modified beads with regard to aptamer activity and elution efficiency. Results are listed out in table 3.1.3 1.

Table 3.1.3 1: Characterization of aptamer 6H7 functionalities utilizing purified PFEI

c [μM] ^a	D_{Apt} ^b [pmol/mg beads]	Q_{PFEI} ^c [pmol/mg beads]	E_{PFEI} ^d [pmol/mg beads]	AA_{PFEI} ^e [%]	EE_{PFEI} ^f [%]
0	-0.04 ± 1	-0.6 ± 3			
25	298.8 ± 7	82.9 ± 3	79.4 ± 4	27.7 ± 6	95.8 ± 9
50	429.5 ± 11	107.3 ± 4	45.8 ± 1	25.0 ± 6	42.7 ± 6
100	1166 ± 8	71.4 ± 7	27.5 ± 1	6.1 ± 10	38.5 ± 13

^a applied aptamer concentrations during immobilization, ^b aptamer loading densities on carboxyl-modified magnetic beads, ^c amount of bound PFEI (via IMAC purified) to immobilized aptamer, ^d amount of eluted PFEI, ^e aptamer activity ratio for PFEI ($Q_{\text{PFEI}}/D_{\text{Apt}}$), ^f elution efficiency ratio for PFEI ($E_{\text{PFEI}}/Q_{\text{PFEI}}$).

Table 3.1.3 1 shows the amount of immobilized aptamer 6H7 on the carboxyl-modified magnetic beads, the amount of bound PFEI to immobilized aptamer 6H7, the amount of eluted PFEI, the calculated aptamer binding activity and PFEI elution efficiency under different concentrations of aptamer 6H7 (0, 25, 50 and 100 μM) applied during the EDC-based aptamer immobilization. At aptamer concentration of 25 μM , the highest aptamer binding activity and elution efficiency were reached. The highest aptamer binding activity, however, was only approximately 28%. This could be caused by the high K_d value of the anti-his-tag aptamer. The aptamer binding activities went down with the increase of immobilized aptamer, these rather low aptamer binding activities may also be a result of steric hindrance due to too high dense immobilization. This finding supports the assumption that increase of aptamer density decrease of aptamer binding activity. Figure 3.1.3 2 graphed the influence of different aptamer concentrations applied to carboxyl-modified magnetic beads on the amount of immobilized aptamer 6H7, the amount of bound and eluted PFEI.

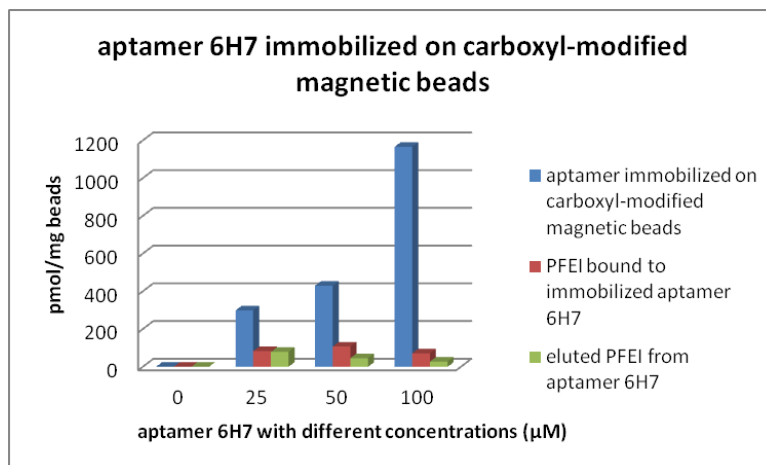


Figure 3.1.3 2: Influence of different aptamer concentrations applied to carboxyl-modified magnetic beads on the amount of immobilized aptamer 6H7, the amount of bound PFEI and eluted PFEI.

In Figure 3.1.3 2, the amount of immobilized aptamers went up with the increase of applied aptamer concentrations. The amount of bound PFEI reached a maximum at aptamer concentration of 50 μM. However, the most eluted PFEI was reached at aptamer concentration of 25 μM. The highest amount of bound PFEI at aptamer concentration of 50 μM could be explained due to the higher aptamer immobilization density. However, at very high aptamer concentration (100 μM), due to extremely reduced aptamer binding activity, aptamers are no longer able to bind properly with their targets. The explanation of most eluted PFEI appeared at aptamer concentration of 25 μM is probably because imidazole can reach the aptamer binding site more easily under this aptamer-loading density on the surface of the supports. At aptamer concentration of 0 μM, there was no aptamer applied to carboxyl-modified beads, resulting in no bound and eluted PFEI. This absence of unspecific binding of PFEI to carboxyl-modified magnetic beads was confirmed by gel electrophoresis (Fig. 3.1.3 3). There was no bands emerged at 30 kDa in eluates (6 and 7), which clearly demonstrated that the binding of the target is based on the affinity of the aptamer. By using carboxyl-modified magnetic beads avoided the unspecific binding of PFEI when utilizing amino-modified beads and improved the poor aptamer loading density when using the capped beads.

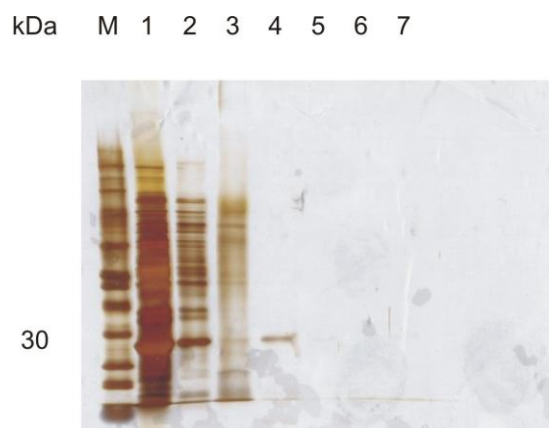


Figure 3.1.3 3: Negative control, binding of PFEI (from *E. coli* lysate) directly on carboxyl-modified magnetic beads without aptamer. Following samples were applied: (M) molecular weight marker, (1) PFEI (from *E. coli* lysate) sample applied to carboxyl-modified magnetic beads, (2) supernatant of PFEI (from *E. coli* lysate) after incubation with carboxyl-modified magnetic beads, (3-5) washing fractions, and (6-7) eluates.

3.1.3.1 Comparison of aptamer functionalities between aptamer 6H7 and 6H5 utilizing carboxyl-modified beads

In order to find out the relation between aptamer types and their performance on the same carrier, aptamer 6H5 was tested and compared with aptamer 6H7. With the help of NanoDropTM spectrophotometer, the amount of immobilized aptamer 6H5 was calculated based on the Lambert-Beer equation by an extinction coefficient of $373 \text{ mM}^{-1}\text{cm}^{-1}$, while the extinction coefficient of aptamer 6H7 is $382 \text{ mM}^{-1}\text{cm}^{-1}$, as mentioned in the previous section. The molecular weight of aptamer 6H5 is 12598 Da. All determinations were analyzed for three times. The average values were used for the comparison. Three different concentrations (10, 25 and 40 μM) of each aptamer were investigated. The concentration of 10 μM was chosen in order to investigate the previous assumption of a decreased aptamer binding activity due to too high aptamer loading density when using an aptamer concentration of 25 μM . Carboxyl-modified magnetic beads were used as solid supports and via IMAC purified PFEI was used for the determination of aptamer functionalities. Results are listed out in table 3.1.3.1 1.

Table 3.1.3.1 1: Comparison of aptamer functionalities between aptamer 6H7 and 6H5 utilizing purified PFEI

c [μM] ^a	D_{Apt} ^b [pmol/mg beads]	Q_{PFEI} ^c [pmol/mg beads]	E_{PFEI} ^d [pmol/mg beads]	AA_{PFEI} ^e [%]	EE_{PFEI} ^f [%]
Apt6H7(10 μM)	157 \pm 13	154.7 \pm 1.4	46.6 \pm 0.3	98.5 \pm 9.2	30.2 \pm 1.5
Apt6H7(25 μM)	501 \pm 42	168.5 \pm 1.5	163.7 \pm 0.8	33.6 \pm 9.2	97.1 \pm 1.3
Apt6H7(40 μM)	1037 \pm 39	213.7 \pm 1.8	98.1 \pm 0.1	20.6 \pm 4.6	45.9 \pm 0.9
Apt6H5(10 μM)	263 \pm 32	244.2 \pm 2	84.4 \pm 0.2	92.9 \pm 13	34.6 \pm 1
Apt6H5(25 μM)	619 \pm 29	276.1 \pm 1.5	233.8 \pm 0.4	44.6 \pm 5.2	84.7 \pm 0.7
Apt6H5(40 μM)	875 \pm 27	358.4 \pm 1.5	146.1 \pm 0.3	40.9 \pm 3.5	40.8 \pm 0.6

^a applied aptamer concentrations during immobilization, ^b aptamer loading densities on carboxyl-modified magnetic beads, ^c amount of bound PFEI (via IMAC purified) to immobilized aptamer, ^d amount of eluted PFEI, ^e aptamer activity ratio for PFEI ($Q_{\text{PFEI}}/D_{\text{Apt}}$), ^f elution efficiency ratio for PFEI ($E_{\text{PFEI}}/Q_{\text{PFEI}}$).

Table 3.1.3.1 1 shows at aptamer concentration of 10 μM , the highest aptamer binding activities were reached. This confirms the finding that aptamer concentrations of 25 μM resulted in high immobilization densities that interfered with high aptamer activity. However, the elution efficiencies at aptamer concentration of 10 μM were very low. The low elution efficiencies were attributed to the unspecific bound PFEI among neighbouring immobilized aptamers. Although the amount of bound PFEI at aptamer concentration of 10 μM was as high as at 25 μM , it seemed that the unspecific bound PFEI among neighbouring aptamers could neither be washed down entirely during the washing steps nor be eluted sufficiently during the elution steps. This effect occurred probably because of the low aptamer cover on the surface of supports, which enables the unspecific protein loading among neighboring aptamers. On the other hand, the highest PFEI elution efficiencies were achieved when using aptamer concentration of 25 μM . At this concentration, imidazole as competitor seemed to reach the aptamer binding site easily and released his-tagged protein PFEI very efficiently. The amount of immobilized aptamer 6H7 and 6H5, the amount of bound and eluted PFEI are shown in Figure 3.1.3.1 1.

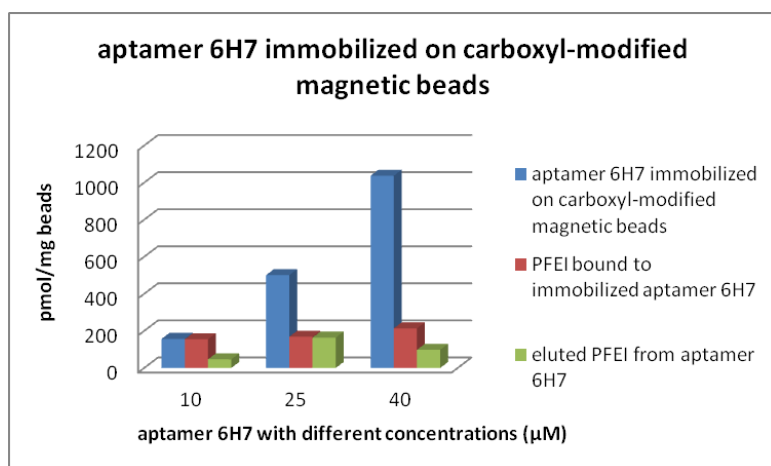
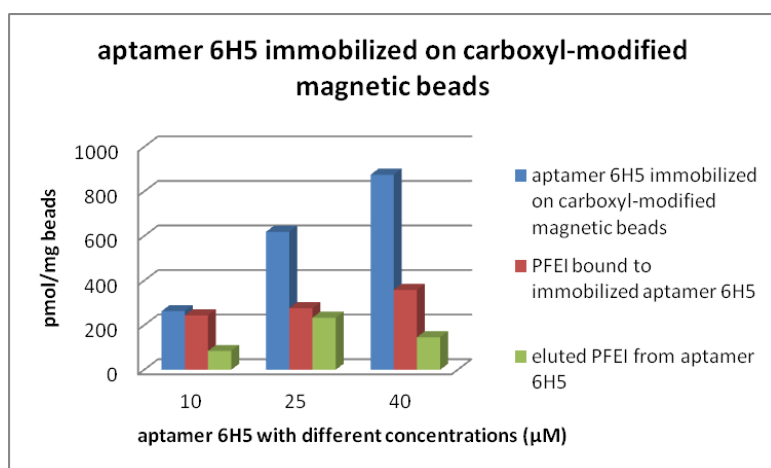
A**B**

Figure 3.1.3.1 1: Comparison of aptamer functionalities between aptamer 6H7 and 6H5 on carboxyl-modified magnetic beads. (A): aptamer 6H7 immobilized on carboxyl-modified magnetic beads; (B): aptamer 6H5 immobilized on carboxyl-modified magnetic beads.

Figure 3.1.3.1 1 shows the functionalities of aptamer 6H7 and aptamer 6H5. Regarding to the immobilization tendency, aptamers 6H7 and 6H5 performed similar. For both types of aptamer, increasing of applied aptamer concentration increased the amount of immobilized aptamers on carboxyl-modified magnetic beads, which resulted in increased amount of bound PFEI. The amount of bound PFEI reached the peak at aptamer concentration of 40 μM, while the largest amount of eluted PFEI was found at aptamer concentration of 25 μM. The reduced amount of eluted PFEI at aptamer concentration of 40 μM is probably because that imidazole could reach aptamer binding site difficultly under higher aptamer density. In this experiment, the highest aptamer activities were reached at aptamer concentration of 10 μM, with a value of over 90%, almost each aptamer binding PFEI and

folding into their 3D structures. But the aptamer cover on the surface was not saturated. The highest PFEI elution efficiency was achieved at aptamer concentration of 25 μM (Table 3.1.3.1 1). In conclusion, the aptamer concentration of 25 μM displayed the optimal results of PFEI purification by using carboxyl-modified magnetic beads. At this concentration, a reasonable compromise between binding capacity of the aptamer-modified magnetic beads and the aptamer binding activity was found. The types of the aptamer (6H5 versus 6H7) seemed to have a little impact on aptamer performance in this case. By using aptamer 6H5, the amount of bound and eluted PFEI was more than that by using aptamer 6H7. To find out more information of the performance between aptamer 6H5 and 6H7, this experiment was repeated by using crude PFEI from *E. coli* lysate. Samples of aptamer 6H5- and 6H7-based PFEI purification from *E. coli* lysate were analysed via SDS PAGE analysis (Figure 3.1.3.1 2). The applied concentrations of aptamer 6H5 and 6H7 were 25 μM . Only slight difference was observed. More unspecific bound PFEI was found in the washing fractions by using 6H7 than 6H5. To summarize, aptamer 6H5 performed better than 6H7 in the purification of PFEI utilizing carboxyl-modified magnetic particles, which indicated higher binding affinity of aptamer 6H5 to targets when compared with aptamer 6H7.

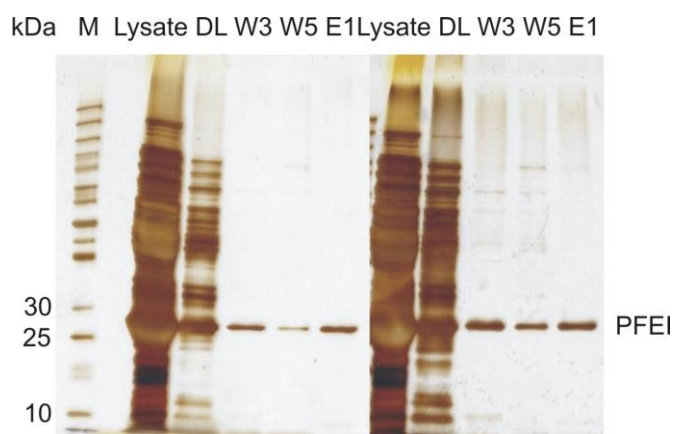


Figure 3.1.3.1 2: Comparison of aptamer functionalities between aptamer 6H5 (left) and 6H7 (right) with concentration of 25 μM on carboxyl-modified magnetic beads. Following samples were applied: (M) molecular weight marker, (Lysate) PFEI (from *E. coli* lysate) sample applied to aptamer-modified magnetic beads, (DL) supernatant of PFEI (from *E. coli* lysate) after incubation with aptamer-modified magnetic beads, (W3, W5) washing fractions, and (E1) eluate.

3.1.3.2 Comparison of aptamer functionalities by using different types of beads

Besides the carboxyl-modified magnetic particles mentioned above, taking into account, whether some other alternatives, which could be used as solid supports in the aptamer-

based downstream processes and probably show more advantages when compared with carboxyl-modified magnetic beads? It was informed by purchasing that the maxi-carboxyl-beads have more functional groups and higher binding capacity than the normal-carboxyl-beads. Thus, maxi-carboxyl-beads were employed to compare with the normal-carboxyl-beads, which were used in the aforementioned experiments. During the investigation, first, same aptamer 6H7s with concentration of 25 μM were immobilized on both of these carboxyl-modified beads. With the help of NanoDropTM 1000 spectrophotometer, 617.8 pmol aptamer per mg beads were found on the normal-carboxyl-beads and 680.7 pmol aptamer per mg beads were detected on the maxi-carboxyl-beads. The difference was not significant, which could be attributed to the saturation of the aptamer. Therefore, aptamer 6H7s with concentration of 100 μM were tested and 871.9 pmol/mg beads aptamer were found on the normal-carboxyl-beads and 1036.3 pmol/mg beads aptamer on the maxi-carboxyl-beads. The results showed that maxi-carboxyl-beads were able to bind more aptamers. To further investigate the impact of beads type on aptamer purification efficiency, aptamer 6H7s with concentration of 100 μM and PFEI from *E. coli* lysate were used for the testing. Samples were examined via SDS PAGE analysis. No difference in purification was observed in the SDS PAGE gel (Fig. 3.1.3.2 1). It can be concluded that the types of beads did not affect the aptamer-based purification efficiency in the same beads concentration. In the following experiments, normal-carboxyl-beads were used further as solid supports.

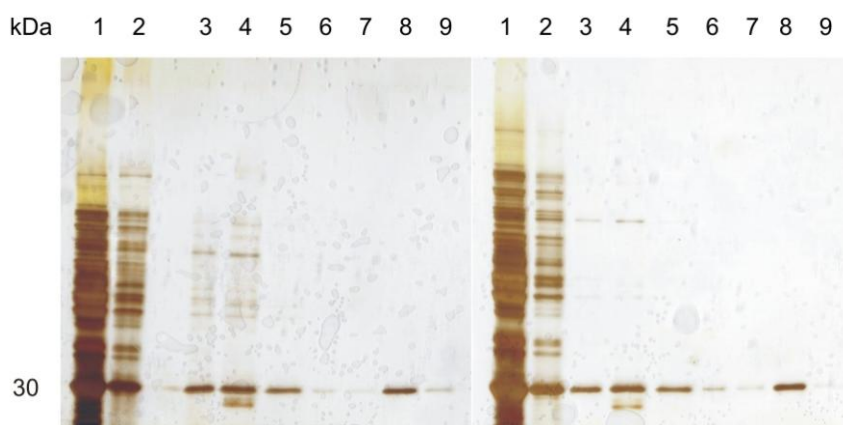


Figure 3.1.3.2 1: Comparison of aptamer functionalities between maxi-carboxyl-beads (left) and normal-carboxyl-beads (right) utilizing 100 μM aptamer 6H7. Following samples were applied: (1) PFEI (from *E. coli* lysate) sample applied to aptamer-modified magnetic beads, (2) supernatant of PFEI (from *E. coli* lysate) after incubation with aptamer-modified magnetic beads, (3–7) washing fractions, and (8-9) eluates.

3.1.4 Aptamer-based automatic purification utilizing a robot

All previous experiments were performed manually. Automation is advantageous with regard on throughput as well as precision. The KingFisher device was chosen as a robot for the automatic purification process. First, the aptamer immobilization, protein binding and elution processes were programmed via corresponding KingFisher software. Afterwards, all samples with 100 μ l (20 mg/ml carboxyl-modified magnetic beads, 25 μ M aptamer 6H5 solutions, 1 mg/ml PFEI from *E. coli* lysate, washing, elution, and aptamer selection buffers) were added into a 96 well plate, which was packed into the KingFisher device before the program was run. The same purification process in manual performance was conducted in automation. The results are displayed via SDS PAGE analysis (Fig. 3.1.4 1).

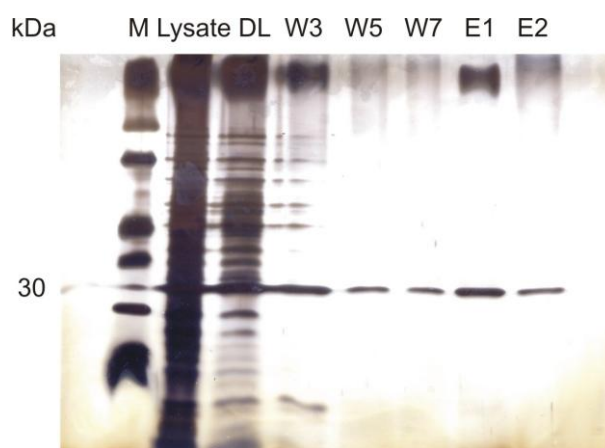


Figure 3.1.4 1: Aptamer 6H5 (25 μ M)-based PFEI automatic purification via KingFisher. Following samples were applied: (M) molecular weight marker, (Lysate) PFEI (from *E. coli* lysate) sample applied to aptamer-modified magnetic beads, (DL) supernatant of PFEI (from *E. coli* lysate) after incubation with aptamer-modified magnetic beads, (W3, W5 and W7) washing fractions, and (E1-E2) eluates.

Even after 7 washing steps, PFEI was washed down from the aptamer-beads-matrix. These appearances could be suspected that the automatic operation was performed at room temperature and the binding between aptamer and target was impaired at higher temperature, which led to the releasing from binding partner. It was difficult to provide an opportunity to fulfil the automatic process at 4 $^{\circ}$ C, as the KingFisher robot must be controlled by computer, in which the corresponding software was installed. To test this hypothesis that aptamers and targets impaired due to room temperature, the same experiment was performed at 4 $^{\circ}$ C manually. The results are shown in Fig. 3.1.4 2.

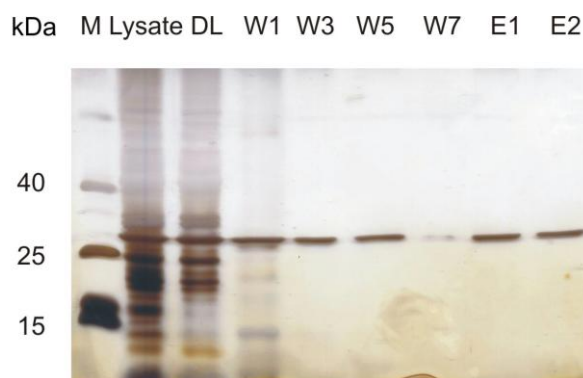


Figure 3.1.4 2: Aptamer 6H5 (25 μ M)-based PFEI manually purification at 4°C. Following samples were applied: (M) molecular weight marker, (Lysate) PFEI (from *E. coli* lysate) sample applied to aptamer-modified magnetic beads, (DL) supernatant of PFEI (from *E. coli* lysate) after incubation with aptamer-modified magnetic beads, (W1-W7) washing fractions, and (E1-E2) eluates.

In the gel analysis, little PFEI released during the last washing step. The purity degree of both eluates was 100%, as determined by densitometry.

To summarize, in order to enable the automated aptamer-based purification, KingFisher was introduced in this study for the aptamer-based PFEI purification utilizing carboxyl-modified magnetic beads. The results were not as good as that by manual, as aptamers and targets impaired during the downstream process. It could be that the binding affinity between aptamers and PFEI is low in the room temperature. It is recommended that these experiments be run in the cooling chamber at 4°C in the further.

3.1.5 Aptamer-based purification of his-tagged HLA utilizing carboxyl-modified magnetic beads

PFEI was utilized as a model protein to determine the functionalities of immobilized aptamers directed against his-tag. In order to examine the general applicability of the developed purification strategy, his-tagged human leukocyte antigen (HLA) was used. HLA consists of a heavy chain (40 kDa) and a light chain (12 kDa). The aptamer 6H5-based purification of HLA via carboxyl-modified magnetic beads was investigated. The purification process for HLA is generally the same as for PFEI. However, because HLA is relatively sensible to salt, salt was avoided in washing buffer. Thus, the selection buffer, which was used for aptamer selection was used as washing buffer. Similar to PFEI, before the incubation with immobilized aptamers, HLA was first transferred to the selection buffer.

Fig. 3.1.5 1 shows the SDS PAGE gel of the aptamer 6H5 (25 μ M)-based HLA purification utilizing carboxyl-modified magnetic beads.

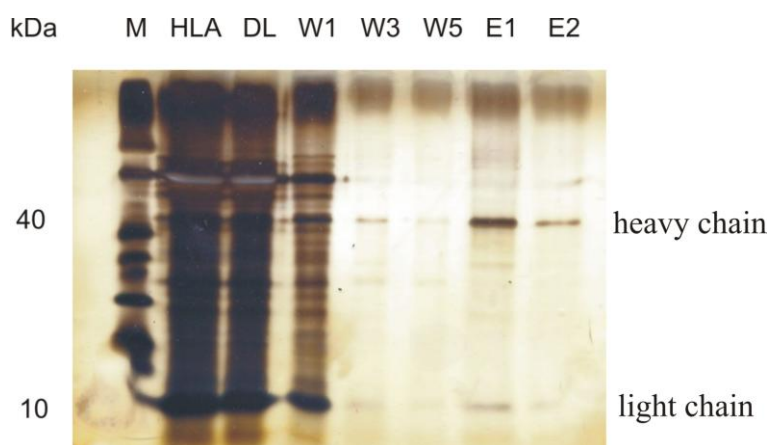


Figure 3.1.5 1: Aptamer 6H5 (25 μ M)-based HLA purification by using carboxyl-modified magnetic beads. Following samples were applied: (M) molecular weight marker, (HLA) HLA (from cell-culture supernatant) sample applied to aptamer-modified magnetic beads, (DL) supernatant of HLA (from cell-culture supernatant) after incubation with aptamer-modified magnetic beads, (W1–W5) washing fractions, and (E1-E2) eluates.

In both eluates E1 and E2, two bands were discovered. At 40 kDa were heavy chains and over 10 kDa were light chains of HLA. With a little contamination at the very beginning of the running gel, the purity degree of the first eluate reached 85.2%, as determined by densitometry.

3.1.6 Conventional IMAC-based downstream process by using his-select nickel magnetic agarose beads

The aforementioned successful purification of his-tagged proteins utilizing aptamer-modified magnetic beads confirmed the applicability of aptamers in the application of downstream processes. Because aptamers exhibit several advantages over conventional methods, comparative experiments between aptamer-based methods and conventional methods were considered and carried out. Conventionally, his-tagged proteins are purified via immobilized metal chelate affinity chromatography (IMAC). Here, the affinity of different transition metal ions towards histidine is exploited to purify the protein. The IMAC method shows disadvantages. First, a part of used metal ions from this nickel magnetic agarose beads are carcinogens [36]. Secondly, because the metal ions are complexed on the surface of material, the metal ligand could be leached from the column

during the purification process. This problem could be solved via the developed aptamer-based downstream process. Since aptamers are covalently immobilized on the solid supports, they will not be leached during the purification procedure. To compare the purification obtained via aptamer-modified magnetic beads, his-select nickel magnetic agarose beads were used to purify PFEI from *E. coli* lysate. PFEI from lysate was first diluted in PBST-6H7 + 20 mM imidazole buffer to 1 mg/ml and then incubated with his-select nickel agarose beads. Specific bound proteins were eluted with increased imidazole concentration of 250 mM. Different fractions of this separation were analyzed via SDS-PAGE analysis (Fig. 3.1.6 1). The purity degree was 99%, as determined by densitometry.

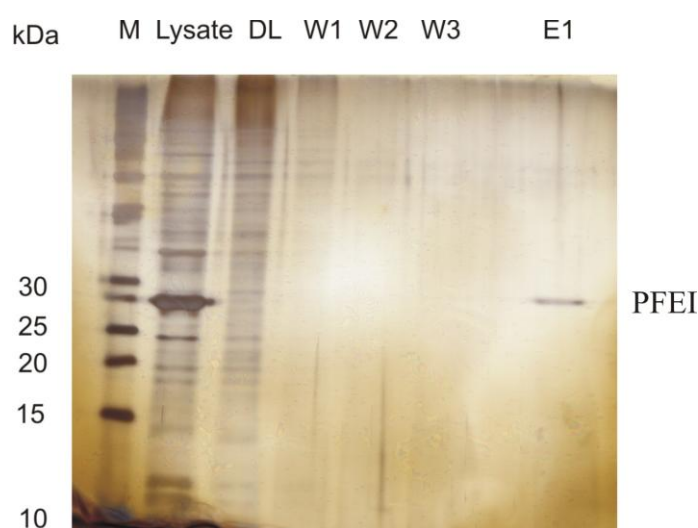


Figure 3.1.6 1: Purification of PFEI from *E. coli* lysate utilizing his-select nickel magnetic agarose beads (IMAC). Following samples were applied: (M) molecular weight marker, (lysate) PFEI (from *E. coli* lysate) sample applied to his-select nickel magnetic agarose beads, (DL) supernatant of PFEI (from *E. coli* lysate) after incubation with his-select nickel magnetic agarose beads, (W1-W3) washing fractions, and (E1) eluate.

Compared with Fig. 3.1.4 2, in which the purity degree of PFEI by using aptamer 6H5 was 100%, the purity degree of 99% utilizing IMAC method showed little difference. The similar purity degrees indicate that aptamer-based purification technology is a good alternative to conventional IMAC method. Taking into account, using aptamers in the downstream process for his-tagged proteins can overcome the disadvantages by using IMAC method. Therefore, aptamer-based downstream process shows great potential to replace the conventional method, especially in the biomedical applications.

All experiments above showed that magnetic beads could be successfully used in the aptamer-based downstream process for his-tagged proteins. Although biomolecules can be

quickly and easily extracted via magnetic particles, it is very difficult to scale-up the aptamer-based downstream processes by using them, which limited the application in the industry in future. In order to provide a possibility to expand the production, some other materials were considered for the immobilization of aptamers. Sepharose is commonly used in chromatographic separations of biomolecules. It is an excellent base matrix for high performance chromatographic procedures in different kinds of chromatographies and other modes of separation. Therefore NHS-activated Sepharose 4 fast flow was chosen and tested as a further solid support.

3.1.7 Scal-up via binding of aptamers on NHS-modified Sepharose

Amino-modified aptamers could bind directly on NHS-modified Sepharose. The binding mechanism is shown in Fig. 3.1.7 1. Because NHS-functional groups lead to a self-signal, they disturb the measurement of aptamers' absorbance at 260 nm, the absorbance of aptamers during the immobilization on Sepharose could thereby not be determined via NanoDrop™ 1000. The analysis was then performed via developed propidium iodide (PI) assay. The performances of aptamers, which were immobilized on NHS-modified Sepharose were investigated first utilizing via IMAC purified PFEI. The results are listed in table 3.1.7 1.

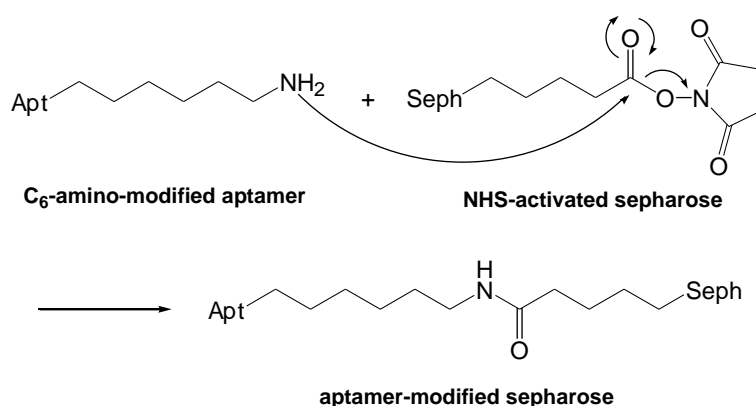


Figure 3.1.7 1: Aptamer immobilization on the NHS-activated Sepharose 4 fast flow.

Table 3.1.7 1: Characterization of aptamer 6H5 functionalities immobilized on sepharose utilizing purified PFEI

c [μM] ^a	D _{Apt} ^b [pmol/200 μl sepharose]	Q _{PFEI} ^c [pmol/200 μl sepharose]	E _{PFEI} ^d [pmol/200 μl sepharose]	AA _{PFEI} ^e [%]	EE _{PFEI} ^f [%]
25	5130 \pm 3	1385.2 \pm 4	344.8 \pm 2	27.0 \pm 1	24.9 \pm 1

^a applied aptamer concentration during immobilization, ^b aptamer loading density on NHS-modified sepharose, ^c amount of bound PFEI (via IMAC purified) to immobilized aptamer, ^d amount of eluted PFEI, ^e aptamer activity ratio for PFEI ($Q_{\text{PFEI}}/D_{\text{Apt}}$), ^f elution efficiency ratio for PFEI ($E_{\text{PFEI}}/Q_{\text{PFEI}}$).

Table 3.1.7 1 shows the amount of immobilized aptamer 6H5 (25 μM) on sepharose, the amount of bound PFEI on immobilized aptamer, the amount of eluted PFEI, the calculated aptamer binding activity and the PFEI elution efficiency. The low aptamer binding activity of only 27% was occurred probably because sepharose is a pore material, aptamers immobilized within the sepharose pores were hindered in their optimal folding, which led to less specific binding of PFEI. The low PFEI elution efficiency might be caused by the PFEI diffusion in pores of sepharose. Longer elution time or more elution steps may be required to account for diffusion processes within the particles. To determine the purification efficiency, the same experiment was repeated by using PFEI from crude *E. coli* lysates. The SDS PAGE gel is shown in Fig. 3.1.7 2. The purity degree of the first eluate was 97.5%, as determined by densitometry.

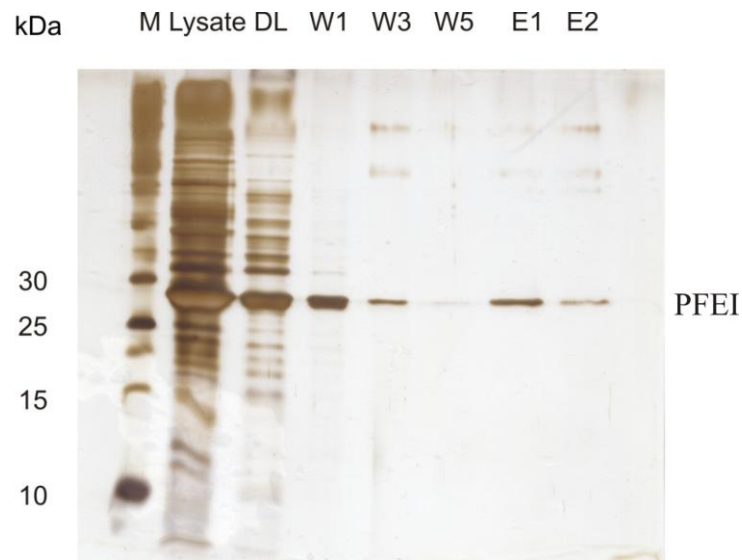


Figure 3.1.7 2: Aptamer 6H5 (25 μ M)-based PFEI (from *E. coli* lysate) purification by using NHS-modified sepharose. Following samples were applied: (M) molecular weight marker, (Lysate) PFEI (from *E. coli* lysate) sample applied to aptamer-modified sepharose, (DL) supernatant of PFEI (from *E. coli* lysate) after incubation with aptamer-modified sepharose, (W1–W5) washing fractions, and (E1–E2) eluates.

In addition to PFEI, HLA was also tested for the aptamer-based scale-up downstream process. Due to HLA’s sensitivity to salt, washing was performed in the aptamer selection buffer.

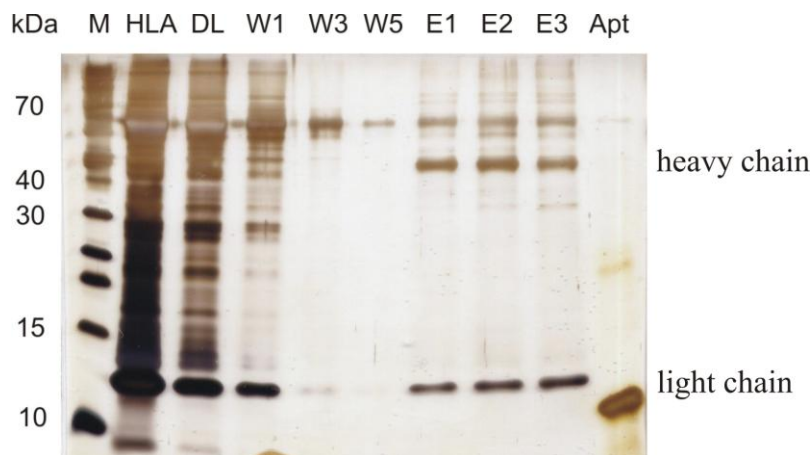


Figure 3.1.7 3: Aptamer 6H5 (25 μ M)-based HLA (from cell-culture supernatant) purification by using NHS-modified sepharose. Following samples were applied: (M) molecular weight marker, (HLA) HLA (from cell-culture supernatant) sample applied to aptamer-modified sepharose, (DL) supernatant of HLA (from cell-culture supernatant) after incubation with aptamer-modified sepharose, (W1–W5) washing fractions, (E1–E3) eluates, and (Apt) aptamer 6H5 (25 μ M).

Fig. 3.1.7 3 shows the gel of aptamer 6H5-based HLA purification utilizing NHS-activated sepharose. After two elution steps, there was still a lot of HLA bound to the immobilized

aptamer 6H5. The sepharose-aptamer-HLA complex was then incubated in Laemmli buffer. The sample was applied to the gel as third elution fraction. SDS PAGE analysis confirmed incomplete elution of HLA after two elution steps. It is presumable that sepharose is a porous media and diffusion processes within the material may require longer processing time. In the future, either the elution time needs to be extended or the elution steps need to be increased. In the elution fractions, HLA was detected with contaminations of BSA (see Fig. 3.1.7 3, by 66.5 kDa). Sample of applied aptamer 6H5 (25 μ M) was also applied in this gel to distinguish the light chain of HLA. It was displayed in gel, that the bands by 12 kDa were actually the HLA light chains. They are not bands of aptamers leached from the sepharose. The purity degree of the first elution fraction by utilizing sepharose was 74.1%, as determined by densitometry.

To summarize, positive results were shown by aptamer-based his-tagged protein purifications. Different aptamers (6H5 and 6H7) were immobilized on different material (magnetic beads and sepharose) and successfully used for the purification of different his-tagged proteins (PFEI and HLA). Furthermore, aptamer-based purification experiments resulted in similar purification efficiency to conventional his-select nickel agarose beads. Nevertheless, the developed purification strategies are only applicable to the isolation of his-tagged proteins. The next chapter of this thesis will describe the development of an aptamer-based purification of F_c fragment and human IgGs.

3.2 Aptamer-based purification of F_c fragment and IgGs

Conventionally, protein A was used for the purification of antibodies. Aptamers were used in this study to test their applicability in the downstream processes for antibodies. In the purification of compounds that are used in pharmaceutical fields, aptamers show several advantages over protein A. First, Due to their *in vitro* production, contaminations with viruses are avoided. Thus, the production of aptamers in compliance with current good manufacturing practice is simplified. Secondly, aptamers have minimal propensity to elicit an antibody response [165]. This is especially advantageous in the downstream process of pharmaceutical antibodies, where the leakage of immunogenic protein A from the chromatographic device is a major concern necessary additional purification steps. Third, besides their lack of immunogenicity, aptamers that may have leaked from the column can be easily removed in the DNA removal step that is essential for the purification of pharmaceutical antibodies. Based on the non-immunogenicity of aptamers, their animal-free and chemical synthesis, the developed aptamer-based downstream processes are especially useful for the purification of pharmaceutical antibodies.

DNA aptamers 264, 265 and 266 against F_c fragment and IgGs as well as aptamer 264 with integrated-spacer PEG6 against IgGs were used in this study. In a previous publication, it was reported that human IgG was successfully purified from cell culture supernatant via an RNA aptamer [148]. In contrast to the work from Miyakawa et al. [148], DNA aptamers, which selected from a MonoLex process for the purification of F_c fragment and IgG were investigated for the first time in this study. These selected DNA aptamers show two main advantages over RNA aptamers, that is, they are more stable and cheap. In order to generate divalent ions dependent aptamers with 3D conformations, aptamers were selected in a buffer containing Mg²⁺ and Ca²⁺. This approach was chosen to enable the destruction of the 3D structures with chelating agents as a potential strategy for the mild elution of bound proteins. This mild elution condition described by Roming et al. [129] is contrary to the harsh acidic elution condition required for protein A-based purifications, which enables aptamer as strongly competitive alternative to protein A in the downstream process.

3.2.1 Immobilization of aptamers on magnetic beads

According to the published literature [36], an aptamer-based purification method for his-tagged proteins utilizing amino-modified magnetic beads was tested in the aforementioned chapter of this work. It was introduced in chapter 3.1.1 that aptamer 6H7 was activated via cyanuric chloride and consequently immobilized onto amino-modified magnetic beads. This method was transferred to aptamers directed against human IgG as a cornerstone. A gentle elution process was developed and performed via adding 300 mM chelating agent EDTA to remove divalent ions and thereby destroy the aptamers' 3D structure. The successful results of binding and elution of human IgG were demonstrated in Fig. 3.2.1 1A. This verified activities of immobilized aptamer and confirmed that the folding of aptamer's 3D structure depends on divalent ions. The possibility of regenerating aptamer-modified magnetic beads was also investigated. Regeneration of the aptamers could be achieved by washing and incubation with the selection buffer (Fig.3.2.1 2). After immobilization, the aptamer (blue) was folded into their three-dimensional structure by incubation them in the selection buffer including divalent ions. The target could be eluted by EDTA-induced unfolding of the aptamer. The aptamer-modified magnetic beads could be stored at 4 °C and then be used repeated for 3 times without losing aptamer functionalities.

In complex IgG samples containing 10% fetal calf serum (FCS), unspecific binding of BSA to aptamer-modified magnetic beads was observed (Fig. 3.2.1 1B). Also observed was a rather low utilization of the applied aptamer. Only 19% of the applied aptamer were immobilized on the amino-modified particle surface when using 25 μ M aptamer during the immobilization. This low efficiency may be attributed to either incomplete activation of the aptamer or by hydrolysis of the activated aptamer. It is also known, that amino-modified surfaces may interact electrostatically with the phosphate backbone of aptamers which will result in misfolding and reduced binding activity of immobilized aptamer [122].

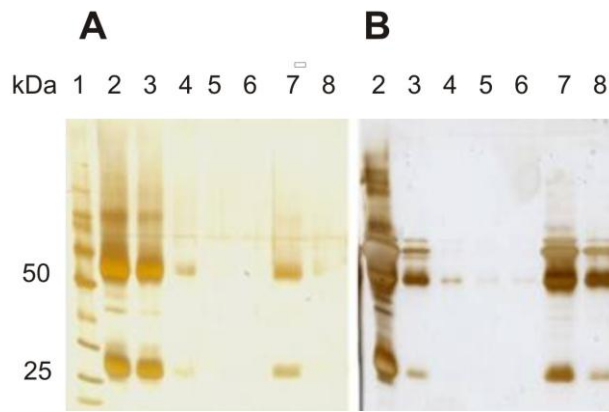


Figure 3.2.1 1: Binding studies utilizing pure human IgG (A) and human IgG supplemented with 10% 1 mg/ml FCS (B). Following samples were applied: (1) molecular weight marker, (2) IgG samples applied to aptamer-modified amino magnetic beads, (3) supernatant of IgG samples after incubation with aptamer-modified amino magnetic beads, (4-6) washing fractions, and (7-8) eluates.

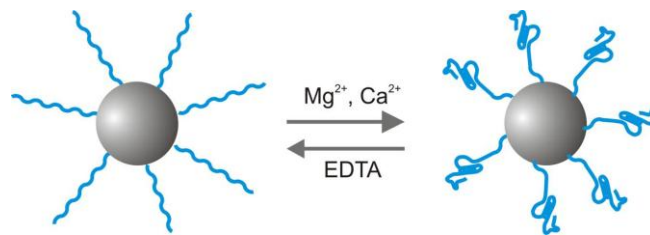


Figure 3.2.1 2: Schematic regeneration of aptamer-modified magnetic beads.

To overcome the limitations by using aptamers immobilized on amino-modified magnetic beads, an EDC-based immobilization strategy by using carboxyl-modified magnetic beads was used in the following researches. This developed method increased aptamer immobilization efficiency. Aptamer 264, 265, 266 were tested for the immobilization and binding with corresponding targets. Because aptamer 264 showed the best functionalities to their targets (data not shown), the following discussion only involves aptamer 264.

3.2.2 Optimization of aptamer activity and binding capacity

As aptamer binding activity ratio (AA) was defined as the the amount of bound protein divided by the amount of immobilized aptamers on the solid supports, it described the amount of appropriately immobilized aptamers that maintain binding property upon immobilization. It was found in the aforementioned chapter for aptamer-based purification of his-tagged protein that decreasing the amount of immobilized aptamer could provide more space for aptamers to fold correctly and thereby increase aptamer binding activity. On the other hand, a decrease of aptamer loading density may result in reduced binding

capacity because not enough aptamers exist to bind to their targets. It was also verified that higher amount of immobilized aptamer could reduce aptamer binding activity, because aptamers folding into their 3D structures might be interfered by steric or electrostatic hindrance due to neighboring aptamers. In order to achieve high binding activity of immobilized aptamers, as well as high binding capacity, the procedure was optimized with regard to the amount of immobilized aptamer. In this study, several different concentrations of aptamer 264 (0, 5, 10, 25, 50, 75, 100 μM) were tested during the immobilization (Fig. 3.2.2 1), 0 μM aptamer 264 was chosen as a negative control and 100 μM was chosen as the amount of immobilized aptamer was presumably saturated under this concentration.

Figure 3.2.2 1 shows that the amount of immobilized aptamer increased with increasing of applied concentration of aptamer until the level of 50 μM , where a maximum aptamer loading of approximately 1200 pmol/mg beads was reached.

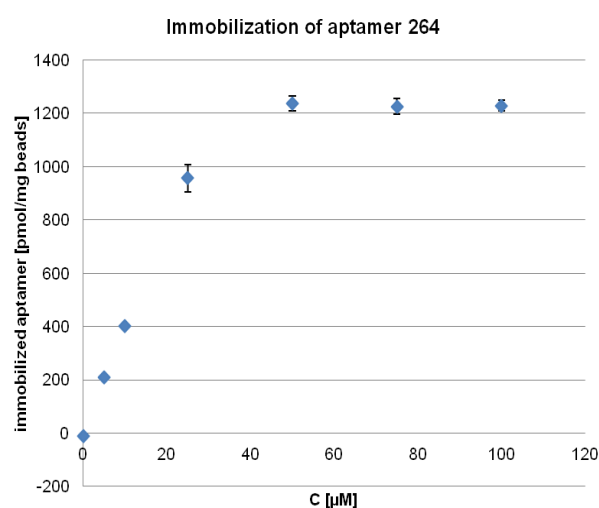


Figure 3.2.2 1: Aptamer loading on carboxyl-modified magnetic beads as a function of applied aptamer concentration during EDC coupling.

To identify the optimal aptamer concentration for an optimal aptamer binding activity and binding capacity, pure commercial F_c fragment and IgG were incubated with aptamer-modified magnetic beads respectively. The amount of immobilized aptamer on the magnetic beads (D_{Apt}) was quantified as well as the amount of bound and eluted F_c fragment (Q_{F_c} and E_{F_c}) and the amount of bound and eluted IgG (Q_{IgG} and E_{IgG}). The amount of immobilized aptamer 264 was calculated based on the Lambert–Beer equation by an extinction coefficient of $614 \text{ mM}^{-1}\text{cm}^{-1}$. The molecular weight of aptamer 264 is

19532 Da. Due to the presence of EDTA in eluate solutions, the determination of concentrations by using NanoDrop™ 1000 was disturbed. Therefore, the Bradford assay was used for the measurement of bound and eluted F_c fragment as well as IgG. The increase of absorbance at 595 nm corresponded to the protein concentration in a solution. Bovine serum albumin (BSA) was used as reference in the concentration range of 0-200 µg/ml. These values were used to calculate the aptamer binding activity ratio (AA) which was defined as the percentage of immobilized aptamer that has bound to target protein. Four different concentrations of aptamer 264 (0, 10, 25, 50 µM) resulting in no, low, medium and high aptamer loading were investigated. The aptamer concentration of 0 µM was used as a negative control, which performed as non-aptamer-modified carboxyl-magnetic beads. The results are shown in table 3.2.2 1 and table 3.2.2 2.

Table 3.2.2 1: Characterization of aptamer functionalities for binding study with pure F_c fragment

c [µM] ^a	D _{Apt} ^b [pmol/mg beads]	Q _{Fc} ^c [pmol/mg beads]	E _{Fc} ^d [pmol/mg beads]	AA _{Fc} ^e [%]	EE _{Fc} ^f [%]
0		219 ± 1	71 ± 7		32.3 ± 10
10	387 ± 31	386 ± 4	324 ± 5	99.8 ± 9	84 ± 3
25	780 ± 35	759 ± 3	698 ± 6	97.3 ± 5	92 ± 1
50	1251 ± 20	683 ± 7	644 ± 8	54.6 ± 3	94.3 ± 2

^a applied aptamer concentrations during immobilization, ^b aptamer loading densities on carboxyl-modified magnetic beads, ^c amount of bound F_c fragment to immobilized aptamer, ^d amount of eluted F_c fragment, ^e aptamer activity ratio for F_c fragment (Q_{Fc}/D_{Apt}), ^f elution efficiency ratio for F_c fragment (E_{Fc}/Q_{Fc}).

Table 3.2.2 2: Characterization of aptamer functionalities for binding study with pure IgG

c [µM] ^a	D _{Apt} ^b [pmol/mg beads]	Q _{IgG} ^c [pmol/mg beads]	E _{IgG} ^d [pmol/mg beads]	AA _{IgG} ^e [%]	EE _{IgG} ^f [%]
0		347 ± 3	282.8 ± 4		81.6 ± 2
10	329 ± 91	327 ± 1	326.9 ± 7	99.4 ± 28	99.9 ± 2
25	758 ± 15	738 ± 2	681.9 ± 2	97.4 ± 2	92.4 ± 1
50	1042 ± 103	727 ± 1	619.1 ± 4	69.8 ± 10	85.1 ± 1

^a applied aptamer concentrations during immobilization, ^b aptamer loading densities on carboxyl-modified magnetic beads, ^c amount of bound IgG to immobilized aptamer, ^d amount of eluted IgG, ^e aptamer activity ratio for IgG (Q_{IgG}/D_{Apt}), ^f elution efficiency ratio for IgG (E_{IgG}/Q_{IgG}).

Table 3.2.2 1 shows the binding of F_c fragment. The aptamer binding activity reached the highest value of 99.8% at aptamer concentration of 10 μM. At aptamer concentration of 25 μM, the aptamer binding activity was 97%. However, the amount of bound F_c fragment of 386 pmol/mg beads at 10 μM was rather low. The aptamer concentration of 25 μM showed the most optimal results. At this concentration level, aptamer loading density was higher than that of 10 μM and thereby had sufficient binding capacity to the target protein. It resulted in the highest amount of bound F_c fragment with a value of 759 pmol/mg beads, which was almost twice as high as that at aptamer concentration of 10 μM. When the applied concentration level was increased to 50 μM, the highest aptamer loading density was reached. Nevertheless, the amount of bound F_c fragment was down to 683 pmol/mg beads and the aptamer binding activity reduced almost half. These results supported the hypothesis that a very high aptamer density could lead to steric or electrostatic hindrance and resulted in reduced aptamer binding activity and decreased binding capacity.

The experiment was repeated with IgG. Table 3.2.2 2 shows the results of IgG binding study. Similar results were observed. Aptamer concentrations of 10 μM and 25 μM resulted in higher aptamer binding activities, ranging between 97% and 99%. An aptamer concentration of 50 μM resulted in reduced aptamer binding activity at level of only 69.8%. In conclusion, an aptamer concentration of 25 μM achieved the most optimal aptamer functionalities with approximately 750 pmol immobilized aptamers per mg beads.

Besides aptamer binding activity ratio (AA), also the elution efficiency (EE) was determined since this value is relevant for the recovery of purified proteins. As expected, in the binding studies of F_c fragment and IgG respectively, the best elution efficiencies were also reached at aptamer concentration of 25 μM. Determined by Bradford assay, 759 pmol F_c fragment were found to be bound to the immobilized aptamer 264 (25μM) and 698 pmol F_c fragment were eluted, resulting in elution efficiency of 92% (Table 3.2.2 1). While 738 pmol IgG were found to be bound to the immobilized aptamer 264 (25μM) and 682 pmol IgG were eluted, the elution efficiency reached 92.4% (Table 3.2.2 2).

The results in table 3.2.2 1 and table 3.2.2 2 also revealed unspecific binding of F_c fragment and IgG to carboxyl-modified magnetic beads. The unspecific binding of IgG can be explained by its isoelectric point between 7 and 9.5 [166], which resulting in a positive net charge of IgG in SB (pH 7.3). Between the carboxyl-modified magnetic beads and IgG,

electrostatic attraction was formed. This ionic interaction led to the unspecific binding of IgG directly onto the carboxyl-modified magnetic beads. This explanation for the unspecific binding of IgG can be extended to the unspecific binding of F_c fragment.

3.2.3 Aptamer-based purification of F_c fragment from FCS

To test the aptamer-based purification efficiency for F_c fragment, 10% fetal calf serum (FCS) was added into pure commercial F_c fragment and this F_c fragment in FCS serum was incubated with aptamer 264-modified magnetic beads. Samples were analyzed via SDS-PAGE analysis (Fig. 3.2.3 1). Within the three elution fractions, F_c fragment was found with minor contaminations of BSA. In the third elution fraction, aptamer 264 was found. This circumstance occurred is probably because that the last elution step was performed over night in Laemmli buffer. Aptamers showed their unstable property when they were incubated over night in Laemmli buffer. The purity degree of the first eluate for F_c fragment was 82.9%, as determined by densitometry.

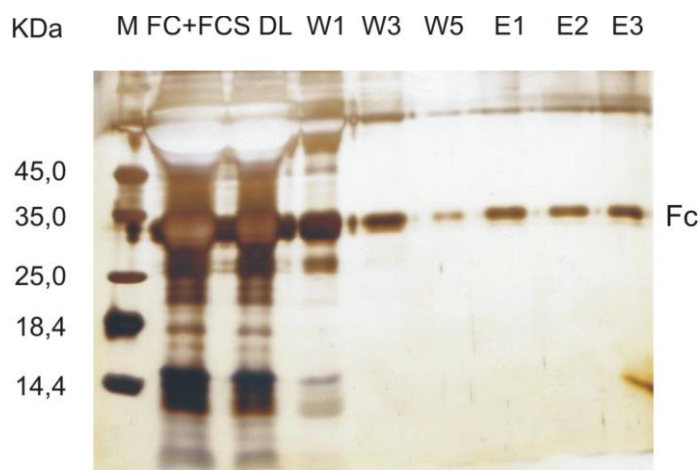


Figure 3.2.3 1: SDS PAGE analysis of aptamer-based purification of F_c fragment from 10% FCS. Following samples were applied: (M) molecular weight marker, (Fc) F_c (from 10% FCS) sample applied to aptamer-modified magnetic beads, (DL) supernatant of F_c (from 10% FCS) after incubation with aptamer-modified magnetic beads, (W1-W5) washing fractions, and (E1-E3) eluates.

3.2.4 Aptamer-based purification of human IgG from FCS

In order to investigate the aptamer-based purification of IgG from complex samples, pure commercial IgG supplemented with 10% FCS was incubated with aptamer 264-modified magnetic beads and the process was analyzed via SDS-PAGE analysis (Fig. 3.2.4 1). Within the first elution fraction (Fig. 3.2.4 1, lane 6), IgG was found with minor

contaminations of BSA. The purity degree of IgG in the first elution fraction was 97%, as determined by densitometry.

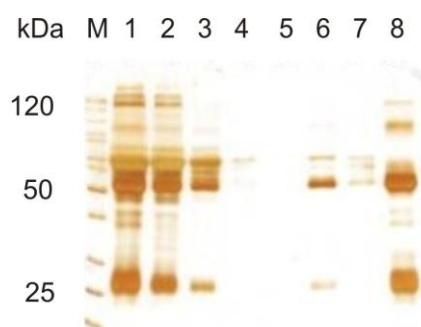


Figure 3.2.4 1: SDS PAGE analysis of aptamer-based purification of IgG from complex sample. Following samples were applied: (M) molecular weight marker, (1) IgG (from 10% FCS) sample applied to aptamer-modified magnetic beads, (2) supernatant of IgG (from 10% FCS) after incubation with aptamer-modified magnetic beads, (3-5) washing fractions, (6-7) eluates and (8) standard IgG.

3.2.5 Conventional protein A-based downstream process

BioMag[®] Protein A was conventionally used for the purification of antibodies. The following experiments were conducted to compare the purification of antibodies with protein A and aptamer-based method.

To test the protein A-based purification method, F_c fragment and IgG supplemented with 10% FCS were used. In the eluates, purified F_c fragment was obtained with no visible contaminants (Fig. 3.2.5 1A), while IgG was purified with a little contamination of BSA (Fig. 3.2.5 1B). The purity degree of F_c fragment from 10% FCS in the first eluate was 94.7%, while the purity degree of IgG from 10% FCS in the first eluate was 79.3%, as determined by densitometry.

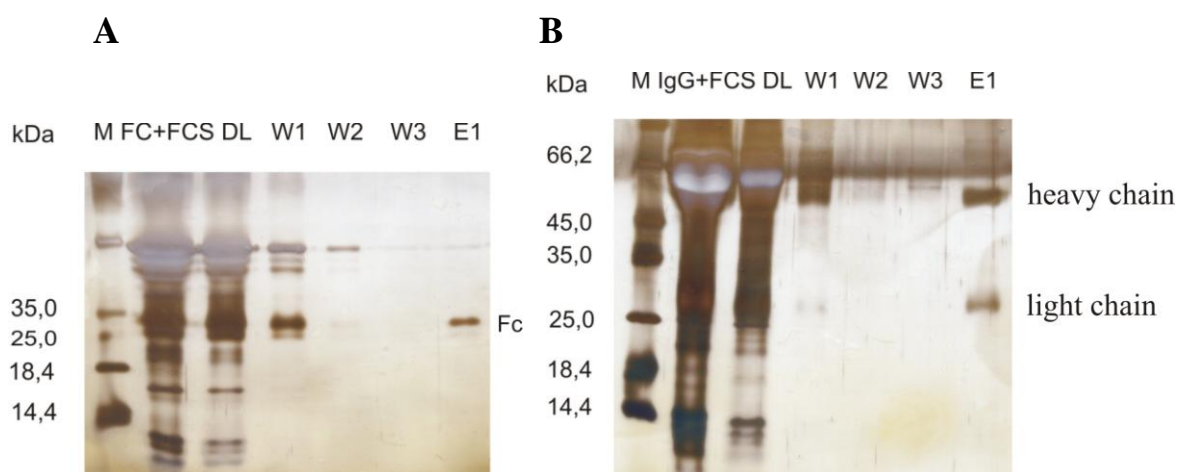


Figure 3.2.5 1: (A) SDS PAGE analysis of protein A-based purification of F_c fragment from 10% FCS. Following samples were applied: (M) molecular weight marker, (F_c+FCS) F_c fragment (from 10% FCS) sample applied to protein A, (DL) supernatant of F_c fragment (from 10% FCS) after incubation with protein A, (W1-W3) washing fractions, and (E1) eluate. (B) SDS PAGE analysis of protein A-based purification of IgG from 10% FCS. Following samples were applied: (M) molecular weight marker, (IgG+FCS) IgG (from 10% FCS) sample applied to protein A, (DL) supernatant of IgG (from 10% FCS) after incubation with protein A, (W1-W3) washing fractions, and (E1) eluate.

The results of aptamer-based purification of F_c fragment and IgG from 10% FCS utilizing carboxyl-modified magnetic beads showed purity degree of 82.9% for F_c fragment and 97% for IgG, similar to those from conventional protein A-based method. Moreover, 1 ml (5 mg) BioMag Protein A can bind approximately 0.2 mg IgG, while the calculated binding capacity of aptamer-based IgG purification showed a similar value of 0.25 mg per 5 mg beads. However, aptamers are produced more easily, are more stable and require less harsh elution terms (*e. g.* 300 mM EDTA, pH 7.3). In contrast, protein A-based protein purification required harsher elution conditions (*e. g.* 100 mM glycine, pH 2.5). Under this harsher elution condition, the properties of purified IgG would be changed. Therefore, the aptamer-based purification process is a valuable and competitive alternative to protein A-based purification of antibodies.

3.2.6 Scale-up via binding of aptamers on NHS-modified sepharose and methyl-carboxyl-modified CIM[®] DISK

Based on the successfully developed aptamer-based downstream processes utilizing carboxyl-modified magnetic beads, sepharose 4 fast flow was selected to enable an efficient scale-up of aptamer-based purification for F_c fragment and IgG. Concerning the

immobilization of aptamer 264 on NHS-activated sepharose, the binding mechanism was introduced in chapter 3.1.7 (Fig. 3.1.7 1).

As a negative control, sepharose was treated in the same way as normal aptamer immobilization but without addition of aptamer during the immobilization procedure. The functionalities of aptamer-modified sepharose were first investigated by binding study with pure F_c fragment. SDS PAGE analysis showed that F_c fragment bound specifically to the immobilized aptamer (Fig. 3.2.6 1A), no binding occurred for the negative control (Fig. 3.2.6 1B). To judge the purification efficiency, the experiment was repeated with F_c fragment supplemented with 10% FCS. In the resulting eluates, F_c fragment was obtained with minor contaminants (Fig. 3.2.6 2). The purity degree of F_c fragment with 10% FCS in both eluates (Fig. 3.2.6 2) was 96.4%, as determined by densitometry.

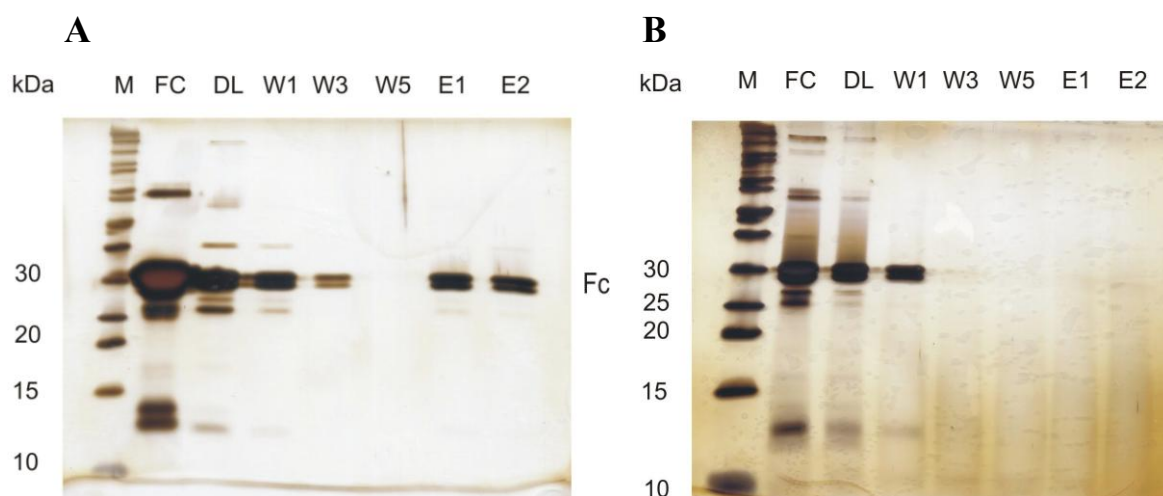


Figure 3.2.6 1: SDS PAGE analysis of F_c binding to aptamer-modified sepharose (A) and sepharose without aptamer (B). Following samples were applied: (M) molecular weight marker, (F_c) pure F_c sample applied to aptamer-modified sepharose, (DL) supernatant of pure F_c after incubation with aptamer-modified sepharose, (W1-W5) washing fractions, and (E1-E2) eluates.

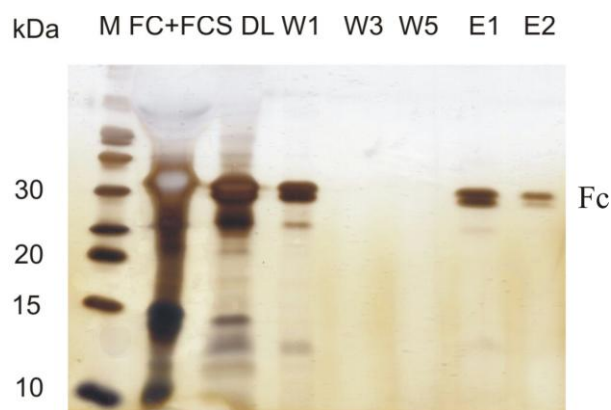


Figure 3.2.6 2: SDS PAGE analysis of the purification of F_c fragment from 10% FCS utilizing aptamer-modified sepharose. Following samples were applied: (M) molecular weight marker, (F_c + FCS) F_c (from 10% FCS) sample applied to aptamer-modified sepharose, (DL) supernatant of F_c (from 10% FCS) after incubation with aptamer-modified sepharose, (W1-W5) washing fractions, and (E1-E2) eluates.

Table 3.2.6 1: Characterization of aptamer functionalities immobilized on sepharose utilizing pure F_c fragment

c [μM] ^a	D _{Apt} ^b [pmol/200 μl sepharose]	Q _{Fc} ^c [pmol/200 μl sepharose]	E _{Fc} ^d [pmol/200 μl sepharose]	AA _{Fc} ^e [%]	EE _{Fc} ^f [%]
25	536 ± 31	300.8 ± 3	291.8 ± 1	56.1 ± 7	97 ± 1

^a applied aptamer concentration during immobilization, ^b aptamer loading density on NHS-activated sepharose, ^c amount of bound F_c fragment to immobilized aptamer, ^d amount of eluted F_c fragment, ^e aptamer activity ratio for F_c fragment (Q_{Fc}/D_{Apt}), ^f elution efficiency ratio for F_c fragment (E_{Fc}/Q_{Fc}).

Table 3.2.6 1 shows 536 pmol of aptamer 264 were immobilized on 200 μL NHS-modified sepharose. The values of bound and eluted F_c fragment were 300 pmol and 292 pmol. The aptamer binding activity showed a value of 56% and the elution efficiency ratio of F_c fragment was 97%. Compared with aptamer 264-based purification of F_c fragment utilizing carboxyl-modified magnetic beads the aptamer binding activity decreased on sepharose. One explanation for reduced aptamer binding activity may be that the immobilized aptamer 264 within the pores of sepharose could not fold correctly due to the small pores, which led to the lower aptamer binding capability to F_c fragment.

The functionality of aptamer-modified sepharose was further investigated by binding study with IgG. The SDS PAGE gel demonstrated that IgG could not bind to the immobilized aptamer (data not shown). It was assumed that IgG has a higher spatial demand compared to F_c fragment. One possible source of decreased aptamer binding activity is steric

hindrance of target binding which may occur when the aptamer is immobilized too close to the carrier surface [122]. In this case, a suitable additional spacer could be helpful for the binding between aptamer 264 and IgG. Spacer can either be built on the surface of sepharose or linked to aptamer 264 [167]. Because the coupling between NHS-activated sepharose and amino-modified aptamer 264 worked very well, aptamer 264 with integrated spacer (PEG6) was chosen for the further experiment. The immobilization and incubation procedures were performed the same way as that of aptamer 264 without integrated spacer.

SDS PAGE analysis showed that IgG supplemented with 10% FCS bound to the immobilized aptamer 264 with integrated spacer PEG6 (Fig. 3.2.6 3). In the eluates, IgG was obtained with BSA contaminants and aptamer 264 fell down partially during the elution (at ca. 13 kDa). This effect occurred probably because part of the covalent bindings between aptamer 264 with integrated spacer PEG6 and NHS-modified sepharose did not work correctly. The purity degree of IgG in both eluates (Fig. 3.2.6 3) was 60.9%, as determined by densitometry.



Figure 3.2.6 3: SDS PAGE analysis of the purification of IgG from 10% FCS utilizing aptamer 264 with integrated spacer and NHS-activated sepharose. Following samples were applied: (M) molecular weight marker, (IgG + FCS) IgG (from 10% FCS) sample applied to aptamer-modified sepharose, (DL) supernatant of IgG (from 10% FCS) after incubation with aptamer-modified sepharose, (W1-W5) washing fractions, and (E1-E2) eluates.

Pure IgG was utilized to characterize the binding efficiency and elution efficiency ratio by using aptamer 264 with integrated spacer PEG 6 (Table 3.2.6 2). The amount of immobilized aptamer 264 was calculated based on the Lambert–Beer equation by an extinction coefficient of $614 \text{ mM}^{-1}\text{cm}^{-1}$. The molecular weight of aptamer 264 with integrated spacer PEG 6 is 19876 Da.

Table 3.2.6 2: Characterization of aptamer functionalities utilizing pure IgG

c [μM] ^a	D_{Apt} ^b [pmol/200 μL sepharose]	Q_{IgG} ^c [pmol/200 μL sepharose]	E_{IgG} ^d [pmol/200 μL sepharose]	AA_{IgG} ^e [%]	EE_{IgG} ^f [%]
25	771 \pm 84	120.6 \pm 12	15.4 \pm 2	15.6 \pm 21	12.8 \pm 23

^a applied concentration of aptamer 264 with integrated spacer PEG6 during immobilization, ^b aptamer with integrated spacer loading density on NHS-activated sepharose, ^c amount of bound IgG to immobilized aptamer, ^d amount of eluted IgG, ^e aptamer activity ratio for IgG ($Q_{\text{IgG}}/D_{\text{Apt}}$), ^f elution efficiency ratio for IgG ($E_{\text{IgG}}/Q_{\text{IgG}}$).

Table 3.2.6 2 reports the amount of immobilized aptamer 264 with integrated spacer PEG6 on the NHS-activated sepharose, the amount of bound and eluted IgG, the calculated aptamer binding activity and the elution efficiency ratio of IgG. Compared to the purification of F_c fragment utilizing aptamer 264 and NHS-activated sepharose, the value of bound IgG was one third of the bound F_c fragment. The aptamer binding activity was also low. This finding supported the assumption that IgG has a higher spatial demand. The value of elution efficiency was only 12.78%. This rather low elution efficiency could be explained as the pore size of sepharose is small, the IgGs, which diffused within sepharose particles were obstructed. A long elution process could be required. The success of using aptamer-modified sepharose for the purification of F_c fragment and IgG implies the industrial application in the future.

The relatively poor purification results of F_c fragment and IgG by using aptamer 264-modified sepharose could be attributed to small pore size. To diminish the influence of pore size, CIM[®] monolithic columns (BIA separations, Ljubljana, Slovenia) containing big internal pore size (porosity 5 μm) were used. The disc-shaped CIM[®] DISK consists of a methylcarboxylate-based porous polymer matrix [129]. Especially, they can be used as a stationary phase for ion exchange chromatography and the purification process by using CIM[®] DISK can be automated via FPLC. The immobilization of aptamer on the CIM[®] monolithic columns was performed similarly as that of carboxyl-modified magnetic beads. EDC was used in the coupling process. The aptamer immobilization was induced via a chemical reaction, in which amino-modified aptamers were covalently coupled to EDC-activated CIM[®] DISK (Fig.3.2.6 4).

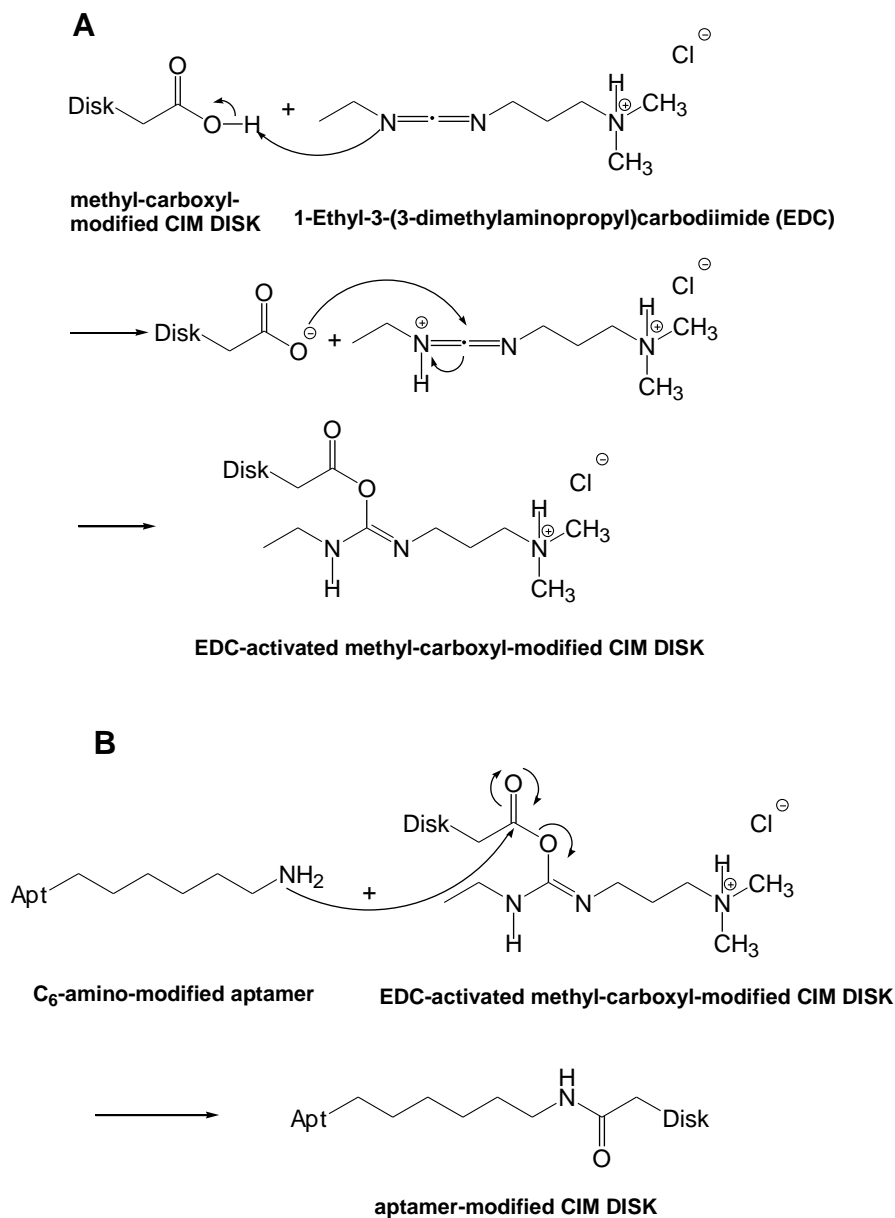


Figure 3.2.6 4: Aptamer immobilization on the methylcarboxyl-modified CIM[®] DISK via EDC. (A) The methylcarboxyl-modified CIM[®] DISK is activated via EDC. (B) The amino-modified aptamer is immobilized on EDC-activated CIM[®] DISK.

The binding study with aptamer-modified CIM[®] monolithic columns was performed with pure F_c fragment. SDS PAGE analysis showed that F_c fragment was bound to the immobilized aptamer and was successfully eluted with 300 mM EDTA (Fig. 3.2.6 5). Within the first elution fraction, F_c fragment was found as a weak band, while within the second elution fraction F_c fragment displayed a strong and thick band. This is probably because that during the first elution step, the elution buffer was diluted through wash buffer remained in the pores of the material from the last washing step. Different from magnetic beads, a complete buffer exchange was hampered for the porous CIM material.

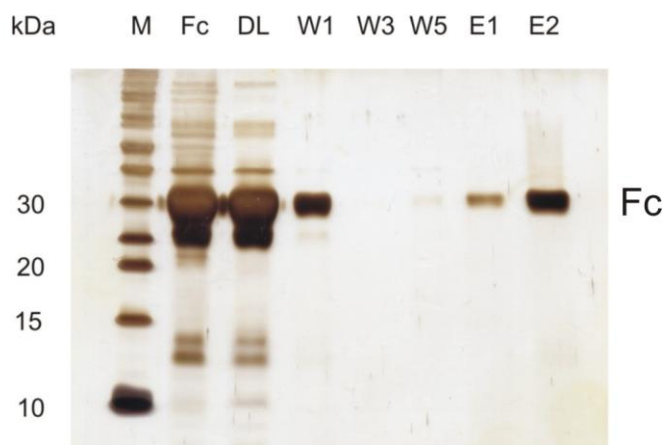


Figure 3.2.6 5: SDS PAGE analysis of F_c fragment binding to aptamer-modified CIM[®] monolithic columns. Following samples were applied: (M) molecular weight marker, (F_c) pure F_c fragment sample applied to aptamer-modified CIM[®] monolithic columns, (DL) supernatant of pure F_c fragment after incubation with aptamer-modified CIM[®] monolithic columns, (W1-W5) washing fractions, and (E1-E2) eluates.

Table 3.2.6 3: Characterization of aptamer functionalities utilizing pure F_c fragment

c [μM] ^a	D _{Apt} ^b [pmol/CIM DISK]	Q _{Fc} ^c [pmol/CIM DISK]	E _{Fc} ^d [pmol/CIM DISK]	AA _{Fc} ^e [%]	EE _{Fc} ^f [%]
25	9721.3 ± 39.8	6876.5 ± 12.9	1423.4 ± 14.1	70.7 ± 1	20.7 ± 1

^a applied aptamer concentration during immobilization, ^b aptamer loading density on CIM[®] DISK, ^c amount of bound F_c fragment to immobilized aptamer, ^d amount of eluted F_c fragment, ^e aptamer activity ratio for F_c fragment (Q_{F_c}/D_{Apt}), ^f elution efficiency ratio for F_c fragment (E_{F_c}/Q_{F_c}).

Table 3.2.6 3 shows that 9721 pmol aptamer 264 were immobilized on the CIM monolithic columns and 6876 pmol F_c fragment were bound with immobilized aptamer 264, 1423 pmol F_c fragment was eluted. The aptamer activity ratio reached 71% and the elution efficiency ratio was 21%. Compared with the purification method by using aptamer 264-modified sepharose, the amount of immobilized aptamer, the amount of bound and eluted F_c fragment and the calculated aptamer binding activity increased significantly. The results supported the hypothesis that pore size interfered in the aptamer performance for sepharose. The relatively low elution efficiency by using CIM[®] DISK implied an incomplete elution process. An extension of elution time or more elution steps could improve elution as well as the automatic elution process via FPLC.

3.3 Aptamer-based purification and depleting of small molecules

In the previous parts, the aptamer-based purification of proteins was discussed. In this section, an aptamer-based purification and depleting of small molecules would be explored. This developed method not only tries to purify small molecules but also deplete disturbed components (for example, toxins). Aptamers have already been selected against small molecules. Several publications have reported the binding possibilities of RNA aptamers for theophylline [86, 168, 169]. In this study, theophylline was selected to examine the applicability of aptamers in the downstream processes for small molecules for the first time. Because malathion is unstable, a little publication has reported about malathion. However, malathion was investigated in this work and represented the contaminants to test the applicability of aptamers to deplete disturbed components for the first time too. Based on the binding property, aptamer-based purification of theophylline and depleting of malathion were examined as model systems.

While the aptamer directed against theophylline was composed of RNA [170], an RNA/DNA chimera against theophylline was used in this study. Because Chavez et al. have reported that RNA/DNA chimera enhance the stability against degradation [171].

According to the patent US 2008/0161236 A1.2008 [172], two given DNA aptamer sequences (forward and reversed) were tested. Only one of these sequences can recognize and bind with malathion, which was not indicated in the patent.

3.3.1 Aptamer-based purification of theophylline

Theophylline ($C_7H_8N_4O_2$, $M_r = 180.2$ g/mol) is used as medicinal tablet, or an injection preparation in the market (Euphylline®, aminophylline®, generics). It was approved in Switzerland in 1954. It is a white, crystalline powder, difficult to dissolve in water. It is a methylxanthine and it is structurally related to caffeine (Fig. 3.3.1 1). Theophylline can expand bronchus, can be used as antiphlogistic and diuretic tablets as well as anti-vascular sclerosis drug, which leads to the vascular dilatation of respiratory tracts and vasculature.

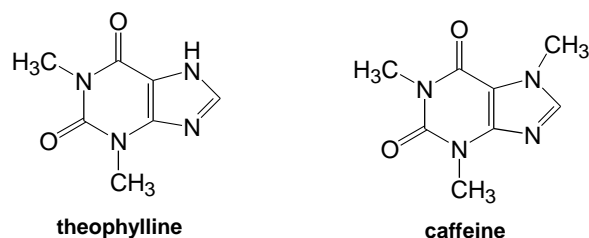


Figure 3.3.1 1: Schematic structure of theophylline and caffeine.

Zimmermann et al. (2000) reported an RNA aptamer containing a 15-nt binding site showing high affinity and specificity for the theophylline [86]. Several RNA aptamers showed reduced binding affinity to their targets because of lack of divalent ions. By high-affinity theophylline binding, divalent ions are also absolutely required. Therefore, removing the divalent ions and adding EDTA in the elution buffer would elute bound theophylline. Secondly, heating destroys the aptamers' secondary structures. Heat denaturation would be investigated for the elution of small molecules. Third, it was reported that there was no binding of theophylline at pH 5 [173]. Therefore the pH value of elution buffer would be adjusted to 5 to obtain the elution of theophylline.

In the previous sections, 20 mg/ml beads were used for the immobilization of aptamer. It was assumed that high beads-concentration could be probably advantageous for small molecules' binding, the commercial 20 mg/ml carboxyl-modified magnetic beads were concentrated to 50 mg/ml. 25 μ M theophylline aptamer was used and immobilized on the concentrated beads, as it was demonstrated by aptamer-based protein purification that an aptamer concentration of 25 μ M resulted in best aptamer functionalities. The amount of immobilized aptamer was calculated based on the Lambert–Beer equation by an extinction coefficient of 416 $\text{mM}^{-1}\text{cm}^{-1}$. The molecular weight of theophylline aptamer is 15710 g/mol. To determine the average amount of immobilized aptamer, three individual immobilization procedures were performed in parallel. All samples were measured three times with the help of NanoDrop. The results of three immobilization procedures are shown in table 3.3.1 1. The average value of 423 pmol immobilized aptamer per mg beads was achieved in table 3.3.1 1.

Table 3.3.1 1: amount of immobilized aptamers (25 μ M) on carboxyl-modified magnetic beads, three individual immobilization procedures were performed in parallel, all resulting samples were measured in triplicates with Nanodrop

	concentration of immobilized theophylline aptamer on carboxyl beads (pmol/mg beads)
immobilization 1	417 \pm 7
immobilization 2	418 \pm 7
immobilization 3	432 \pm 6
average value	423 \pm 8

It was reported by Zimmermann et al. (2000) that theophylline was bound to aptamer-modified magnetic beads via heating to 65 °C [86]. In this experiment, binding was performed first by heating to 65 °C in the selection buffer (100 mM HEPES, 50 mM NaCl, 5 mM MgCl₂, pH 7.3) for 30 minutes at 600 rpm. After slowly cooled in room temperature, the binding procedure was performed for additional two hours at room temperature. Different elution methods were investigated to elute the bound theophylline. Divalent ions were removed in all elution buffers (100 mM HEPES, 50 mM NaCl, pH 7.3). First elution strategy was to use 100 mM EDTA in the elution buffer as the binding of theophylline to aptamer depended on the presence of divalent ions. EDTA removed divalent ions by chelating them and destroyed the correct folding of the aptamer. The second elution method was to use heat denaturation at 95 °C twice, 15 minutes each. With heat denaturation, the secondary structure of aptamers could be destroyed. The third elution method was to change pH-value from 7.3 to 5.0 in the elution buffer. Zimmermann et al. observed no binding of theophylline at pH 5 because of improper aptamer folding at decreased pH value, at pH 5, base A₇ of theophylline aptamer was protonated (Fig. 3.3.1 2) [173]. The quantification of theophylline was performed by company symrise (holzminden, Germany) and the results of theophylline binding and elution efficiency are calculated and listed in table 3.3.1 2.

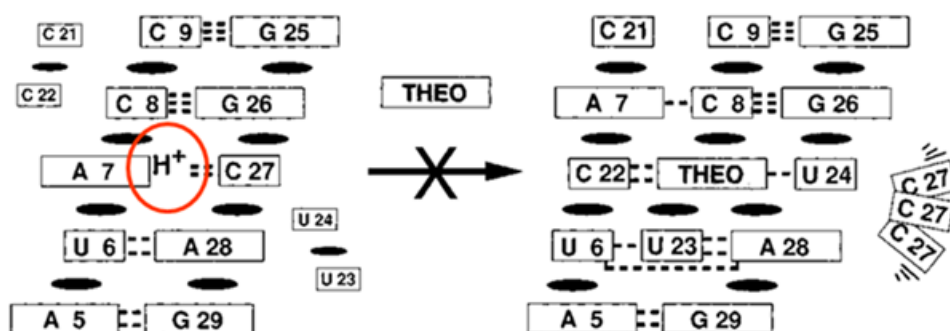


Figure 3.3.1 2: Diagram of base protonation at low pH-value [173]

Table 3.3.1 2: characterization of theophylline binding and elution efficiency ratio utilizing aptamer-modified carboxyl beads under three different elution methods

Elution methods	c [μM] ^a	D_{Apt} ^b [pmol/mg beads]	$Q_{\text{theophylline}}$ ^c [pmol/mg beads]	$E_{\text{theophylline}}$ ^d [pmol/mg beads]	$AA_{\text{theophylline}}$ ^e [%]	$EE_{\text{theophylline}}$ ^f [%]
1 (EDTA)	25	423 ± 8	0.53	0.11	0.13	20
2 (heating)	25	423 ± 8	0.53	0.20	0.13	39
3 (pH 5)	25	423 ± 8	0.53	0.10	0.13	19

^a applied aptamer concentration during immobilization, ^b aptamer loading density on carboxyl-modified magnetic beads, ^c amount of bound theophylline to immobilized aptamer, ^d amount of eluted theophylline, ^e aptamer activity ratio for theophylline ($Q_{\text{theophylline}}/D_{\text{Apt}}$), ^f elution efficiency ratio for theophylline ($E_{\text{theophylline}}/Q_{\text{theophylline}}$).

The results listed in table 3.3.1 2 were not ideal as the amount of bound theophylline was very low. Thus the binding method was optimized. Instead of cooling slowly to room temperature after binding at 65 °C, rapid cooling to room temperature was performed. Results showed no significant difference between slow cooling and rapid colling methods. Theophylline aptamer was first immobilized on concentrated carboxyl-modified magnetic beads (50 mg/ml). Three identical immobilization procedures were performed parallely. The average amount of immobilized aptamer (applied concentraion of 25 μM) was 535 pmol/mg beads. All three manuscripts were combined for the binding of theophylline. Tenfold molar excess of theophylline (48.19 μg / ml) was added into the 300 μl aptamer-modified beads suspension.

Three developed elution methods were used to test the elution efficiency of theophylline. Heat denaturation was retained as this method showed the best elution efficiency ratio in

the aforementioned experiments. A potential reason for incomplete elution of theophylline by heating may be that they were re-bound to aptamers. To avoid re-binding of theophylline, a combined elution strategy of heat denaturation and decreased pH was designed. The combination of using heating at 95°C and adjusting pH-value of 5 in the elution buffer was chosen as the second elution method. Urea was often used for elution [44]. 7 M urea was used in the elution buffer as another candidate for the elution strategy. The binding and elution data were provided by symrise (table 3.3.1 3) and the results of theophylline binding and elution efficiency are calculated and listed out in table 3.3.1 4.

Table 3.3.1 3: theophylline binding on aptamer-modified carboxyl beads

	theophylline [ppb] in 100 µl	theophylline [pmol] in 100 µl
Applied theophylline	61100	33.91
Theophylline supernatant	50480	28.01
Wash fraction 1	8004	4.44
Wash fraction 2	1428	0.79
Wash fraction 3	323	0.18
Wash fraction 4	131	0.07
Wash fraction 5	76	0.04
Wash fraction 6	65	0.04
E1 with elution method 1 (heating, pH 7.3)	467	0.26
E2 with elution method 1 (heating, pH 7.3)	89	0.05
E3 with elution method 1 (heating, pH 7.3)	20	0.01
E1 with elution method 2 (heating, pH 5)	440	0.24
E2 with elution method 2 (heating, pH 5)	79	0.04
E3 with elution method 2 (heating, pH 5)	14	0.01
E1 with elution method 3 (urea)	49	0.03
E2 with elution method 3 (urea)	52	0.03

Table 3.3.1 4: characterization of theophylline binding and elution efficiency ratio on aptamer-modified carboxyl beads under three different elution methods

Elution methods	c [μM] ^a	D _{Apt} ^b [pmol/mg beads]	Q _{theophylline} ^c [pmol/mg beads]	E _{theophylline} ^d [pmol/mg beads]	AA _{theophylline} ^e [%]	EE _{theophylline} ^f [%]
95°C pH 7.3	25	535	0.34	0.29	0.1	85
95°C pH 5	25	535	0.34	0.32	0.1	94
urea	25	535	0.34	0.06	0.1	18

^a applied aptamer concentration during immobilization, ^b aptamer loading density on carboxyl-modified magnetic beads, ^c amount of bound theophylline to immobilized aptamer, ^d amount of eluted theophylline, ^e aptamer activity ratio for theophylline ($Q_{\text{theophylline}}/D_{\text{Apt}}$), ^f elution efficiency ratio for theophylline ($E_{\text{theophylline}}/Q_{\text{theophylline}}$).

Table 3.3.1 4 shows by using heating at a pH-value of 7.3, the elution efficiency of theophylline was 85%; by heating at a pH-value of 5, the elution efficiency reached the highest value of 94%. The high elution efficiency from both methods revealed that heating played a very important role in the elution process. The relatively higher elution efficiency at pH-value of 5 supported the hypothesis that adjusting pH-value of 5 in the elution buffer prevented the reversing reaction and thereby promoted the elution efficiency. Moreover, elution via urea showed a less efficient elution effect, less theophylline being eluted during the elution steps. This is probably because that 7 M urea was not efficient enough for the aptamer denaturation, which led to the difficulty of releasing the binding between theophylline and aptamer.

Based on the successful elutions by utilizing heating and different pH-values, the reusability of theophylline-aptamer-beads was investigated. The elution data were provided by symrise (table 3.3.1 5, table 3.3.1 6).

Table 3.3.1 5: elution data of theophylline from regenerated aptamer-modified carboxyl beads

	theophylline [ppb] in 100 μl	theophylline [pmol] in 100 μl
Wash fraction 6 (95°C, pH 5)	75	0.04
E1 (95°C, pH 5)	771	0.43
E2 (95°C, pH 5)	119	0.07
E3 (95°C, pH 5)	24	0.01

The particles could be successfully reused with the elution method of heating at a pH-value of 5. There was even a larger amount of theophylline (**176 %** in comparison of the first use

of aptamer-modified beads with the same elution method, table 3.3.1 3) eluted from the reused aptamer-modified carboxyl beads. This effect can be explained that the elution was completed from the preceding experiment.

Table 3.3.1 6: elution data of theophylline from regenerated aptamer-modified carboxyl beads

	theophylline [ppb] in 100 μ l	theophylline [pmol] in 100 μ l
Wash fraction 6 (95°C, pH 7.3)	60	0,03
E1 (95°C, pH 7.3)	676	0,38
E2 (95°C, pH 7.3)	107	0,06
E3 (95°C, pH 7.3)	14	0,01

The results of the reusability via heating at a pH-value of 7.3 were similar to heating at pH 5. A larger amount of theophylline (**155 %** in comparison of the first use of aptamer-modified beads with the same elution method, table 3.3.1 3) was eluted from the reused aptamer-modified carboxyl beads.

Zimmermann et al. (2000) also reported that caffeine was added to the aptamer in tenfold excess and the NMR spectra showed no evidence for binding [86]. There was no interaction between caffeine and the aptamer binding site, where theophylline could be specifically bound. This finding from Zimmermann emphasized that the RNA aptamer could discriminate the extremely closely related molecules (Fig. 3.3.1 1).

To replicate the results of their study, three experiments were conducted. In the first experiment, only theophylline was incubated with aptamer-modified beads as a positive control. In the second experiment, equimolar amounts of theophylline, theobromine and caffeine (Fig. 3.3.1 3) were mixed and incubated with aptamer-modified beads. In the third experiment, theophylline, theobromine and caffeine containing 10 % coffee were mixed and incubated with aptamer. The binding and elution data were provided by symrise. Data and results are displayed in the following tables and figures.

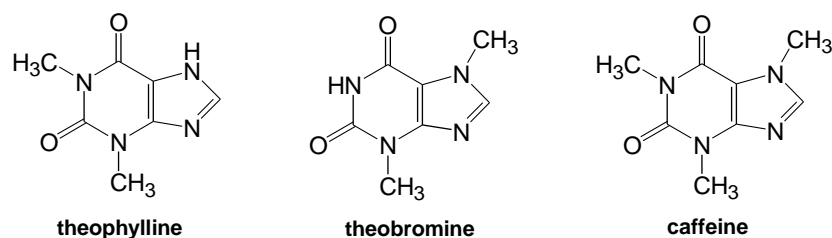


Figure 3.3.1 3: Structure of theophylline, theobromine and caffeine.

Table 3.3.1 7 shows the concentrations of theophylline in different fractions during the binding and elution process. Pure theophylline was applied (data provided by symrise) in this experiment as a positive control. The amount of eluted theophylline in the first eluate was 1.7 ppb, while the amount of theophylline in the last washing fraction was 0, which demonstrated that theophylline was successfully bound and eluted from aptamer-modified magnetic beads.

Table 3.3.1 7: Purification data from pure theophylline

	theophylline [ppb]
sample	253
DL	207
Wash fractions (1-7)	34.2
Wash fraction 8	0
Elution 1	1.7
Elution 2	0.5
Elution 3	0.1

Table 3.3.1 8 shows no binding either between theobromine and aptamer-modified beads or between caffeine and aptamer-modified beads in the second experiment. Only theophylline was bound and successfully eluted from the mixture utilizing aptamer-modified magnetic beads, which emphasized the aptamer's binding specificity. The percentage of theophylline in the applied sample was determined to be 34%. In the elution theophylline was isolated with a purity of 100% (data provided by symrise).

Table 3.3.1 8: Purification data from mixture of theophylline, theobromine and caffeine

	theophylline [ppb]	theobromine [ppb]	caffeine [ppb]	theophylline percentage [%]
sample	254	228	260	34
DL	210	195	222	
Wash fractions (1-7)	37,7	29,57	31,6	
Wash fraction 8	0,2	0	0	
Elution 1	1.6	0	0	100
Elution 2	0.2	0	0	
Elution 3	0.1	0	0	

Fig. 3.3.1 4 graphed the results from table 3.3.1 8.

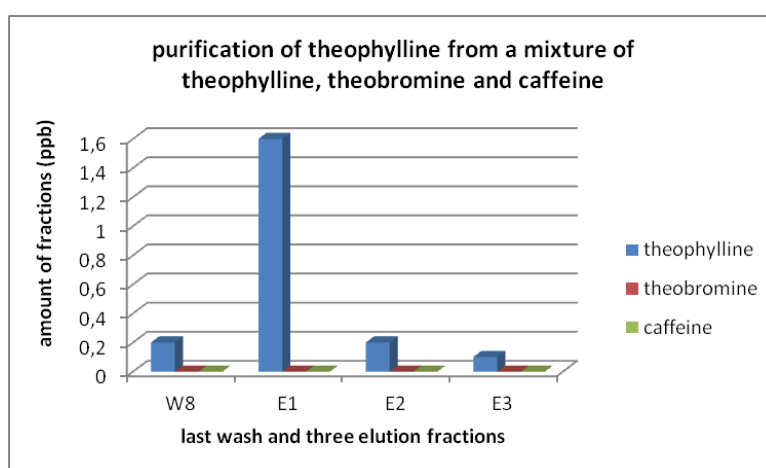


Figure 3.3.1 4: Purification of theophylline from a mixture of theophylline, theobromine and caffeine utilizing aptamer-modified carboxyl beads. Following samples were applied: (W8) wash fraction 8 (last wash fraction), and (E1-E3) eluates.

Fig. 3.3.1 4 clearly indicates that only theophylline was bound and eluted from the aptamer. The third experiment of purification from a mixture of theophylline, theobromine and caffeine containing 10 % coffee was done to simulate a complex sample. A little binding of theobromine and caffeine containing 10% coffee was detected in the eluates. However, theophylline showed the best binding and elution results. The percentage of theophylline in the applied sample was determined to be 26%. In the elution theophylline was isolated with a purity of 85%. The results are reported in table 3.3.1 9 (data provided by symrise).

Table 3.3.1 9: purification of theophylline from a mixture of theophylline, theobromine and caffeine containing 10% coffee

	theophylline [ppb]	theobromine [ppb]	caffeine containing 10% coffee [ppb]	theophylline percentage [%]
sample	253	215	510	26
DL	203	182	433	
Wash fractions (1-7)	43.3	35.53	75.67	
Wash fraction 8	0,2	0	0	
Elution 1	3.1	0.06	0.5	85
Elution 2	0.8	0	0.2	
Elution 3	0.2	0	0	

Fig. 3.3.1 5 graphed the results from table 3.3.1 9.

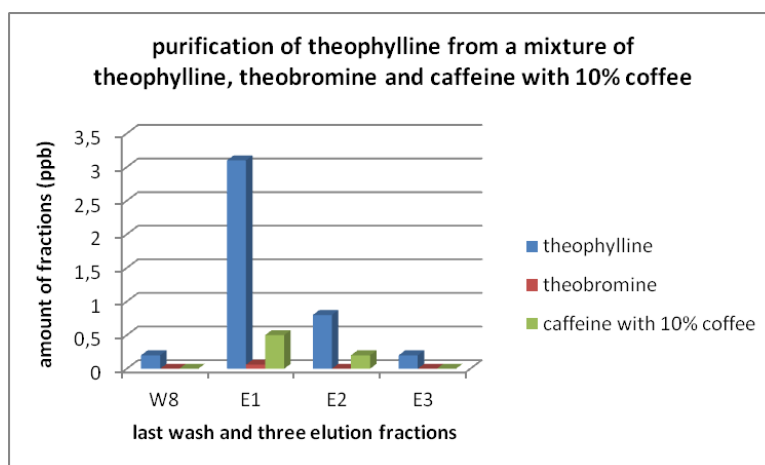


Figure 3.3.1 5: Purification of theophylline from a mixture of theophylline, theobromine and caffeine containing 10% coffee utilizing aptamer-modified carboxyl beads. Following samples were applied: (W8) wash fraction 8 (last wash fraction) and (E1-E3) eluates.

Figure 3.3.1 5 shows theophylline was successfully purified from the mixture. However, compared with the purification from the second experiment where a mixture of theobromine and caffeine was conducted, a little theobromine was contaminated in the first elution fraction and a little caffeine containing 10% coffee was contaminated in the first and second elution fractions. This is probably because that coffee is composed of more substances, like saccharides, cellulose, different acids, phenols, lignin, lipids, trigonelline and so forth [174]. It was assumed that some of these small substances could interfere in the specific binding of aptamers.

3.3.2 Aptamer-based depleting of malathion

Based on the successful purification of theophylline, the method was transferred to another target malathion (O, O'-dimethyl S-(1, 2-dicarbethoxyethyl) phosphorodithioate) to test the aptamer-based depleting of small molecules. Malathion ($C_{10}H_{19}O_6PS_2$, $M_r = 330.4$ g/mol) is an organophosphorus insecticide and acaricide. It is a racemate (Fig. 3.3.2 1). It is clear, colorless or slight yellow liquid, difficult to dissolve in water. This organophosphorus exhibits low mammalian toxicity. Even though the hazardous effects of malathion on human health and the ecosystems were already reported [175, 176], it continues to be one of the most utilized insecticides. In addition, malathion degrades in the environment by hydrolysis, photolysis, and biotransformation. It was reported that breakdown products of malathion are more toxic than the pesticide itself [177]. By hydrolysis at pH-value of about 6, the half-life of malathion reduced to one or two weeks [178]. Under a condition of pH 6 and 70 °C, malathion showed a half-life of 7 to 8 hours in 20% ethanol and water mixture [179]. In this thesis, malathion was chosen as a model system to demonstrate the applicability of aptamer-modified magnetic beads for the depletion of toxic compounds.

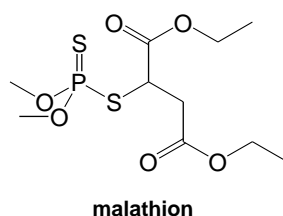


Figure 3.3.2 1: structure of malathion

In order to find out the actual aptamer sequence which directed against malathion. Both of these aptamer sequences, which were indicated in patent were first immobilized on carboxyl-modified magnetic beads with concentrations of 50 mg/ml and 20 mg/ml. Here, two beads concentrations were examined to find out a suitable aptamer loading density for the binding of malathion. The amount of immobilized aptamer (forward) was calculated based on the Lambert–Beer equation by an extinction coefficient of $765 \text{ mM}^{-1}\text{cm}^{-1}$, while the extinction coefficient of aptamer (reversed) is $657 \text{ mM}^{-1}\text{cm}^{-1}$. The molecular weight of malathion aptamer is 22616 g/mol. 173.9 pmol aptamer forward and 172.9 pmol aptamer reversed per mg beads were bound by beads concentration of 50 mg/ml. 387.3 pmol aptamer forward and 379.65 pmol aptamer reversed per mg beads were bound by beads concentration of 20 mg/ml. The beads concentration of 50 mg/ml resulted in lower

malathion aptamer immobilization than the beads concentration of 20 mg/ml. Concerning the molecular weight of malathion is smaller as PFEI, presumably higher aptamer loading density could be helpful for more binding of malathion. Therefore, beads with concentration of 20 mg/ml were used for the binding study with malathion.

To assess the functionalities of immobilized aptamers with forward and reversed sequences, the binding of malathion was performed. 10 fold excess malathion (5.48 $\mu\text{g/ml}$) of aptamer was added for the incubation. Binding buffer (500 mM NaCl, 10 mM Tris-HCl, 1 mM MgCl_2 , pH 7.2-7.4) was used for binding and washing. To release the bound malathion, three elution strategies were investigated. First, it was reported that Mg^{2+} might promote the aptamers' 3D folding [130]. 100 mM EDTA was added into the elution buffer (500 mM NaCl, 10 mM Tris-HCl, pH 7.2-7.4) as the first elution method. As already described for theophylline, binding of the target to the aptamer depended on the pH value, thus different pH values (3, 4, 9, 10) were adjusted in the elution buffer as the second elution method. Third, heating to 95°C was used to destroy the binding between aptamer and malathion. For this elution method, elution of malathion may not only be promoted by unfolding of the aptamer but also by destruction of malathion itself, which is known to be instable at elevated temperature [179].

The samples from first and third elution methods were analyzed by symrise (data not shown), no malathion was eluted from either aptamer forward or aptamer reversed. This is probably because malathion is poorly soluble in water. The chelate reaction by using EDTA was interfered. To solve this problem, 5% DMSO was added into the washing and elution buffer. Even after the optimization, no better results were seen. Regarding to the heat denaturation, malathion was degraded during heating at 95°C as prediction. It was also assumed that the analysis for malathion must be done as soon as possible, as malathion is very unstable. Thus, the samples from the second elution method (changing pH values) with optimized binding and elution conditions were analyzed via HPLC in our institut. 5% DMSO was added in the binding and elution buffer to overcome the disadvantage of malathion's poor solvability. Analysis was done directly after the downstream process.

Via HPLC, a peak appeared from the first elution fraction by using aptamer forward at pH 10 (Fig. 3.3.2 2). No peaks were seen by using aptamer reversed, which means that only the sequence of aptamer forward could bind to malathion. To determine the optimal pH

value for the elution of bound malathion, further three experiments were performed with pH values of 10, 10.5 and 11 in elution buffer. The results from HPLC showed that malathion could only be eluted by pH 10. Under pH values of 10.5 and 11, several peaks were shown in the elution fraction (data not shown), which indicated that malathion decomposed rapidly when using extreme pH values.

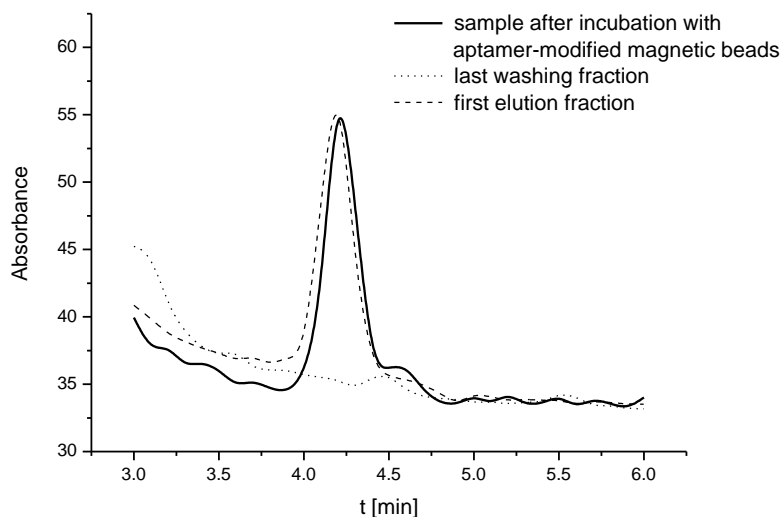


Figure 3.3.2 2: HPLC chromatography of different fractions originating from the aptamer-based capture of malathion.

To summarize, malathion can bind with the sequence of aptamer forward and can be eluted at pH 10 with adding 5% DMSO in the binding and elution buffer. Malathion is unstable. It degraded already partly during the downstream processes, especially under extreme pH values or higher temperature. In the further work, it is recommended to bind and elute malathions in dark at 4°C and the analysis should be conducted as soon as possible.

3.4 Aptamer-based detection of proteins via quantum dots

In addition to the application of aptamers in downstream processes, aptamers can also be used in the detection field. For example, aptamers are used in the field of aptasensors for detection of various substances [126, 127]. In this study, aptamer-based detection of proteins via quantum dot 525 was investigated.

525 ITKTM carboxyl-modified Quantum Dot (QD) was used. This QD was modified with carboxyl groups on the surface. First, aptamer 6H7 (200 μ M) was immobilized on 50 μ l QD 525, resulting in immobilization of 15 aptamer per QD, while PFEI (1 mg/ml, 0.5 μ l/per spot) as positive control and BSA (1mg/ml, 0.5 μ l/per spot) as negative control were printed on a nitrocellulose slide. After incubation the slide printed with PFEI and BSA with aptamer-modified QD 525, photo of the slide under UV irradiation is shown in Fig.3.4 1.



Figure 3.4 1: Detection of binding between aptamer and PFEI. Following samples were applied: (P) PFEI (positive control), (N) BSA (negative control).

In this photo, obvious binding was seen in the row of P (positive control), but no binding track was seen in the row of N (negative control). This result indicated that only PFEI can bind with anti-his-tag aptamer (6H7). It emphasized aptamer's binding specificity.

In addition to PFEI, HLA was also tested for the aptamer detection capability. 1 mg/ml HLA (0.5 μ l/per spot) was printed on the nitrocellulose slide, BSA (1mg/ml, 0.5 μ l/per spot) was used as negative control. Different concentrations of aptamer 6H7 (50 μ M, 100 μ M and 200 μ M) were immobilized on QD 525 and incubated with the slide. The photo of slide under UV irradiation is shown in Fig. 3.4 2.

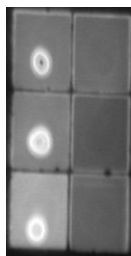


Figure 3.4 2: Detection of binding between aptamer and HLA. Left row: HLA (positive control), right row: BSA (negative control), from top to bottom: aptamer concentrations (50 μ M, 100 μ M, 200 μ M).

HLA was also successfully bound with aptamer 6H7. At aptamer concentration of 200 μ M, the slide displayed a strong background, which indicated the slide needed to be washed more times after incubation with aptamer-modified QD to reduce the background interference. Also, no binding track between aptamer 6H7 and BSA was found.

To examine if PFEI or HLA could bind directly on QDs, PFEI and HLA were printed on the nitrocellulose slide and incubated with QD 525 without aptamer. No binding track was found (data not shown). This demonstrated again the binding of his-tagged proteins were based on aptamer's specificity and affinity. In the future, F_c fragment or IgG can also be tested against aptamer-modified QDs. Moreover, instead of printing protein manually per pipette on the surface of slides, slides can be coated automatically via spotters. The automatic coating process by using for example a noncontact spotter enables the unity and presiseness of slide coating and allows the characterization via GenePix®Pro 6.1.

4 Summary and outlook

This study focused on the investigation of aptamer-based downstream processes for proteins and small molecules utilizing the recognition and binding properties of aptamers. The purification methods were developed on the basis of aptamer-modified magnetic beads and further transferred to aptamer-modified sepharose and CIM[®] DISK for the scale-up of protein purification. Besides, the basic aptamer-based protein detection was investigated via quantum dots.

4.1 Aptamer-based purification of his-tagged proteins

In a previous publication, amino-modified magnetic beads were used as solid supports for aptamers' immobilization and binding to their corresponding targets [36]. However, the amino-modified beads showed several disadvantages in the downstream processes. First, BSA and his-tagged protein PFEI bound unspecifically to the amino-modified surface. Secondly, the amino-modified surface may interact electrostatically with the phosphate backbone of aptamer which would result in misfolding and reduced binding activity of immobilized aptamer [122]. Third, toxic cyanuric chloride was required for the immobilization of amino-modified aptamers to the amino-modified beads. In order to overcome these disadvantages, an EDC-based immobilization strategy was developed in this study. Carboxyl-modified magnetic beads were employed for the EDC coupling chemistry. First, no unspecific binding of his-tagged proteins was determined on carboxyl-modified beads. Secondly, the purity degree of PFEI reached 100% (Table 4 1), which was even higher than by using amino-modified magnetic beads, which was 93%, as published in the literature [36]. Third, the elution efficiency of PFEI utilizing aptamer 6H7 immobilized on carboxyl-modified magnetic beads reached a high value of 97%, which was in accordance with that of amino-modified magnetic beads.

His-tagged protein HLA was used to demonstrate the general applicability of the developed aptamer-based purification strategy. The purity degree of HLA was 85.2% (Table 4 1) by using aptamer 6H5 (25 μ M) immobilized on carboxyl-modified beads.

To explore an automatic process, KingFisher was introduced. The automatic purification via KingFisher was successfully done. Results showed the automatic method was not suitable for the purification of proteins, which are sensible to room temperature.

Comparative experiments were made between aptamer-based methods and conventional purification methods. In this work, IMAC method for his-tagged proteins utilizing his-select nickel magnetic agarose beads was performed. Results showed no significant difference. The purity degree of PFEI by using conventional IMAC method was 99%, while utilizing aptamer 6H5-based purification, the purity degree of PFEI reached 100% (Table 4 1). By the aptamer-based purification strategy, the use of toxic transition metal could be avoided. Thus, the aptamer-based process has potential to replace IMAC in the purification of proteins that should for example be used in biomedical applications.

4.2 Aptamer-based purification of antibodies

It was reported in a previous publication that human IgG was successfully purified from cell culture supernatant via an RNA aptamer and purification efficiencies equivalent to protein A were achieved [148]. In this study, instead of RNA aptamer, DNA aptamers were introduced to purify F_c fragment and IgGs by using the purification method developed for his-tagged proteins. The used DNA aptamers show two main advantages over RNA aptamers, they are more stable and cheap. The obtained purity degree was 82.9% for F_c fragment and 97% for IgG (Table 4 1). Furthermore, elution efficiency for both F_c fragment and IgG reached 92% (Table 4 2).

Comparative experiments were performed utilizing protein A. Results showed no significant difference. For F_c fragment, the purity degree by using aptamer 264 immobilized on carboxyl-modified beads was 82.9%, while by using protein A was 94.7%. For IgG, the purity degree by using aptamer 264 immobilized on carboxyl-modified beads reached 97%, while by using protein A was only 79.3% (Table 4 1). Given the advantages of aptamers, that is, they are more easily to be produced, more stable and can be worked under milder conditions, aptamer-based downstream process has great potential to replace the conventional methods. Moreover, especially in the context of pharmaceutical antibody purification, the aptamers' non-immunogenicity is advantageous as well as their cell-free production.

4.3 Scale-up

In order to allow scale-up of aptamer-based purification strategies, the developed methods were transferred to sepharose 4 fast flow and CIM DISK. Compared with carboxyl-modified beads, there was no unspecific binding by using NHS-activated sepharose. Table 4 2 listed out the aptamers' functionalities by using different kinds of solid supports. In order to compare the results, all values are transferred to mg immobilized aptamer or mg bound and eluted target per mg solid support (Table 4 2). Carboxyl-modified magnetic beads, however, showed the highest amount of immobilized aptamer as well as bound and eluted protein per mg of support. This effect may be attributed to the optimized downstream processes for aptamer-modified magnetic beads. 25 μ M aptamer was found to be the optimal aptamer concentration during the immobilization for magnetic beads. This aptamer concentration was applied for 2 mg magnetic beads and was tested for the aptamer immobilization on 200 μ l of sepharose and one CIM DISK. It was estimated that 200 μ l sepharose correspond to 22.2 mg of dry sepharose, it was also weighted that one CIM DISK was 156.2 mg. Therefore, a higher applied aptamer concentration or a higher volume of applied aptamer solution could presumably enhance the aptamer loading density on sepharose and CIM DISK, resulting in improved binding capacity of the aptamer-modified material. Furthermore, the rather low aptamer activity of 56.1% for F_c fragment via aptamer 264-modified sepharose may be caused by the small pore size of sepharose interfering with the functionality of aptamer 264 (Table 4 2). This finding was confirmed by binding study with IgG. Because of a higher spatial demand of IgG, it could not bind with aptamer 264, which was immobilized on sepharose. On the contrary, F_c fragment was successfully purified with purity degree of 96.4% (Table 4 1) and elution efficiency of 97% (Table 4 2). To realize the binding of IgG, a spacer of PEG6 linked to the aptamer was introduced. The purity degree of IgG by using aptamer with integrated spacer immobilized on sepharose reached 60.9% (Table 4 1).

Based on the assumption that the small pore size of sepharose could lead to difficulties of aptamer functionality and result in limitations of diffusion for larger proteins, CIM[®] DISK with big internal pore size was chosen as an alternative support material for the scale-up. F_c fragment was successfully bound and eluted via aptamer-modified CIM[®] monolithic columns. The increased aptamer activity of 70.7% by using CIM DISK with big pore size supported the assumption (Table 4 2).

4.4 Aptamer-based purification and depleting of small molecules

Several publications have reported high affinity RNA aptamers for theophylline [86, 168, 169]. In this work, aptamer-based purification of theophylline utilizing carboxyl-modified magnetic beads was explored for the first time. An RNA/DNA chimera against theophylline was used as Chavez et al. have reported that chimera could enhance the stability against degradation [171]. Utilizing this RNA/DNA chimera and carboxyl-modified beads, theophylline was successfully bound and eluted. The elution efficiency reached 94%. After successful binding studies, the aptamer-based purification of theophylline from complex samples was tested. From an equimolar mixture of theophylline, theobromine and caffeine, theophylline was isolated with a purity degree of 100% (Table 4 1). From a mixture of theophylline, theobromine and caffeine containing 10% coffee, theophylline was purified with a purity degree of 85% (Table 4 1). These experiments emphasized that aptamers can discriminate extremely closely related molecular compounds. Moreover, the aptamer-beads-matrix was successfully regenerated. In addition, malathion was chosen to test the possibility of depleting contaminants by using aptamers. Results showed that malathion could bind to corresponding DNA aptamer and be eluted at pH 10 in the aptamer binding buffer with 5% DMSO.

4.5 Aptamer-based detection of proteins

Another purpose of this work was to investigate the aptamer-based protein detection. His-tagged proteins PFEI and HLA were employed. Quantum dot 525 was introduced as support material. Results showed that anti-his-tag aptamers bound specifically on corresponding his-tagged proteins. No binding between aptamers and BSA was found.

Table 4 1: list of purity degrees via aptamer-based purification methods and conventional methods

aptamer	type of solid supports	targets	purity (%)
6H5	carboxyl magnetic beads	PFEI (from <i>E. coli</i> lysate)	100
6H5	sepharose	PFEI (from <i>E. coli</i> lysate)	97.5
	agarose beads *	PFEI (from <i>E. coli</i> lysate)	99
6H5	carboxyl magnetic beads	HLA (from cell-culture supernatant)	85.2
6H5	sepharose	HLA (from cell-culture supernatant)	74.1
264	carboxyl magnetic beads	F _c fragment (from 10% FCS)	82.9
	protein A **	F _c fragment (from 10% FCS)	94.7
264	carboxyl magnetic beads	IgG (from 10% FCS)	97
	protein A **	IgG (from 10% FCS)	79.3
264	sepharose	F _c fragment (from 10% FCS)	96.4
264 + PEG 6	sepharose	IgG (from 10% FCS)	60.9
264	CIM DISK	F _c fragment (from 10% FCS)	100
theophylline aptamer	carboxyl magnetic beads	Theophylline (from a mixture with theobromine and caffeine)	100
theophylline aptamer	carboxyl magnetic beads	Theophylline (from a mixture with theobromine and caffeine containing 10% coffee)	85

* comparative experiments utilizing agarose beads for the purification of his-tagged proteins via IMAC

** comparative experiments utilizing protein A-modified magnetic beads

Table 4 2: list of aptamers' functionalities by using different kinds of solid supports

targets	types of solid supports	different aptamers c [25µM] ^a	D _{Apt} ^b [mg/mg beads or sepharose or disk]	Q _{target} ^c [mg/mg beads or sepharose or disk]	E _{target} ^d [mg/mg beads or sepharose or disk]	AA _{target} ^e [%]	EE _{target} ^f [%]
PFEI	carboxyl beads*	6H5	3.11x10 ⁻³	6.39x10 ⁻³	5.85x10 ⁻³	86.4	91.4
PFEI	sepharose**	6H5	2.91x10 ⁻³	1.87x10 ⁻³	4.66x10 ⁻⁴	27	24.9
F _c	carboxyl beads*	264	1.52x10 ⁻²	3.8x10 ⁻²	3.49x10 ⁻²	97.3	92
F _c	sepharose**	264	4.72x10 ⁻⁴	6.77x10 ⁻⁴	6.57x10 ⁻⁴	56.1	97
F _c	CIM DISK***	264	1.22 x10 ⁻³	2.2 x10 ⁻³	4.56 x10 ⁻⁴	70.7	20.7
IgG	carboxyl beads*	264	1.48x10 ⁻²	4.91x10 ⁻²	4.53x10 ⁻²	43.1	92.4
IgG	sepharose**	264+PEG6	6.9x10 ⁻⁴	8.15x10 ⁻⁴	1.04x10 ⁻⁴	15.6	12.8

^a applied different aptamers with concentration of 25 µM during immobilization, ^b aptamer immobilized on different types of solid supports, ^c targets bound to immobilized aptamer, ^d eluted targets, ^e aptamer efficiency ratio for targets (Q_{target}/D_{Apt}), ^f elution efficiency ratio for targets (E_{target}/Q_{target}).

* dry weight of carboxyl-modified beads was calculated via the indication provided by producer

** dry weight of NHS-activated sepharose was estimated from a swelling factor (4-5 ml/g) of sepharose

*** dry weight of CIM DISK was weighed without the ring

4.6 Outlook

The successive aptamers' immobilization on different kinds of solid supports developed in this study can be used as a versatile tool box for the purification of various proteins and small molecules, as well as for protein detection applications. Yet there are still many fields in this area to be further explored and investigated. For example, how reaction conditions of the aptamers' immobilization on different surfaces can be further optimized; how aptamer functionalities can be increased; how the binding and elution conditions for the targets can be modified; how the downstream process can be simplified; how the automatic purification procedure can be improved; how the operations utilizing fast protein liquid chromatography (FPLC) can be standardized. Furthermore, as larger proteins exhibit big spatial demands, suitable spacers between aptamers and surfaces of solid supports should be studied. Finally, aptamer-modified quantum dots for analytical applications should be further investigated in future work.

This study has provided aptamer-based downstream processes for proteins and small molecules via various solid supports and aptamer-based protein detection via quantum dots. It is hoped that it will contribute to a better understanding of aptamer properties and functionalities and the development of more stable purification methods by using aptamers.

5 Appendices

5.1 Materials

5.1.1 Chemicals

1-Ethyl-3-(3-dimethylaminopropyl)carbodiimid (EDC)	Sigma-Aldrich, Steinheim, DE
2-(N-morpholino) ethanesulfonic acid (MES)	Sigma-Aldrich, Steinheim, DE
Acetic acid	Fluka, Buchs, CH
Agarose	Fluka, Buchs, CH
Bovine serum albumin (BSA)	Sigma-Aldrich, Steinheim, DE
Bromophenol blue	Fluka, Buchs, CH
Calcium chloride	Fluka, Buchs, CH
Cobalt sulfate	Merck, Darmstadt, DE
Copper sulfate	Merck, Darmstadt, DE
Cyanuric chloride	Sigma-Aldrich, Steinheim, DE
Dimethyl sulfoxide (DMSO)	Sigma-Aldrich, Steinheim, DE
Disodium hydrogen phosphate	Sigma-Aldrich, Steinheim, DE
Ethanol (95%)	Merck, Darmstadt, DE
Ethidium bromide	Fluka, Buchs, CH
Ethylenediaminetetraacetic acid (EDTA)	Fluka, Buchs, CH
Formaldehyde solution (36.5%)	Fluka, Buchs, CH
Glycerol	Fluka, Buchs, CH
Hydrochloric acid	Fluka, Buchs, CH
Imidazole	Merck, Darmstadt, DE
Magnesium chloride	Fluka, Buchs, CH
Malathion	Sigma-Aldrich, Steinheim, DE
Monosodium phosphate	Merck, Darmstadt, DE
potassium chloride	Fluka, Buchs, CH
Potassium hexacyanoferrate (III)	Sigma-Aldrich, Steinheim, DE
Rhamnose	Sigma-Aldrich, Steinheim, DE
Sodium acetate	Carl Roth GmbH, Karlsruhe, DE
Sodium bicarbonate	Merck, Darmstadt, DE
Sodium carbonate	Merck, Darmstadt, DE
Sodium chloride	Fluka, Buchs, CH
Sodium dodecyl sulfate	Sigma-Aldrich, Steinheim, DE
Sodium hydroxide	Fluka, Buchs, CH
Sulfuric acid	Fluka, Buchs, CH
Theophylline	Sigma-Aldrich, Steinheim, DE
Tris-HCl	Carl Roth GmbH, Karlsruhe, DE

Tris-Base
 Tween 20
 Yeast extract

Carl Roth GmbH, Karlsruhe, DE
 Sigma-Aldrich, Steinheim, DE
 Fluka, Buchs, CH

5.1.2 Buffers and solutions

All buffer salts were purchased from Fluka (Buchs, Switzerland) and Sigma-Aldrich (Steinheim, Germany) and all are per analysis quality. All solutions were prepared with Millipore quality (MQ) water (ARIUM, Sartorius Stedim Biotech, Göttingen, Germany) and were filtered prior to use (Sartolab, bottle top filters, PES 0.2 µm pore size, Sartorius Stedim, Göttingen). The solutions for protein purification were also filtered and degassed in an ultrasonic bath. All used pipette tips, react-, centrifuger- and plastic-vessels were sterile.

Standard buffer:

LB-Medium	10 g/l tryptone, 10 g/l NaCl, 5 g/l yeast extract, autoclaved
PBS	137 mM NaCl, 2.7 mM KCl, 4.3 mM Na ₂ HPO ₄ , 1.4 mM KH ₂ PO ₄ , pH 7.5
TGS	25 mM Tris, 192 mM Glycin, 0,1 % SDS, pH 8.3
equilibration buffer for FPLC (IMAC)	0.1 M sodium acetate, 500 mM NaCl, pH 4.5
binding buffer for FPLC (IMAC)	50 mM NaH ₂ PO ₄ , 500 mM NaCl, pH 8.0
elution buffer for FPLC (IMAC)	50 mM NaH ₂ PO ₄ , 500 mM NaCl, 250 mM imidazole, 50% glycerine, pH 8.0

Aptamer selection buffer:

PBST-6H7	50 mM K ₂ HPO ₄ , 150 mM NaCl, 0.05% Tween 20, pH 7.5
264 - 266	20 mM Tris/HCl, 150 mM NaCl, 4 mM KCl, 1 mM MgCl ₂ , 1 mM CaCl ₂ , pH 7.3
theophylline	100 mM HEPES, 50 mM NaCl, 5 mM MgCl ₂ , pH 7.3
malathion	500 mM NaCl, 10 mM Tris-HCl, 1 mM MgCl ₂ , pH 7.2-7.4

5.1.3 Biomolecules

5.1.3.1 Aptamers

Aptamers 6H5 and 6H7 against his-tagged proteins were produced and modified by the company Biospring (Frankfurt, Germany). C₆-amino-linker was attached at the 5'-end of the aptamer. They are 40 nt full length aptamer.

Aptamers 264, 265 and 266 were also synthesized by the company BioSpring (Frankfurt am Main, DE) and 5'-modified with (C₆)-NH₂. Aptamers against the F_C fragment of human IgG (264, 265, 266) were selected by Aptares (Mittelwalde, Germany) utilizing the MonoLex process [103]. Selection was performed in selection buffer and the library was composed of:

TACGACTCACTATAGGGATCC-N₂₁-GAATTCCTTTAGTGAGGGTT, resulting in 63 nt full length aptamers. Aptamer 264_5'NH₂PEG6 is 65 nt full length aptamer.

The chimera (RNA/DNA-T) against theophylline is 49 nt full length DNA/RNA. Selection was performed in selection buffer.

Malathion aptamer is 72 nt full length DNA. Selection was performed in selection buffer.

6H7 [180]	GCTATGGGTGGTCTGGTTGGGATTGGCCCCGGGAGCTGGC
6H5 [180]	GGCTTCAGGTTGGTCTGGTTGGGTTTGGCTCCTGTGTACG
264 [103]	TACGACTCACTATAGGGATCCTTGCTTACATTACGACGTA CTGAATTCCTTTAGTGAGGGTT
265 [103]	TACGACTCACTATAGGGATCCATAGAAAACCCCTAAACGC CCGAATTCCTTTAGTGAGGGTT
266 [103]	TACGACTCACTATAGGGATCCTACGTCATTATGGAAACCG ACGAATTCCTTTAGTGAGGGTT
264+PEG6 [103]	12T ACG ACT CAC TAT AGG GAT CCT TGC TTA CAT TAC GAC GTA CTG AAT TCC CTT TAG TGA GGG TT
RNA/DNA-T [171]	CTCATCTGTGATCTAAGGCGAUACCAGCCGAAAGGCCCUU GGCAGCGUC
Malathion aptamer forward [172]	ATA CGG GAG CCA ACA CCA GCA GTC AAG AAG TTA AGA GAA AAA CAA TTG TGT ATA AGA GCA GGT GTG ACG GAT
Malathion aptamer reversed [172]	ATCCGTCACACCTGCTCTTATACACAATTGTTTTTCTCTTAA CTTCTTGACTGCTGGTGGTGGCTCCCGGTAT

5.1.3.2 Antibodies

Human F _c fragment	Dianova, Hamburg, DE
Human Immunoglobulin 1	Sigma, Traufkirchen, DE
Human Immunoglobulin 2	Sigma, Traufkirchen, DE
Human Immunoglobulin 3	Sigma, Traufkirchen, DE
Human Immunoglobulin 4	Sigma, Traufkirchen, DE
Human Immunoglobulin	Sigma, Traufkirchen, DE

5.1.3.3 Proteins

<i>Pseudomonas Fluorescens Esterase I</i> (PFEI)	Institut für Technische Chemie, Hannover, DE
Human leukocyte antigen (HLA)	Medical school Hannover, DE

5.1.3.4 Other materials

PageRuler™ Unstained Protein Ladder	Fermentas, St. Leon-Rot, DE
Unstained Protein Marker 26610	Thermo Scientific Inc., Bremen, DE
BioMag Amine-terminated magnetic beads	Polysciences, Inc., Warrington, PA
BioMag Carboxyl-terminated magnetic beads	Polysciences, Inc., Warrington, PA
BioMag Maxi Carboxyl-terminated magnetic beads	Polysciences, Inc., Warrington, PA
NHS-activated Sepharose 4 Fast Flow	GE Healthcare Bio-Sciences AB. (Sweden)
CIM® DISK, Monolithic Column	BIA Separations
His-Select Nickel Magnetic Agarose Beads	Sigma-Aldrich, Inc., DE
BioMag Protein A	QIAGEN, DE
Carboxyl-modified quantum dot 525	Labeling & detection, life technologies

5.1.3.5 Protein sequences

Nucleotide sequence of *Pseudomonas Fluorescens Esterase I* (PFEI) [164]:

```
mstfvakdgt qiyfkdwgsg kpvlfshgwl ldadmweyqm eylssrgyrt iafrdrpvwpl  
Gptldrqrlr hlrrrrhrpvd rtpgpqggdp gglhgrrrc gplhrppqr tggprgaagr  
Rhpavrpear lsagcpvdfv arfktellkd raqfisdfna pfyginkqv vsqgvqtql  
qiallaslka tvdcvtgspk ptsartwprs typpwypwrw rlrscsrpp akwrrs
```

5.1.4 Consumables

Centrifugal filter units	Millipore, Billerica, USA
Falcon tubes	Sarstedt, Nümbrecht, DE
Micro titer plate	Abgene, Rochester, USA
Minisart high flow filters	Sartorius, Göttingen, DE
PLASTIBRAND pipette tips	Brand, Wertheim, DE
Slide-A-Lyzer dialysis unit mini	Thermo Scientific, Waltham, USA
Vivaspins	Sartorius, Göttingen, DE

5.1.5 Equipments

Autoclave	Systec V-150	Systec GmbH, Wettengel, DE
Centrifuges	Centrifuge 5415 R Megafuge 1.0 RS	Eppendorf, Hamburg, DE Heraeus Instruments, Osterode, DE
FPLC	BioLogic DuoFlow System	BIO-RAD, München, DE
Gel electrophoresis	Thermo EC 105	Thermo Scientific, Waltham, USA
Incubator	CertomatR HK	B. Braun, Melsungen, DE
KingFisher	Thermo EC	Thermo Scientific, Waltham, USA
pH meter	HI 221 Calibration Check	Hanna Instruments, Kehl, DE
Plate welder	ALPSTM 50 V	Thermo Scientific, Waltham, USA
Rotator-mixer	Bio RS-24 Multi	PeQLab Biotechnologie GmbH, DE
Separator	6 Tube Magnetic Stand	Applied Biosystems Deutschland GmbH, Darmstadt
Shaker	MTS 4	IKA, Staufen, DE
Spectrophotometer	Nanodrop ND-1000 Nanodrop ND-3300	NanoD. Techn., Wilmington, USA NanoD. Techn., Wilmington, USA
Thermomixer	Thermomixer comfort	Eppendorf, Hamburg, DE
Ultrasonic bath	Sonorex Super RK 510 H	BANDELIN, Berlin, DE
UV desk	UV-SYSTEM	INTAS Science Imaging Instruments GmbH, Göttingen, DE
Water Purification System	Arium 611	Sartorius, Göttingen, DE
PI measuring	Fluoroskan Ascent	Thermo Electron Corporation, DE
Spectrophotometer	Multiskan Spectrum	Thermo Electron Corporation, DE

5.1.6 Software

SkanIt RE for MSS 2.1	Thermo Electron Corporation, DE
Ascent software for Fluoroskan Ascent	Thermo Electron Corporation, DE

KingFisher	Thermo Scientific, Waltham, USA
NanoDrop ND-1000	NanoD. Techn., Wilmington, USA
NanoPlotter NPC16	GeSiM, Großerkmannsdorf, DE

5.2 Methods

In the following sections, the methods frequently used in this study will be described. Subsequently, the optimized protocols of this thesis will be discussed chronologically.

5.2.1 General methods

5.2.1.1 Determination of concentrations of immobilized aptamers as well as bound and eluted proteins via NanoDropTM

Concentrations of aptamers and proteins can be determined with a NanoDropTM 1000 spectrophotometer (Thermo Scientific, Waltham, MA) by using the respective buffer as blank. For fluorescently labeled aptamers and proteins, NanoDropTM 3000 spectrophotometer can be utilized. To determine the average concentration value, all samples were measured 3 times.

The aptamer concentration can be determined via NanoDropTM 1000 by measuring the absorbance at $\lambda = 260$ nm. The concentrations were calculated based on the Lambert-Beer equation utilizing the respective extinction coefficients. Accordingly, following relation between the absorbance A and concentration C exists:

$$C = \frac{A}{\varepsilon \cdot d} \quad \text{(Formula 5.2.1.1: Lambert-Beer Law)}$$

C : aptamer concentration in $\mu\text{mol/l}$

A: absorbance by $\lambda = 260$ nm

ε : molar decadic extinction coefficients ε in ($\text{mM}^{-1}\text{cm}^{-1}$) – (provided by Biospring)

d: the layer thickness in cm (d= 1 cm)

With the help of NanoDrop ND 1000, the concentration of protein can be determined by measuring the absorbance at $\lambda = 280$ nm utilizing the Beer-Lambert law (formula 5.2.1.1). Accordingly, following relation between the absorbance A and concentration C exists:

$$C = \frac{A}{\varepsilon \cdot d} \quad \text{(Formula 5.2.1.1: Lambert-Beer Law)}$$

C: protein concentration in $\mu\text{mol/l}$

A: absorbance by $\lambda = 280 \text{ nm}$

ε : molar decadic extinction coefficients ε in ($\text{mM}^{-1}\text{cm}^{-1}$) – (calculated by online protein extinction coefficient calculator – BioMol.Net)

d: the layer thickness in cm ($d = 1 \text{ cm}$)

5.2.1.2 Determination of concentrations of immobilized aptamers via propidium iodide (PI) assay

Concentrations of aptamers can also be determined via PI assay. Per experiment, 25 μl solution of PI (0.1 mg/ml diluted in 0.9% NaCl) were added into 100 μl of sample solution (max. 5 μM DNA, as the calibration curve is no longer linear for DNA concentrations of 5-10 μM). After thoroughly mixing, the mixture was incubated in the dark for 30 minutes at room temperature. Measurements could be conducted in the fluoroskan ascent device with Abs/Em = 536/617 nm.

5.2.1.3 Determination of concentrations of bound and eluted proteins via Bradford assay

Concentrations of proteins can also be determined via Bradford protein assay [163] utilizing coomassie-Blue in a 96well Plate. Bovine serum albumin (BSA) was selected as standard protein for generating a calibration curve. This BSA standard curve is linear over a short range, from 0 $\mu\text{g/ml}$ to 200 $\mu\text{g/ml}$, the linearity is lost if the concentration is over 200 $\mu\text{g/ml}$. Thus it is necessary to dilute samples within the range before analysis. Concentrations of samples were calculated from absorbance values utilizing the formula of corresponding linear equations. Instead of using BSA, pure target protein can also be used as standard assay, in this study, pure IgG was also used as standard protein for the determination of IgG concentrations in the complex sample. First, BSA solutions (2 mg/ml in 0.9% NaCl solution) or pure IgG solutions were diluted in corresponding buffer to reach the concentrations of 0 $\mu\text{g/ml}$, 20 $\mu\text{g/ml}$, 40 $\mu\text{g/ml}$, 100 $\mu\text{g/ml}$, 150 $\mu\text{g/ml}$, and 200 $\mu\text{g/ml}$. Secondly, all samples for analysis were diluted in the range between 0 and 200 $\mu\text{g/ml}$. Third, 250 μl Bradford reagent were added to corresponding BSA (50 μl) and protein (50 μl) samples simultaneously. Afterwards, they were thoroughly mixed so that the developing colour was homogeneous. All samples were then pipetted into a 96-well plate.

After 15 minutes incubation at room temperature, the measurement of the absorbance was carried out at 595 nm by using multiskan spectrum device. Based on these measured values, a calibration curve can be obtained and taking into account the dilution factor used to calculate the protein concentration of the sample.

5.2.1.4 Determination of the amount of immobilized aptamers

To calculate the amount of aptamer in each fraction, the sample volume was required (Formula 5.2.1.4 A). The amount of immobilized aptamer was calculated via subtraction of the amount of the aptamer remaining in solution after immobilization (including the aptamer found in the washing fractions) from the amount of aptamer in the original solution (formula 5.2.1.4 B).

$$\text{Aptamer } [\mu\text{mol}] = C \left[\frac{\mu\text{mol}}{L} \right] * V [\mu\text{L}] * 10^{-3}$$

Formula 5.2.1.4 A: Calculation the amount of aptamer in each fraction (μmol)

$$\text{immobilized Aptamer } [\mu\text{mol}] = \text{Aptamer}_{(\text{applied})} [\mu\text{mol}] - \text{Aptamer}_{(\text{DL})} [\mu\text{mol}] - \text{Aptamer}_{(\text{Wash } 1)} [\mu\text{mol}] - \text{Aptamer}_{(\text{Wash } 2)} [\mu\text{mol}] - \text{Aptamer}_{(\text{Wash } 3)} [\mu\text{mol}] - \text{Aptamer}_{(\text{Wash } 4)} [\mu\text{mol}] \dots$$

Formula 5.2.1.4 B: Calculation the amount of immobilized Aptamer (μmol)

5.2.1.5 Determination of the amount of bound and eluted proteins

The same formulas were used to calculate the amount of bound and eluted protein in each fraction, taking into account the measured sample volume, the amount of bound protein was calculated via subtraction of the amount of the protein remaining in solution after incubation (including the protein found in the washing fractions) from the amount of protein in the original solution. Because imidazole disturbs the results adsorbtion at 280 nm determined by NanoDrop, eluates were first treated with dialysis (see 5.2.1.8) against the selection buffer. The amount of eluted protein was calculated via addition of the amount of the protein which was found in the elution fractions.

5.2.1.6 Calculation of aptamer activity

The aptamer activity was defined as the proportion of the immobilized aptamer that was able to bind the target. The activity can be calculated as the percentage of the amount of bound protein divided by immobilized aptamer on the solid supports according to formula 5.2.1.6.

$$\text{Aptamer activity (\%)} = \frac{\text{bound protein } [\mu\text{mol}]}{\text{immobilized aptamer } [\mu\text{mol}]} * 100\%$$

Formula 5.2.1.6: Calculation of aptamer activity (%)

5.2.1.7 Calculation of the elution efficiency

The elution efficient is the percentage of the amount of eluted protein divided by bound protein. The elution efficiency can be calculated according to formula 5.2.1.7.

$$\text{Elution efficiency (\%)} = \frac{\text{eluted protein } [\mu\text{mol}]}{\text{bound protein } [\mu\text{mol}]} * 100\%$$

Formula 5.2.1.7: Calculation of elution efficiency (%)

5.2.1.8 Dialysis

Slide-A-Lyzer mini dialysis units were used for the dialysis. Because imidazole interferes with the determination of protein concentration by using NanoDrop™ 1000, it is necessary to remove imidazole in the eluates via dialysis. Protein eluates contaminated with imidazole were pipetted into the dialysis units and incubated overnight in the corresponding aptamer selection buffer at 4°C.

5.2.1.9 Buffer exchange by ultrafiltration

The proteins originally dissolved in PBS buffer were rebuffed via ultrafiltration in the aptamer selection buffer. The ultrafiltration is based on the separation of proteins by using a membrane filter. Here, the membrane filter should have a defined pore size, which is smaller as the molecular weight of corresponding protein. Protein solution was added into the membrane filter. Higher molecular weight components, which are larger than the pore size of membrane, remained in the retentate after centrifugation.

300 µl solution of protein was concentrated to 100 µl via centrifugation at 13,000 rpm and 4°C for 2 minutes. Afterwards, 200 µl selection buffer was added into the concentrated protein solution and the centrifugation was repeated. After six times of rebuffering, the concentration of protein was set to 1 mg/ml in the selection buffer.

5.2.1.10 SDS-PAGE

- SDS-running buffer: 25 mM Tris, 192 mM Glycin, 0,1% SDS; pH 8,3 (1 x TGS)
- SDS-sample buffer: 20 mM Tris/HCl, 2 mM EDTA (Na-salt), 5% SDS, 0,02% Bromophenol blue in 90 ml H₂O, directly before use, 10% 2- Mercaptoethanol and 10% Glycerin (55%) were added to the sample buffer.

Table 5.2.1.10: Composition of separation gel (A) and stacking gel (B).

A			B	
component	12%	16%	component	6%
Polyacrylamide/Bisacrylamide -mixture (37.5:1), 40%	4.5 ml	6 ml	Polyacrylamide/Bisacrylamide -mixture (37.5:1), 40%	750 µl
SDS (1%)	1.5 ml	1.5 ml	SDS (1%)	300 µl
Tris/HCl (1.5 M), pH 8.8	4.2 ml	4.2 ml	Tris/HCl (1.5 M), pH 6.8	630 µl
ddH ₂ O	4.8 ml	3.3 ml	ddH ₂ O	3700 µl
TEMED	30 µl	30 µl	TEMED	10 µl
APS (25%)	30 µl	30 µl	APS (25%)	10 µl

The components of the separation gel were mixed and the solution was pipetted into the SDS-PAGE apparatus. After the polymerization of the separation gel (ca. 20 min.), the stacking gel was poured into the apparatus, after 20 minutes, the stacking gel was polymerized.

The protein samples were mixed 1:1 with the SDS-sample buffer and then heated for 10 minutes at 95°C. Subsequently, 10 µl of the samples and 3.5 µl of the protein-Ladder (Unstained Protein Ladder) were applied to the gel.

The separation was carried out first at 100 V. After the samples passed through the stacking gel, the running voltage was changed to 150 V. As soon as the bromphenol blue runned on of the bottom of the gel, the electrophoresis was stopped.

Silver staining

- Fixer: 500 ml H₂O, 500 ml EtOH, 100 ml acetic acid
- Farmers reducer: 0.1% potassium hexacyanoferrat (III) und 0.1% sodium thiosulfate
- 2.5% sodium carbonate solution
- 5% acetic acid
- 0.1% silver nitrate solution

The silver staining of the gel was performed on a shaker. First, the gel was incubated in fixer for 30 minutes at room temperature and 300 rpm. After two short washing steps with ultrapure water, the gel was incubated in 100 ml Farmers reducer solution for 2.5 min at room temperature and 300 rpm. Subsequently, the gel was washed with ultrapure water for three times, 10 minutes each and then incubated in 0.1% silver nitrate solution for 30 min at room temperature and 300 rpm. The gel was then washed with ultrapure water twice, 30 second each and rinsed with 2.5% sodium carbonate solution. To have a band development, the gel was incubated in 100 ml of 2.5% sodium carbonate solution with 400 µl formaldehyde solution (36.5%). To stop staining, the gel was put into the 5% acetic acid solution for 10 minutes. Afterwards, it was stored in ddH₂O.

5.2.2 Production of the target protein PFEI

5.2.2.1 His-Tag-Protein PFEI

His-tagged protein PFEI was produced from *E. coli* cells and purified by FPLC. The extraction and purification of the protein PFEI is described below.

5.2.2.1.1 Cultivation

For the preparation of pre-culture, 40 ml of LB-medium, 200 µl *E. coli* from frozen culture and 120 µl 25 mg/ml ampicillin derived solution were added into a 100 ml shake flask. The culture was incubated overnight in the shaker at 37°C and 150 rpm.

For the main-culture, 100 ml of LB-medium, 200 µl ampicillin solution (25 mg/ml) and 1 ml of the preculture were added into 500 ml shake flasks, respectively. The culture was

incubated in the shaker for 2-4 hours at 37 °C and 150 rpm. At an OD₆₀₀-value of 0.8-1.0, 1 ml rhamnose (0.2 g/ml) was added for the induction of PFEI-his. The cultures were incubated for further 4 h in the shaker at 37 °C and 150 rpm.

5.2.2.1.2 Cell harvest and disruption

The cultures were transferred into 50 ml centrifuge tubes and centrifuged with 4000 g for 15 minutes at 4°C. The supernatant was discarded as PFEI is expressed intracellularly. The cell pellets were then resuspended in 2-4 ml of 1 x PBS buffer and disrupted via ultrasonication for three times, one minute each (90 W, 0.6 sec pulse duration) under ice cooling. The cell constituents were centrifuged and the supernatant was selected. The successful expression was determined by SDS-PAGE analysis.

5.2.2.1.3 Purification via FPLC

- equilibration buffer: 0.1 M sodium acetate, 0.5 M NaCl, pH 4.5
- metal salt solutions: 0.1 M cobaltchloride (CoCl₂*6H₂O) in equilibration buffer, pH 4.5
- binding buffer: 50 mM NaH₂PO₄, 0.5 M NaCl, pH 8.0
- elution buffer: 0.1 M sodium acetate, 0.5 M NaCl, 0.1 M imidazole, 50% glycerol, pH 4.5

The implementation of the PFEI purification via FPLC is described below. Sartobind IDA 75 module was used as the membrane adsorber. All buffers and lysates were sterile filtered before. All buffers were degassed in an ultrasonic bath before use. The purification was carried out with a flow rate of 1 ml / min, and was monitored with a flow detector at 280 nm.

- The membrane adsorber was flushed with 10 ml of equilibration buffer.
- Subsequently, the membrane was loaded with 10 ml of 0.1 M cobaltchloride salt solution.
- Excess metal salt was washed away with 20 ml equilibration buffer.
- The membrane was rinsed with 20 ml binding buffer.
- The protein-containing sample was diluted in the binding buffer and passed through the adsorber.

- PFEI was eluted with 20 ml elution buffer.
- For membrane regeneration, the membrane was washed with 10 ml equilibration buffer and the metal ions were removed with 10 ml of 1 M sulfuric acid.
- The membrane was washed with 20 ml equilibration buffer and was stored in equilibration buffer supplemented with 0.02% sodium azide.

The success of the purification was monitored via SDS-PAGE analysis.

5.2.3 Immobilization of aptamers on different solid supports

The coupling of aptamers and the subsequent washing steps of all the following experiments were performed in eppendorf tubes (except for CIM[®] DISK, which was performed in the 6-well-plate) under rotation of 20 rpm by utilizing a rotator (Shaker Rotator Bio-RS-24, Peqlab, Erlangen, Germany). Magnetic separations were performed manually by using a magnetic separator (6 Tube Magnetic Stand, Applied Biosystems Deutschland GmbH, Darmstadt).

5.2.3.1 Immobilization of aptamers on magnetic beads

As an alternative to columns, magnetic nanoparticles were developed for a quick and easy extraction of biomolecules. The immobilization of aptamers on two types of magnetic beads is described below.

5.2.3.1.1 Immobilization of aptamers on amino-modified magnetic beads

To achieve the covalent binding between amino-modified aptamers and amino-modified magnetic beads, either the amino-linker from aptamer or the amino-groups on the surface of magnetic beads need to be activated. First, the amino-modified aptamers were activated via cyanuric chloride.

- Aptamer activation via cyanuric chloride

Aptamer 6H7 (5'-GCT ATG GGT GGT CTG GTT GGG ATT GGC CCC GGG AGC TGG C-3') was diluted in ddH₂O to adjust the concentration to 220 μM.

100 μl aptamer 6H7 (220 μM) was further diluted in 100 μL 0.2 M sodium borate buffer (1.2366 g Boric acid in 100 ml ddH₂O, pH 8.4) to get an aptamer concentration of 110 μM – the concentration was determined with the help of NanoDrop ND 1000 [1:100 diluted in 0.1 M sodium borate buffer (0.6183 g Boric acid in 100 ml ddH₂O, pH 8.4)].

22 μl freshly prepared cyanuric chloride solution (9.2 mg cyanuric chloride diluted in 10 ml acetonitrile) were added into 100 μl aptamer 6H7 (110 μM) solution and incubated for one hour at room temperature.

Excess of cyanuric chloride was removed by buffer exchange with in 0.1 M sodium borate buffer for 6 times by using vivaspins with 3 kDa membrane – the concentration was determined again with the help of NanoDrop ND 1000 (1:100 diluted in 0.1 M sodium borate buffer).

- Immobilization of activated aptamer on the amino-modified magnetic beads

100 μl of the amino-modified magnetic particle suspension (20 mg/ml) were washed with 100 μl 0.1 M sodium borate buffer (pH 8.4) twice, 15 minutes each. 100 μl activated aptamer 6H7 solution diluted in 0.1 sodium borate buffer (pH 8.4) to achieve three different aptamer concentrations (25 μM , 45 μM and 85 μM), these three aptamer 6H7 solutions were added into the washed magnetic beads and incubated with them for 2 hours at room temperature. To remove unbound aptamer, the aptamer-modified magnetic beads were washed with 100 μl of 0.1 M sodium borate buffer (pH 8.4) for three times, 15 minutes each. Finally, the aptamer 6H7 modified-magnetic beads were washed with selection buffer (50 mM K₂HPO₄, 150 mM NaCl, 0.05% Tween 20, pH 7.5) for 15 minutes, transferred to fresh SB and stored at 4°C.

5.2.3.1.2 *Capping of amino-modified magnetic beads*

Because PFEI can bind directly on the amino-modified magnetic beads, comparatively not directly on the carboxyl-modified magnetic beads, amino surface was modified via succinic anhydride (capping) before binding with aptamer.

Per capping, 100 μ l amino-modified magnetic beads suspension (20 mg/ml) was collected via magnetic separator. 100 μ l succinic anhydride solutions [0.138 g succinic anhydride + 8.5 ml dimethyl sulfoxide (DMSO) + 0.5 ml 0.1 M sodium bicarbonate, pH 9.4] were added to the collected beads and incubated with them for 5 minutes at room temperature. Afterwards, the beads were washed with 100 μ l ddH₂O for three times, one minute each at room temperature. Finally, the beads were further washed with 100 μ l 25 mM MES buffer [2-(N-morpholino) ethanesulfonic acid, pH 6.0] twice, 10 minutes each at room temperature. After capping, the amino groups were transferred to carboxyl groups. In order to immobilize amino-modified aptamers onto capped magnetic beads, an EDC-mediated coupling was used.

5.2.3.1.3 Immobilization of aptamers on carboxyl-modified magnetic beads

Two binding processes for the aptamer immobilization on carboxyl-modified magnetic beads were tested.

First, the two steps coating process was performed. Thereby 100 μ L of carboxyl-modified magnetic beads suspension (20 mg/ml) was washed with 100 μ l 25 mM MES buffer (pH 6) twice, 10 minutes each at room temperature. A freshly prepared mixture of 16.7 μ l solution of NHS and 16.7 μ l solution of EDC (50 mg/ml in ice cold 25 mM MES buffer, pH 6) was added into the washed beads and incubated with them for 30 minutes at room temperature. After incubation, the beads were washed with 100 μ l 25 mM MES buffer (pH 6) twice, 10 minutes each. Afterwards, 100 μ l of 100 μ M amino-modified aptamer 6H7 in 25 mM MES (pH 6) were added into the activated beads and incubated for one hour at room temperature. In order to remove the unbound aptamers, the aptamer-beads mixture was washed with 100 μ l 50 mM Tris buffer (pH 7.4) for four times, 15 minutes each at room temperature. Consequently, the coated beads were resuspended to 100 μ l selection buffer (PBST-6H7) and stored at 2-8 °C.

By one step coating procedure, 100 μ l of the carboxyl-modified magnetic particle suspension (20 mg/ml) were washed with 100 μ l 25 mM MES (pH 6) twice, 10 min each. Afterwards 100 μ l of 25 μ M (for some experiment, different concentrations of aptamers were applied) aptamer solution in MES (pH 6) was added into washed beads and incubated with them for 30 minutes at room temperature. EDC solution (10 mg/ml) was freshly prepared in ice cold MES (pH 6) and 30 μ l of this solution were added to the aptamer and

magnetic beads suspension. The coupling was performed at 4°C overnight. To remove unbound aptamer, the aptamer-modified magnetic beads were washed with 100 µl of 50 mM Tris buffer (pH 7.4) for four times, 10 minutes each. Finally, the magnetic beads were washed with selection buffer (SB, pH 7.5) for 30 minutes, transferred to fresh SB and stored at 4°C.

5.2.3.2 Immobilization of aptamers on NHS-modified sepharose

200 µl NHS-modified sepharose suspension were pipetted into a 2 ml eppendorf tubes, the sepharose particles were washed with 1 ml ice cold HCl (1 mM) for four times, 10 minutes each at 4°C and 20 rpm. After each washing fraction, particles were settled down for 20 minutes and 900 µl supernatant were removed. 200 µl aptamer (diluted in standard buffer: 25 µM in 0.2 M NaHCO₃, 0.5 M NaCl, pH 8.3) were added into the washed sepharose particles. After incubation over night at 4°C, the aptamer-modified sepharose was then blocked with 1 ml Tris buffer (50 mM, pH 7.4) for 8 times, 15 minutes each at 4°C. Consequently, to fold the immobilized aptamer, the aptamer-modified sepharose was washed with 1 ml aptamer selection buffer (20 mM Tris, 150 mM NaCl, 4 mM KCl, 1 mM MgCl₂, 1 mM CaCl₂, pH7.3) twice, 15 minutes each at 4°C. After washing, the aptamer-modified sepharose was stored in SB at 4°C.

5.2.3.3 Immobilization of aptamers on methyl-carboxyl-modified CIM[®] DISK

The washing and incubation process of CIM[®] DISK was performed in a 6 well-plate. The CIM[®] DISK was washed first with 1 ml MES buffer (25 mM, pH 6) twice, 30 min each at room temperature. Afterwards, 1 ml of 25 µM aptamer was added into the washed CIM[®] DISK and incubated with it for 30 minutes at roomtemperature. After incubation, 300 µl ice-cold freshly prepared EDC (10 mg/ml in MES buffer) were added into the solution. The reaction was further performed over night at 4°C and 300 rpm. In order to remove unbound aptamer, the aptamer-modified CIM[®] DISK was washed with 1 ml Tris buffer (50 mM, pH 7.4) for four times, 15 minutes each at 4°C. Consequently, the aptamer-modified CIM[®] DISK was washed with 1 ml aptamer selection buffer for 15 minutes at 4°C.

5.2.4 Aptamer-based downstream process for his-tagged proteins

5.2.4.1 Aptamer-based purification of PFEI

The self produced PFEI was first rebuffered into the aptamer selection buffer (50 mM K_2HPO_4 , 150 mM NaCl, 0.05% Tween 20, pH 7.5), in which the aptamers were selected. The rebuffering process was performed in a VIVASPIN 500 membrane (10,000 MWCOPEs). Afterwards, the rebuffered PFEI was diluted to a concentration of 1 mg/ml. 100 μ L of PFEI (1 mg/ml) was then added to and incubated with aptamer-modified-matrix for four hours at 4°C. To remove unbound and unspecifically bound PFEI, the aptamer-modified matrix bound with PFEI was washed with 100 μ L of wash buffer 1 (SB + 350 mM NaCl, pH 7.5) for 10 minutes at 4°C, and then washed with wash buffer 2 (SB + 350 mM NaCl + 1 M KCl, pH 7.5) for another 10 minutes at 4°C, and one time more with wash buffer 1 for 30 minutes at 4°C. Afterwards, PFEI was eluted with elution buffer (SB + 1M imidazole, pH 7.5) twice (30 min. + 10 min.) at 4°C. Finally, the aptamer-modified matrix was transferred to fresh SB and stored at 4°C.

5.2.4.2 Aptamer-based purification of HLA

His-tagged protein HLA was first rebuffered into the selection buffer (50 mM K_2HPO_4 , 150 mM NaCl, 0.05% Tween 20, pH 7.5), in which the aptamers were selected. The rebuffering process was performed in a VIVASPIN 500 membrane (10,000 MWCOPEs). The concentration of rebuffered HLA was set to 1 mg/ml. 100 μ L of HLA (1 mg/ml) was then added to and incubated with aptamer-modified-matrix for four hours at 4°C. To remove unbound and unspecifically bound HLA, the aptamer-modified matrix bound with HLA was washed with 100 μ L of selection buffer for three times (2x10 min., 1x30 min.) at 4°C and 20 rpm. Subsequently, HLA was eluted with elution buffer (SB + 1M imidazole, pH 7.5) twice (30 min. + 10 min.) at 4°C. Finally, the aptamer-modified matrix was transferred to fresh SB and stored at 4°C.

5.2.4.3 Aptamer-based automatic downstream process via KingFisher

KingFisher was used to achieve the automatic aptamer-based downstream process. First, the automatic procedure was programmed with the help of KingFischer software. All

samples and buffers were pipetted into the 96-well-plate. The automatic process is described below:

- 1) 100 μ l of with MES buffer (25 mM, pH 6.0) washed carboxyl-beads – collect beads
- 2) 100 μ l aptamer (diluted in MES) + 30 μ l EDC (in 25 μ M ice-cold MES), 2 hours incubation, slowly – collect beads
- 3) 100 μ l Tris (50 mM, pH 7.4), 15 minutes washing, slowly – collect beads
- 4) 100 μ l Tris (50 mM, pH 7.4), 15 minutes washing, slowly – collect beads
- 5) 100 μ l Tris (50 mM, pH 7.4), 15 minutes washing, slowly – collect beads
- 6) 100 μ l Tris (50 mM, pH 7.4), 15 minutes washing, slowly – collect beads
- 7) 100 μ l PBST-6H7 buffer (pH 7.5), 30 minutes washing, slowly – collect beads
- 8) 100 μ l PBST-6H7 buffer – regeneration

The finished samples were stored at 4°C.

5.2.5 Aptamer-based downstream process for antibodies

The commercial F_c fragment and IgG were first rebuffered into the SB (20 mM Tris, 150 mM NaCl, 4 mM KCl, 1 mM MgCl₂, 1 mM CaCl₂, pH 7.3), in which the aptamers were selected. The rebuffering process was performed utilizing a 10 kDa centrifugal membrane. Afterwards, the F_c fragment and IgG were diluted to a concentration of 1 mg/ml. 100 μ l (except for CIM[®] DISK was 1 ml) each of these samples was then added and incubated with aptamer-modified matrix for four hours at 4°C. To remove unbound and unspecifically bound F_c fragment and IgG, the aptamer-modified matrix bound with F_c fragment or IgG was washed with 100 μ l (for sepharose and CIM[®] DISK were 1 ml) of wash buffer 1 (SB + 500 mM KCl, pH 7.3) for 20 minutes at 4°C, and then washed with SB (pH 7.3) for two times more, 20 minutes each at 4°C. Afterwards, the F_c fragment or IgG was eluted with elution buffer (20 mM Tris, 300 mM EDTA, pH 7.3) twice, 30 minutes each at 4°C. Finally, the aptamer-modified matrix was transferred to fresh SB and stored at 4°C.

5.2.6 Aptamer-based downstream process for small molecules

5.2.6.1 Aptamer-based purification of theophylline

20 mg/ml carboxyl-modified magnetic particle suspension was concentrated to 50 mg/ml. Three identical experiments were done in parallel. Per experiment, 100 μ l of the magnetic particle suspension (50 mg/ml) was washed with 100 μ l MES buffer (25 mM, pH 6) twice, 10 minutes each. Afterwards 100 μ l of 25 μ M theophylline aptamer solution in MES (pH 6) was added and incubated for 30 minutes at room temperature. EDC solution (10 mg/ml) was prepared in ice-cold MES buffer (pH 6) immediately before 30 μ l of this solution was added to the aptamer and magnetic beads suspension. The coupling was performed at 4°C overnight. To remove unbound aptamer, the aptamer-modified magnetic beads were washed with 100 μ l of 50 mM Tris buffer (pH 7.4) for four-times, 15 minutes each and washed further with theophylline binding buffer (100 mM HEPES, 50 mM NaCl, 5 mM MgCl₂, pH 7.3) for 30 minutes at 4°C. Finally, the aptamer-modified magnetic beads were transferred to fresh theophylline binding buffer and stored at 4°C.

All aptamer-modified magnetic beads resulting from the three experiments were combined. 10-fold excess of theophylline was added and incubated with 300 μ l aptamer-modified magnetic particle suspension for 30 minutes at 65°C and 600 rpm. During the incubation, the suspension was resuspended every 5 minutes. Afterwards, the suspension was cooled to 20°C. The temperature dropped ca. 5°C in every 3 minutes, while the suspension was resuspended every 3 minutes. The theophylline-aptamer-beads suspension was incubated for further 2 hours at room temperature. After incubation, the suspension was washed with theophylline binding buffer for 6 times, 15 minutes each. Consequently, the bound theophylline was eluted via different elution methods.

First, theophylline was eluted with elution buffer 1 (100 mM HEPES, 100 mM EDTA, 50 mM NaCl, pH 7.3) for two times (1x30 min. and 1x15 min.). Secondly, theophylline was eluted via heating at 95°C in elution buffer 2 (100 mM HEPES, 50 mM NaCl, pH 7.3) twice, 15 minutes each. During the heating, the suspension was resuspended in every 5 minutes. Third, theophylline was eluted via heating at 95°C in elution buffer 3 (100 mM HEPES, 50 mM NaCl, pH 5) for two times (1x30 min. and 1x15 min.). Last, theophylline was eluted with elution buffer 4 (100 mM HEPES, 7 M urea, 50 mM NaCl, pH 7.3) for twice, 15 minutes each.

5.2.6.2 Aptamer-based purification of malathion

100 µl of the carboxyl-modified magnetic particle suspension (20 mg/ml and 50 mg/ml) were washed with 100 µl MES buffer (25 mM, pH 6) twice, 10 minutes each. Afterwards 100 µl of 25 µM malathion aptamer (forward and reversed) solution in MES (pH 6) was added and incubated for 30 minutes at room temperature. EDC solution (10 mg/ml) was prepared in ice-cold MES buffer (pH 6) immediately before 30 µl of this solution was added to the aptamer and magnetic beads suspension. The coupling was performed at 4°C overnight. To remove unbound aptamer, the aptamer-modified magnetic beads were washed with 100 µl of 50 mM Tris buffer (pH 7.4) for four times, 15 minutes each. Finally, the aptamer-modified magnetic beads were washed with malathion binding buffer (500 mM NaCl, 10 mM Tris-HCl, 1 mM MgCl₂, pH 7.2-7.4) for 30 minutes at 4°C and transferred to fresh malathion binding buffer and stored at 4°C.

Malathion can be purified via aptamer-modified magnetic beads. Before incubation with malathion, the aptamer-modified magnetic beads were first heated at 95°C for 5 minutes. After heating, the aptamer-beads matrix was incubated with SB for 5 hours at 4°C. 10-fold excess malathion (5.48 µg/ml) of aptamer was added and incubated with the aptamer-modified beads over night at 4°C. The malathion aptamer-modified beads were then washed with malathion binding buffer (500 mM NaCl, 10 mM Tris-HCl, 1 mM MgCl₂, pH 7.2-7.4) for three times (2x10 min. and 1x30 min.) at 4°C. Consequently, malathion was eluted with binding buffer under different pH-values (binding buffer, pH 3, 4, 9, 10).

5.2.7 Conventional purification methods

5.2.7.1 Purification of lysate (PFEI) via his-select nickel magnetic agarose beads

PFEI containing *E. coli* lysate was first rebuffered into 1xPBS buffer, the rebuffered PFEI was diluted in a buffer of PBST-6H7 + 20 mM imidazole to a concentration of 1 mg/ml. 100 µl of prepared PFEI (1 mg/ml) were added and incubated with 100 µl his-select nickel magnetic agarose beads for 4 hours and 20 rpm at 4°C. After incubation, the nickel magnetic agarose beads were washed with 1 ml wash buffer (50 mM sodium phosphate, pH 8.0, 0.3 M sodium chloride, 10 mM imidazole) for three times, 10 minutes each at 4°C and 20 rpm. Consequently, PFEI was eluted with 500 µl elution buffer (50 mM sodium phosphate, pH 8.0, 0.3 M sodium chloride, 250 mM imidazole) for 15 minutes at 4°C.

5.2.7.2 Purification of antibodies via BioMag[®] Protein A

100 μl BioMag[®] Protein A particles were pipetted into a 1.5 ml microcentrifuge tube. The BioMag particles were washed with 750 μl protein A buffer (0.1 M Tris-HCl, 0.15 M NaCl, pH 7.5) for three times, 10 minutes each. After washing, 50 μl of 1 mg/ml F_c fragment and 10% FCS or 50 μl of 1 mg/ml IgG and 10% FCS were diluted in 50 μl protein A buffer and added to the BioMag particles and then incubated for 1 hour at room temperature. During the incubation, the tube was vortexed every 5 minutes. Afterwards, the BioMag particles were washed with 750 μl protein A buffer for three times, 15 minutes each. 50 μl glycine (0.1 M) was added, the pH-value was adjusted to 2.5. The tube was vortexed and incubated for 5 minutes at room temperature. Consequently, 2.5 μl NaOH (1 M) was added to the eluted fraction.

5.2.8 Aptamer-based detection of proteins via quantum dots

5.2.8.1 Immobilization of aptamers on ITK carboxyl-modified quantum dots

50 μl of 8 μM carboxyl-modified quantum dots 525 were washed with 200 μl MES buffer (100 mM, pH 6.0) via 10 kDa MWCO centrifugal membrane with 4000 g for 2.5 minutes at room temperature. The volume was concentrated from 250 μl to 50 μl . The washed quantum dots were diluted with MES to 400 μl and transferred into an eppendorf tube. 196 μl quantum dots were transferred into another eppendorf tube, 49 μl aptamer solutions (300 μM) were added and incubated with 196 μl quantum dots for 30 minutes at room temperature. After incubation, 9.8 μl ice-cold freshly prepared EDC (5.75 mg/ml in MES) were added to the solution. The reaction was performed over night at 4°C and 20 rpm.

After immobilization of aptamers to quantum dots, 100 μl aptamer-modified quantum dots were pipetted into a 100 kDa MWCO centrifugal membrane. 400 μl Tris buffer (50 mM Tris, pH 7.4) were added into the centrifugal membrane. The solution was centrifuged with 4000 g and this washing step was repeated 6 times, 2.5 minutes each at 4°C. 400 μl flow-throughs from each washing fraction were stored in eppendorf tubes at 4°C for the quantification. After 6 times washing, the supernatant was diluted with Tris buffer to 200 μl . 100 μl of this solution were dialysed in PBST-6H7 at 4°C overnight.

5.2.8.2 Detection of proteins via aptamer-modified quantum dots

After diaysis, volume of the remaining solution was measured via pipettes. The concentration of aptamer-modified quantum dots (19220.23 pmol aptamer were immobilized to 76.9 μ l 8 μ M QD 525) was determined via NanoDrop™ 3000. 40 μ l solutions were selected and diluted with 760 μ l PBST-6H7 buffer.

0.5 μ l PFEI (1 mg/ml) (or HLA, 1 mg/ml) and 0.5 μ l BSA (1 mg/ml, as negative control) were pipetted on a nitrocellulose slide. The slide was then incubated for 30 minutes at room temperature. Afterwards, the slide surface was blocked with 2% milk powder (in PBS buffer) for 45 minutes at room temperature. The slide was then washed with PBST-6H7 buffer for three times, 5 minutes each at room temperature. 800 μ l aptamer-modified quantum dots solutions were incubated with the slide via an adhesive film in a plastic box over night at room temperature under light exclusion. After incubation, the slide was washed with PBST-6H7 in the dark for 3 times, 10 minutes each. Consequently, the slide was dried under a stream of nitrogen. The slide was detected under a UV light (312 nm).

5.3 Abbreviations

μM:	μ mol/L
3D:	Three dimensional
ADP:	Adenosine d iphosphate
AMP:	Adenosine m onophosphate
APS:	Ammonium p ersulfate
ATP:	Adenosine t riphosphate
AVP:	Arginine- v asopressin
BSA:	B ovine S erum A lbumin
CEC:	C apillary E lectro C hromatography
CHO:	C hinese H amster O vary
ddH₂O:	D idistilled water
DMSO:	D imethyl S ulfoxide
DNA:	D eoxyribo n ucleic a cid
EC:	E fficiency r ation
EDC:	1-Ethyl-3-(3- d imethylaminopropyl) c arbodiimid

EDTA:	Ethylenediaminetetraacetic acid
ELISA:	Enzyme-linked immuno sorbent assay
FCS:	Fetal Calf Serum
FMN:	Flavin Mononucleotide
FPLC:	Fast Protein Liquid Chromatography
HCV:	Hepatitis C Virus
HLA:	Human Leukocyte Antigen
HPLC:	High-pressure Liquid Chromatography
IgG:	Immunoglobulin G
kDa:	Kilodalton
LC:	Liquid Chromatography
MHH:	Medical School Hannover
MES:	2-(N-Morpholino)ethanesulfonic acid
NAD:	Nicotinamide adenine dinucleotide
NHS:	N-Hydroxysuccinimide
NMR:	Nuclear Magnetic Resonance
PBS:	Phosphate Buffered Saline
PCR:	Polymerase Chain Reaction
PEG:	Polyethylene glycol
PFEI:	Pseudomonas Fluorescens Esterase
PI:	Isoelectric Point
PI:	Propidium Iodide
QD:	Quantum Dot
RNA:	Ribonucleic acid
rpm:	rounds per minute
RT-PCR:	Real Time - Polymerase Chain Reaction
SB:	Selection Buffer
SDS:	Sodium Dodecyl Sulfate
SDS PAGE:	Sodium Dodecyl Sulfate Polyacrylamide Gel Electrophoresis
SELEX:	Systematic Evolution of Ligands by Exponential enrichment
TEMED:	Tetramethylethylenediamine
Tris:	Tris(hydroxymethyl)aminomethane
UV:	Ultraviolet

6 References

1. Ellington, A.D. and J.W. Szostak, *In vitro selection of RNA molecules that bind specific ligands*. Nature, 1990. **346**(6287): p. 818-22.
2. Wieland, M., et al., *Artificial ribozyme switches containing natural riboswitch aptamer domains*. Angew Chem Int Ed Engl, 2009. **48**(15): p. 2715-8.
3. Sinha, J., S.J. Reyes, and J.P. Gallivan, *Reprogramming bacteria to seek and destroy an herbicide*. Nat Chem Biol. **6**(6): p. 464-70.
4. Tuerk, C. and L. Gold, *Systematic evolution of ligands by exponential enrichment: RNA ligands to bacteriophage T4 DNA polymerase*. Science, 1990. **249**(4968): p. 505-10.
5. Daksis, J.I. and G.H. Erikson, *Specific triplex binding capacity of mixed base sequence duplex nucleic acids used for single-nucleotide polymorphism detection*. Genet Test, 2005. **9**(2): p. 111-20.
6. Catz, S.D., J.L. Johnson, and B.M. Babior, *Characterization of the nucleotide-binding capacity and the ATPase activity of the PIP3-binding protein JFC1*. Proc Natl Acad Sci U S A, 2001. **98**(20): p. 11230-5.
7. Paszkiewicz-Gadek, A., A. Gindzienski, and H. Porowska, *Nucleotide-sugar binding to ribosomes. Comparison of affinity and capacity of gastric mucosa and liver ribosomes to sugar-nucleotides*. Roczn Akad Med Białymst, 1996. **41**(2): p. 305-15.
8. Hong, E.S., et al., *Mass spectrometric studies of alkali metal ion binding on thrombin-binding aptamer DNA*. J Am Soc Mass Spectrom. **21**(7): p. 1245-55.
9. Noeske, J., H. Schwalbe, and J. Wohnert, *Metal-ion binding and metal-ion induced folding of the adenine-sensing riboswitch aptamer domain*. Nucleic Acids Res, 2007. **35**(15): p. 5262-73.
10. Sussman, D., J.C. Nix, and C. Wilson, *The structural basis for molecular recognition by the vitamin B 12 RNA aptamer*. Nat Struct Biol, 2000. **7**(1): p. 53-7.
11. Battig, M.R., B. Soontornworajit, and Y. Wang, *Programmable release of multiple protein drugs from aptamer-functionalized hydrogels via nucleic acid hybridization*. J Am Chem Soc. **134**(30): p. 12410-3.
12. Patel, D.J. and A.K. Suri, *Structure, recognition and discrimination in RNA aptamer complexes with cofactors, amino acids, drugs and aminoglycoside antibiotics*. J Biotechnol, 2000. **74**(1): p. 39-60.
13. Zhang, L., et al., *Co-delivery of hydrophobic and hydrophilic drugs from nanoparticle-aptamer bioconjugates*. ChemMedChem, 2007. **2**(9): p. 1268-71.
14. Chen, Y.H., et al., *HIV-1 gp41 contains two sites for interaction with several proteins on the helper T-lymphoid cell line, H9*. AIDS, 1992. **6**(6): p. 533-9.
15. Lupold, S.E., et al., *Identification and characterization of nuclease-stabilized RNA molecules that bind human prostate cancer cells via the prostate-specific membrane antigen*. Cancer Res, 2002. **62**(14): p. 4029-33.
16. Le Tinevez, R., R.K. Mishra, and J.J. Toulme, *Selective inhibition of cell-free translation by oligonucleotides targeted to a mRNA hairpin structure*. Nucleic Acids Res, 1998. **26**(10): p. 2273-8.
17. Pileur, F., et al., *Selective inhibitory DNA aptamers of the human RNase H1*. Nucleic Acids Res, 2003. **31**(19): p. 5776-88.
18. Kim, Y.M., et al., *Specific modulation of the anti-DNA autoantibody-nucleic acids interaction by the high affinity RNA aptamer*. Biochem Biophys Res Commun, 2003. **300**(2): p. 516-23.

19. Berens, C., A. Thain, and R. Schroeder, *A tetracycline-binding RNA aptamer*. *Bioorg Med Chem*, 2001. **9**(10): p. 2549-56.
20. Geiger, A., et al., *RNA aptamers that bind L-arginine with sub-micromolar dissociation constants and high enantioselectivity*. *Nucleic Acids Res*, 1996. **24**(6): p. 1029-36.
21. Gopinath, S.C., et al., *An RNA aptamer that distinguishes between closely related human influenza viruses and inhibits haemagglutinin-mediated membrane fusion*. *J Gen Virol*, 2006. **87**(Pt 3): p. 479-87.
22. Labib, M., et al., *Aptamer-based viability impedimetric sensor for viruses*. *Anal Chem*. **84**(4): p. 1813-6.
23. Hwang do, W., et al., *A nucleolin-targeted multimodal nanoparticle imaging probe for tracking cancer cells using an aptamer*. *J Nucl Med*. **51**(1): p. 98-105.
24. Mairal, T., et al., *Aptamers: molecular tools for analytical applications*. *Anal Bioanal Chem*, 2008. **390**(4): p. 989-1007.
25. Pan, Y., et al., *Selective collection and detection of leukemia cells on a magnet-quartz crystal microbalance system using aptamer-conjugated magnetic beads*. *Biosens Bioelectron*. **25**(7): p. 1609-14.
26. Zhu, X., et al., *Aptamer-based and DNAzyme-linked colorimetric detection of cancer cells*. *Protein Cell*. **1**(9): p. 842-6.
27. Breaker, R.R., *DNA enzymes*. *Nature Biotechnology*, 1997. **15**(5): p. 427-431.
28. Nutiu, R., et al., *Engineering DNA aptamers and DNA enzymes with fluorescence-signaling properties*. *Pure and Applied Chemistry*, 2004. **76**(7-8): p. 1547-1561.
29. Farrow, M.A. and P. Schimmel, *Editing by a tRNA synthetase: DNA aptamer-induced translocation and hydrolysis of a misactivated amino acid*. *Biochemistry*, 2001. **40**(14): p. 4478-83.
30. Konopka, K., et al., *Receptor ligand-facilitated cationic liposome delivery of anti-HIV-1 Rev-binding aptamer and ribozyme DNAs*. *J Drug Target*, 1998. **5**(4): p. 247-59.
31. Golub, E., et al., *Hemin/G-quadruplexes as DNAzymes for the fluorescent detection of DNA, aptamer-thrombin complexes, and probing the activity of glucose oxidase*. *Analyst*. **136**(21): p. 4397-401.
32. Adler, A., et al., *Post-SELEX chemical optimization of a trypanosome-specific RNA aptamer*. *Comb Chem High Throughput Screen*, 2008. **11**(1): p. 16-23.
33. Stoltenburg, R., C. Reinemann, and B. Strehlitz, *FluMag-SELEX as an advantageous method for DNA aptamer selection*. *Anal Bioanal Chem*, 2005. **383**(1): p. 83-91.
34. Zhao, Q., X.F. Li, and X.C. Le, *Aptamer capturing of enzymes on magnetic beads to enhance assay specificity and sensitivity*. *Anal Chem*. **83**(24): p. 9234-6.
35. Tennico, Y.H., et al., *On-chip aptamer-based sandwich assay for thrombin detection employing magnetic beads and quantum dots*. *Anal Chem*. **82**(13): p. 5591-7.
36. Kokpinar, O., et al., *Aptamer-based downstream processing of his-tagged proteins utilizing magnetic beads*. *Biotechnol Bioeng*.
37. Yan, X., et al., *DNA aptamer folding on magnetic beads for sequential detection of adenosine and cocaine by substrate-resolved chemiluminescence technology*. *Analyst*. **135**(9): p. 2400-7.
38. Centi, S., et al., *Different approaches for the detection of thrombin by an electrochemical aptamer-based assay coupled to magnetic beads*. *Biosens Bioelectron*, 2008. **23**(11): p. 1602-9.

39. Oktem, H.A., et al., *Single-step purification of recombinant Thermus aquaticus DNA polymerase using DNA-aptamer immobilized novel affinity magnetic beads*. Biotechnol Prog, 2007. **23**(1): p. 146-54.
40. Mani, R.J., et al., *Bi-cell surface plasmon resonance detection of aptamer mediated thrombin capture in serum*. Biosens Bioelectron. **26**(12): p. 4832-6.
41. Nam, E.J., et al., *Highly sensitive electrochemical detection of proteins using aptamer-coated gold nanoparticles and surface enzyme reactions*. Analyst. **137**(9): p. 2011-6.
42. Wang, J. and H.S. Zhou, *Aptamer-based Au nanoparticles-enhanced surface plasmon resonance detection of small molecules*. Anal Chem, 2008. **80**(18): p. 7174-8.
43. Lee, S.J., et al., *ssDNA aptamer-based surface plasmon resonance biosensor for the detection of retinol binding protein 4 for the early diagnosis of type 2 diabetes*. Anal Chem, 2008. **80**(8): p. 2867-73.
44. Balamurugan, S., et al., *Surface immobilization methods for aptamer diagnostic applications*. Anal Bioanal Chem, 2008. **390**(4): p. 1009-21.
45. Cole, J.R., et al., *Affinity capture and detection of immunoglobulin E in human serum using an aptamer-modified surface in matrix-assisted laser desorption/ionization mass spectrometry*. Anal Chem, 2007. **79**(1): p. 273-9.
46. Shao, K., et al., *Emulsion PCR: a high efficient way of PCR amplification of random DNA libraries in aptamer selection*. PLoS One. **6**(9): p. e24910.
47. Liao, S., et al., *Aptamer-Based Sensitive Detection of Target Molecules via RT-PCR Signal Amplification*. Bioconjug Chem. **21**(12): p. 2183-9.
48. Carothers, J.M., et al., *Informational complexity and functional activity of RNA structures*. J Am Chem Soc, 2004. **126**(16): p. 5130-7.
49. Stead, S.L., et al., *An RNA-aptamer-based assay for the detection and analysis of malachite green and leucomalachite green residues in fish tissue*. Anal Chem. **82**(7): p. 2652-60.
50. Latham, J.A. and T.R. Cech, *Defining the inside and outside of a catalytic RNA molecule*. Science, 1989. **245**(4915): p. 276-82.
51. Cech, T.R., *RNA as an enzyme*. Biochem Int, 1989. **18**(1): p. 7-14.
52. Altman, S., *Ribonuclease P: an enzyme with a catalytic RNA subunit*. Adv Enzymol Relat Areas Mol Biol, 1989. **62**: p. 1-36.
53. Robertson, D.L. and G.F. Joyce, *Selection in vitro of an RNA enzyme that specifically cleaves single-stranded DNA*. Nature, 1990. **344**(6265): p. 467-8.
54. Ellington, A.D. and J.W. Szostak, *Selection in vitro of single-stranded DNA molecules that fold into specific ligand-binding structures*. Nature, 1992. **355**(6363): p. 850-2.
55. Brumby, A., et al., *Chiral stationary phase based on a biostable L-RNA aptamer*. Anal Chem, 2005. **77**(7): p. 1993-8.
56. Lee, K.Y., et al., *Bioimaging of nucleolin aptamer-containing 5-(N-benzylcarboxamide)-2'-deoxyuridine more capable of specific binding to targets in cancer cells*. J Biomed Biotechnol. **2010**: p. 168306.
57. Klevenz, B., K. Butz, and F. Hoppe-Seyler, *Peptide aptamers: exchange of the thioredoxin-A scaffold by alternative platform proteins and its influence on target protein binding*. Cell Mol Life Sci, 2002. **59**(11): p. 1993-8.
58. Watson, S.R., et al., *Anti-L-selectin aptamers: binding characteristics, pharmacokinetic parameters, and activity against an intravascular target in vivo*. Antisense Nucleic Acid Drug Dev, 2000. **10**(2): p. 63-75.

59. Ohuchi, S.P., T. Ohtsu, and Y. Nakamura, *A novel method to generate aptamers against recombinant targets displayed on the cell surface*. *Nucleic Acids Symp Ser (Oxf)*, 2005(49): p. 351-2.
60. Pestourie, C., B. Tavitian, and F. Duconge, *Aptamers against extracellular targets for in vivo applications*. *Biochimie*, 2005. **87**(9-10): p. 921-30.
61. Cox, J.C., et al., *Automated selection of aptamers against protein targets translated in vitro: from gene to aptamer*. *Nucleic Acids Res*, 2002. **30**(20): p. e108.
62. Pestourie, C., et al., *Comparison of different strategies to select aptamers against a transmembrane protein target*. *Oligonucleotides*, 2006. **16**(4): p. 323-35.
63. Schultze, P., R.F. Macaya, and J. Feigon, *Three-dimensional solution structure of the thrombin-binding DNA aptamer d(GGTTGGTGTGGTTGG)*. *J Mol Biol*, 1994. **235**(5): p. 1532-47.
64. Bing, T., et al., *Conservative secondary structure motif of streptavidin-binding aptamers generated by different laboratories*. *Bioorg Med Chem*. **18**(5): p. 1798-805.
65. Kuwahara, M., et al., *Screening of modified DNA aptamers that recognize DNA secondary structure*. *Nucleic Acids Symp Ser (Oxf)*, 2004(48): p. 265-6.
66. Huang, Z. and J.W. Szostak, *Evolution of aptamers with a new specificity and new secondary structures from an ATP aptamer*. *RNA*, 2003. **9**(12): p. 1456-63.
67. Wang, K.Y., et al., *The tertiary structure of a DNA aptamer which binds to and inhibits thrombin determines activity*. *Biochemistry*, 1993. **32**(42): p. 11285-92.
68. Sekiya, S., et al., *Analysis of interaction between RNA aptamer and protein using nucleotide analogs*. *Nucleic Acids Symp Ser*, 2000(44): p. 163-4.
69. Tinoco, I., Jr. and C. Bustamante, *How RNA folds*. *J Mol Biol*, 1999. **293**(2): p. 271-81.
70. Brion, P. and E. Westhof, *Hierarchy and dynamics of RNA folding*. *Annu Rev Biophys Biomol Struct*, 1997. **26**: p. 113-37.
71. Ilyas, A., et al., *Electrical detection of cancer biomarker using aptamers with nanogap break-junctions*. *Nanotechnology*. **23**(27): p. 275502.
72. Deissler, H.L. and G.E. Lang, *[Effect of VEGF165 and the VEGF aptamer pegaptanib (Macugen) on the protein composition of tight junctions in microvascular endothelial cells of the retina]*. *Klin Monbl Augenheilkd*, 2008. **225**(10): p. 863-7.
73. Wyatt, J.R., J.D. Puglisi, and I. Tinoco, Jr., *RNA folding: pseudoknots, loops and bulges*. *Bioessays*, 1989. **11**(4): p. 100-6.
74. Kim, M.Y. and S. Jeong, *RNA aptamers that bind the nucleocapsid protein contain pseudoknots*. *Mol Cells*, 2003. **16**(3): p. 413-7.
75. Lambert, D., et al., *The influence of monovalent cation size on the stability of RNA tertiary structures*. *J Mol Biol*, 2009. **390**(4): p. 791-804.
76. Hamel, E., et al., *Modulation of tubulin-nucleotide interactions by metal ions: comparison of beryllium with magnesium and initial studies with other cations*. *Arch Biochem Biophys*, 1992. **295**(2): p. 327-39.
77. Tajmir-Riahi, H.A., *Interaction of La (III) and Tb (III) ions with purine nucleotides: evidence for metal chelation (N-7-M-PO3) and the effect of macrochelate formation on the nucleotide sugar conformation*. *Biopolymers*, 1991. **31**(9): p. 1065-75.
78. Green, S.M., et al., *Roles of metal ions in the maintenance of the tertiary and quaternary structure of arginase from Saccharomyces cerevisiae*. *J Biol Chem*, 1991. **266**(32): p. 21474-81.

79. Boada, F.E., et al., *Non-invasive assessment of tumor proliferation using triple quantum filtered ²³Na MRI: technical challenges and solutions*. Conf Proc IEEE Eng Med Biol Soc, 2004. **7**: p. 5238-41.
80. Nonaka, Y., K. Sode, and K. Ikebukuro, *Screening and improvement of an anti-VEGF DNA aptamer*. *Molecules*. **15**(1): p. 215-25.
81. McKeague, M., et al., *Screening and initial binding assessment of fumonisin b(1) aptamers*. *Int J Mol Sci*. **11**(12): p. 4864-81.
82. Conn, G.L. and D.E. Draper, *RNA structure*. *Curr Opin Struct Biol*, 1998. **8**(3): p. 278-85.
83. Sakamoto, T., et al., *NMR structures of double loops of an RNA aptamer against mammalian initiation factor 4A*. *Nucleic Acids Res*, 2005. **33**(2): p. 745-54.
84. Westhof, E. and V. Fritsch, *RNA folding: beyond Watson-Crick pairs*. *Structure*, 2000. **8**(3): p. R55-65.
85. Hermann, T. and D.J. Patel, *Adaptive recognition by nucleic acid aptamers*. *Science*, 2000. **287**(5454): p. 820-5.
86. Zimmermann, G.R., et al., *Molecular interactions and metal binding in the theophylline-binding core of an RNA aptamer*. *RNA*, 2000. **6**(5): p. 659-67.
87. Williamson, J.R., *Induced fit in RNA-protein recognition*. *Nat Struct Biol*, 2000. **7**(10): p. 834-7.
88. Zhang, D.W., et al., *A label-free aptasensor for the sensitive and specific detection of cocaine using supramolecular aptamer fragments/target complex by electrochemical impedance spectroscopy*. *Talanta*. **92**: p. 65-71.
89. Nomura, Y., et al., *Conformational plasticity of RNA for target recognition as revealed by the 2.15 Å crystal structure of a human IgG-aptamer complex*. *Nucleic Acids Res*. **38**(21): p. 7822-9.
90. Jayasena, S.D., *Aptamers: an emerging class of molecules that rival antibodies in diagnostics*. *Clin Chem*, 1999. **45**(9): p. 1628-50.
91. Tang, Q., X. Su, and K.P. Loh, *Surface plasmon resonance spectroscopy study of interfacial binding of thrombin to antithrombin DNA aptamers*. *J Colloid Interface Sci*, 2007. **315**(1): p. 99-106.
92. Hianik, T., et al., *Influence of ionic strength, pH and aptamer configuration for binding affinity to thrombin*. *Bioelectrochemistry*, 2007. **70**(1): p. 127-33.
93. Wilson, D.S. and J.W. Szostak, *In vitro selection of functional nucleic acids*. *Annu Rev Biochem*, 1999. **68**: p. 611-47.
94. Tombelli, S., et al., *Aptamer-based biosensors for the detection of HIV-1 Tat protein*. *Bioelectrochemistry*, 2005. **67**(2): p. 135-41.
95. Gold, L., *Oligonucleotides as research, diagnostic, and therapeutic agents*. *J Biol Chem*, 1995. **270**(23): p. 13581-4.
96. Tan, X., et al., *Molecular beacon aptamers for direct and universal quantitation of recombinant proteins from cell lysates*. *Anal Chem*. **84**(19): p. 8272-6.
97. Hou, S., et al., *Study on the interaction between nucleic acids and imidacloprid and its application*. *Nucleosides Nucleotides Nucleic Acids*, 2009. **28**(11): p. 989-97.
98. Yuan, Y., et al., *Prediction of interactiveness of proteins and nucleic acids based on feature selections*. *Mol Divers*. **14**(4): p. 627-33.
99. Li, Y., et al., *Nucleic acids in protein samples interfere with phosphopeptide identification by immobilized-metal-ion affinity chromatography and mass spectrometry*. *Mol Biotechnol*, 2009. **43**(1): p. 59-66.
100. Proske, D., et al., *Aptamers--basic research, drug development, and clinical applications*. *Appl Microbiol Biotechnol*, 2005. **69**(4): p. 367-74.
101. Gopinath, S.C., *Methods developed for SELEX*. *Anal Bioanal Chem*, 2007. **387**(1): p. 171-82.

102. Stoltenburg, R., C. Reinemann, and B. Strehlitz, *SELEX--a (r)evolutionary method to generate high-affinity nucleic acid ligands*. *Biomol Eng*, 2007. **24**(4): p. 381-403.
103. Nitsche, A., et al., *One-step selection of Vaccinia virus-binding DNA aptamers by MonoLEX*. *BMC Biotechnol*, 2007. **7**: p. 48.
104. Kim, Y.S., et al., *Isolation and characterization of enantioselective DNA aptamers for ibuprofen*. *Bioorg Med Chem*. **18**(10): p. 3467-73.
105. Park, H. and I.R. Paeng, *Development of direct competitive enzyme-linked aptamer assay for determination of dopamine in serum*. *Anal Chim Acta*. **685**(1): p. 65-73.
106. Wang, J., et al., *Aptamer-Au NPs conjugates-enhanced SPR sensing for the ultrasensitive sandwich immunoassay*. *Biosens Bioelectron*, 2009. **25**(1): p. 124-9.
107. Shimada, J., et al., *DNA-enzyme conjugate with a weak inhibitor that can specifically detect thrombin in a homogeneous medium*. *Anal Biochem*. **414**(1): p. 103-8.
108. Ferreira, C.S., et al., *DNA aptamers against the MUC1 tumour marker: design of aptamer-antibody sandwich ELISA for the early diagnosis of epithelial tumours*. *Anal Bioanal Chem*, 2008. **390**(4): p. 1039-50.
109. Huang, D.W., et al., *Time-resolved fluorescence aptamer-based sandwich assay for thrombin detection*. *Talanta*. **83**(1): p. 185-9.
110. Pultar, J., et al., *Aptamer-antibody on-chip sandwich immunoassay for detection of CRP in spiked serum*. *Biosens Bioelectron*, 2009. **24**(5): p. 1456-61.
111. O'Donoghue, M.B., et al., *Single-molecule atomic force microscopy on live cells compares aptamer and antibody rupture forces*. *Anal Bioanal Chem*. **402**(10): p. 3205-9.
112. Schlecht, U., et al., *Comparison of antibody and aptamer receptors for the specific detection of thrombin with a nanometer gap-sized impedance biosensor*. *Anal Chim Acta*, 2006. **573-574**: p. 65-8.
113. Dwarakanath, S., et al., *Quantum dot-antibody and aptamer conjugates shift fluorescence upon binding bacteria*. *Biochem Biophys Res Commun*, 2004. **325**(3): p. 739-43.
114. Sanz, J.C., et al., *Assessment of RNA amplification by multiplex RT-PCR and IgM detection by indirect and capture ELISAs for the diagnosis of measles and rubella*. *APMIS*. **118**(3): p. 203-9.
115. Rodriguez-Medina, J.R., et al., *Hepatitis C viral RNA amplification by the polymerase chain reaction allows detection of false positive HCV ELISAs among patients with non-A, non-B hepatitis*. *P R Health Sci J*, 1993. **12**(1): p. 35-8.
116. Shin, S., et al., *An alternative to Western blot analysis using RNA aptamer-functionalized quantum dots*. *Bioorg Med Chem Lett*. **20**(11): p. 3322-5.
117. Yang, X., et al., *Immunofluorescence assay and flow-cytometry selection of bead-bound aptamers*. *Nucleic Acids Res*, 2003. **31**(10): p. e54.
118. Davis, K.A., et al., *Staining of cell surface human CD4 with 2'-F-pyrimidine-containing RNA aptamers for flow cytometry*. *Nucleic Acids Res*, 1998. **26**(17): p. 3915-24.
119. Collett, J.R., et al., *Functional RNA microarrays for high-throughput screening of anti-protein aptamers*. *Anal Biochem*, 2005. **338**(1): p. 113-23.
120. Murray, E., et al., *Microarray-formatted clinical biomarker assay development using peptide aptamers to anterior gradient-2*. *Biochemistry*, 2007. **46**(48): p. 13742-51.
121. Lee, M. and D.R. Walt, *A fiber-optic microarray biosensor using aptamers as receptors*. *Anal Biochem*, 2000. **282**(1): p. 142-6.
122. Walter, J.G., et al., *Systematic investigation of optimal aptamer immobilization for protein-microarray applications*. *Anal Chem*, 2008. **80**(19): p. 7372-8.

123. Cerchia, L., et al., *Cell-specific aptamers for targeted therapies*. Methods Mol Biol, 2009. **535**: p. 59-78.
124. Thiel, K.W. and P.H. Giangrande, *Therapeutic applications of DNA and RNA aptamers*. Oligonucleotides, 2009. **19**(3): p. 209-22.
125. *Preclinical and phase IA clinical evaluation of an anti-VEGF pegylated aptamer (EYE001) for the treatment of exudative age-related macular degeneration*. Retina, 2002. **22**(2): p. 143-52.
126. Sefah, K., et al., *Nucleic acid aptamers for biosensors and bio-analytical applications*. Analyst, 2009. **134**(9): p. 1765-75.
127. Torres-Chavolla, E. and E.C. Alocilja, *Aptasensors for detection of microbial and viral pathogens*. Biosens Bioelectron, 2009. **24**(11): p. 3175-82.
128. Murphy, M.B., et al., *An improved method for the in vitro evolution of aptamers and applications in protein detection and purification*. Nucleic Acids Res, 2003. **31**(18): p. e110.
129. Romig, T.S., C. Bell, and D.W. Drolet, *Aptamer affinity chromatography: combinatorial chemistry applied to protein purification*. J Chromatogr B Biomed Sci Appl, 1999. **731**(2): p. 275-84.
130. Peyrin, E., *Nucleic acid aptamer molecular recognition principles and application in liquid chromatography and capillary electrophoresis*. J Sep Sci, 2009. **32**(10): p. 1531-6.
131. Michaud, M., et al., *A DNA aptamer as a new target-specific chiral selector for HPLC*. J Am Chem Soc, 2003. **125**(28): p. 8672-9.
132. Johanna-Gabriela Walter, F.S., Thomas Scheper, *Aptamers as affinity ligands for downstream processing*. Eng. Life Sci. , 2012. **12**: p. No. 5, 1-11.
133. Deng, Q., et al., *Retention and separation of adenosine and analogues by affinity chromatography with an aptamer stationary phase*. Anal Chem, 2001. **73**(22): p. 5415-21.
134. Deng, Q., C.J. Watson, and R.T. Kennedy, *Aptamer affinity chromatography for rapid assay of adenosine in microdialysis samples collected in vivo*. J Chromatogr A, 2003. **1005**(1-2): p. 123-30.
135. Clark, B.J. and J.E. Mama, *Resolution of chiral compounds by HPLC using mobile phase additives and a porous graphitic carbon stationary phase*. J Pharm Biomed Anal, 1989. **7**(12): p. 1883-8.
136. Clark, S.L. and V.T. Remcho, *Electrochromatographic retention studies on a flavin-binding RNA aptamer sorbent*. Anal Chem, 2003. **75**(21): p. 5692-6.
137. Clark, J.E. and S.V. Olesik, *Technique for ultrathin layer chromatography using an electrospun, nanofibrous stationary phase*. Anal Chem, 2009. **81**(10): p. 4121-9.
138. Zhang, Y., et al., *Development of an immobilized P-glycoprotein stationary phase for on-line liquid chromatographic determination of drug-binding affinities*. J Chromatogr B Biomed Sci Appl, 2000. **739**(1): p. 33-7.
139. Rehder, M.A. and L.B. McGown, *Open-tubular capillary electrochromatography of bovine beta-lactoglobulin variants A and B using an aptamer stationary phase*. Electrophoresis, 2001. **22**(17): p. 3759-64.
140. Ruta, J., et al., *Covalently bonded DNA aptamer chiral stationary phase for the chromatographic resolution of adenosine*. Anal Bioanal Chem, 2008. **390**(4): p. 1051-7.
141. Michaud, M., et al., *Immobilized DNA aptamers as target-specific chiral stationary phases for resolution of nucleoside and amino acid derivative enantiomers*. Anal Chem, 2004. **76**(4): p. 1015-20.
142. Kotia, R.B., L. Li, and L.B. McGown, *Separation of nontarget compounds by DNA aptamers*. Anal Chem, 2000. **72**(4): p. 827-31.

143. Charles, J.A. and L.B. McGown, *Separation of Trp-Arg and Arg-Trp using G-quartet-forming DNA oligonucleotides in open-tubular capillary electrochromatography*. Electrophoresis, 2002. **23**(11): p. 1599-604.
144. Vo, T.U. and L.B. McGown, *Selectivity of quadruplex DNA stationary phases toward amino acids in homodipeptides and alanyl dipeptides*. Electrophoresis, 2004. **25**(9): p. 1230-6.
145. Vo, T.U. and L.B. McGown, *Effects of G-quartet DNA stationary phase destabilization on fibrinogen peptide resolution in capillary electrochromatography*. Electrophoresis, 2006. **27**(4): p. 749-56.
146. Rehder-Silinski, M.A. and L.B. McGown, *Capillary electrochromatographic separation of bovine milk proteins using a G-quartet DNA stationary phase*. J Chromatogr A, 2003. **1008**(2): p. 233-45.
147. Connor, A.C. and L.B. McGown, *Aptamer stationary phase for protein capture in affinity capillary chromatography*. J Chromatogr A, 2006. **1111**(2): p. 115-9.
148. Miyakawa, S., et al., *Structural and molecular basis for hyperspecificity of RNA aptamer to human immunoglobulin G*. RNA, 2008. **14**(6): p. 1154-63.
149. Sugiyama, S., et al., *Crystallization and preliminary X-ray diffraction studies of an RNA aptamer in complex with the human IgG Fc fragment*. Acta Crystallogr Sect F Struct Biol Cryst Commun, 2008. **64**(Pt 10): p. 942-4.
150. Zhao, Q., X.F. Li, and X.C. Le, *Aptamer-modified monolithic capillary chromatography for protein separation and detection*. Anal Chem, 2008. **80**(10): p. 3915-20.
151. Bock, L.C., et al., *Selection of single-stranded DNA molecules that bind and inhibit human thrombin*. Nature, 1992. **355**(6360): p. 564-6.
152. Dick, L.W., Jr. and L.B. McGown, *Aptamer-enhanced laser desorption/ionization for affinity mass spectrometry*. Anal Chem, 2004. **76**(11): p. 3037-41.
153. Ravelet, C., C. Grosset, and E. Peyrin, *Liquid chromatography, electrochromatography and capillary electrophoresis applications of DNA and RNA aptamers*. J Chromatogr A, 2006. **1117**(1): p. 1-10.
154. Ravelet, C., et al., *A L-RNA aptamer chiral stationary phase for the resolution of target and related compounds*. J Chromatogr A, 2005. **1076**(1-2): p. 62-70.
155. Ruta, J., et al., *Aptamer-based enantioselective competitive binding assay for the trace enantiomer detection*. Anal Chem, 2007. **79**(12): p. 4716-9.
156. Zhao, Q., et al., *Aptamer-based affinity chromatographic assays for thrombin*. Anal Chem, 2008. **80**(19): p. 7586-93.
157. Holmberg, A., et al., *The biotin-streptavidin interaction can be reversibly broken using water at elevated temperatures*. Electrophoresis, 2005. **26**(3): p. 501-10.
158. Ruta, J., et al., *Enantiomeric separation using an l-RNA aptamer as chiral additive in partial-filling capillary electrophoresis*. Anal Chem, 2006. **78**(9): p. 3032-9.
159. Collett, J.R., E.J. Cho, and A.D. Ellington, *Production and processing of aptamer microarrays*. Methods, 2005. **37**(1): p. 4-15.
160. Cho, S., et al., *Microbead-based affinity chromatography chip using RNA aptamer modified with photocleavable linker*. Electrophoresis, 2004. **25**(21-22): p. 3730-9.
161. Chung, W.J., et al., *Microaffinity purification of proteins based on photolytic elution: toward an efficient microbead affinity chromatography on a chip*. Electrophoresis, 2005. **26**(3): p. 694-702.
162. Ng, E.W., et al., *Pegaptanib, a targeted anti-VEGF aptamer for ocular vascular disease*. Nat Rev Drug Discov, 2006. **5**(2): p. 123-32.
163. Bradford, M.M., *A rapid and sensitive method for the quantitation of microgram quantities of protein utilizing the principle of protein-dye binding*. Anal Biochem, 1976. **72**: p. 248-54.

164. Choi, K.D.J., G. H.; Rhee. J. S.; Yoo. O. J., *Cloning and nucleotide sequence of an esterase gene from Pseudomonas Fluorescens and expression of the gene in Escherichia coli.* 1990.
165. Sanguineti, S., et al., *Specific recognition of a DNA immunogen by its elicited antibody.* J Mol Biol, 2007. **370**(1): p. 183-95.
166. Prin, C., et al., *Isoelectric restriction of human immunoglobulin isotypes.* Biochim Biophys Acta, 1995. **1243**(2): p. 287-9.
167. Zhu, G., et al., *Characterization of Optimal Aptamer-Microarray Binding Chemistry and Spacer Design.* CHEMICAL ENGINEERING & TECHNOLOGY, 2011. **34**(12): p. 2022-2028.
168. Freedman, H., et al., *Explicitly solvated ligand contribution to continuum solvation models for binding free energies: selectivity of theophylline binding to an RNA aptamer.* J Phys Chem B. **114**(6): p. 2227-37.
169. Latham, M.P., G.R. Zimmermann, and A. Pardi, *NMR chemical exchange as a probe for ligand-binding kinetics in a theophylline-binding RNA aptamer.* J Am Chem Soc, 2009. **131**(14): p. 5052-3.
170. Jenison, R.D., et al., *High-resolution molecular discrimination by RNA.* Science, 1994. **263**(5152): p. 1425-9.
171. Chavez, J.L., et al., *Theophylline detection using an aptamer and DNA-gold nanoparticle conjugates.* Biosens Bioelectron. **26**(1): p. 23-8.
172. Bruno, J.G.M., J. C. , 2008. **US 2008/0161236 A1.**
173. Zimmermann, G.R., et al., *A semiconserved residue inhibits complex formation by stabilizing interactions in the free state of a theophylline-binding RNA.* Biochemistry, 1998. **37**(25): p. 9186-92.
174. Belitz, H.-D., Grosch, W., & Schieberle, *Coffee, tea, cocoa.* Food Chemistry, 2009: p. 938-951.
175. Windham, G.C., et al., *Genetic monitoring of malathion-exposed agricultural workers.* Am J Ind Med, 1998. **33**(2): p. 164-74.
176. Balluz, L.S., et al., *Health complaints related to pesticide stored at a public health clinic.* Environ Res, 2000. **82**(1): p. 1-6.
177. Boyd, E.M. and T.K. Tanikella, *The acute oral toxicity of malathion in relation to dietary protein.* Arch Toxicol, 1969. **24**(4): p. 292-303.
178. Cowart, R.P., F.L. Bonner, and E.A. Epps, Jr., *Rate of hydrolysis of seven organophosphate pesticides.* Bull Environ Contam Toxicol, 1971. **6**(3): p. 231-4.
179. Ruzicka, J.H., J. Thomson, and B.B. Wheals, *The gas chromatographic determination of organophosphorus pesticides. II. A comparative study of hydrolysis rates.* J Chromatogr, 1967. **31**(1): p. 37-47.
180. M. B. Doyle, S.A.M., *Aptamers and methods for their in vitro selection and uses thereof.* 2005. **US2005/0142582 A1.**

7 Resume

Personal data

name: Guohong Zhu
date of birth: 30.11.1976
place of birth: Shanghai
nationality: Chinese

Study

Feb. 2010 – Aug. 2013 PhD study at the Institute of Technical Chemistry,
Gottfried Wilhelm Leibniz Universität Hannover
Oct. 2006 – Oct. 2009 Chemical study at the Institute of Organic Chemistry,
Gottfried Wilhelm Leibniz Universität Hannover
Sep. 1996 – Juni. 2000 Chemical study at Shanghai University of Engineering
Science, Shanghai, China

High school education

Sep.1992 – Juni.1995 high school in Shanghai, China
Sep.1989 – Juni.1992 middle school in Shanghai, China
Sep.1983 – Juni.1989 primary school in Shanghai, China

8 Publications and conference contributions

Publications

1. Characterization of Optimal Aptamer-Microarray Binding Chemistry and Spacer Design. G. Zhu, M. Lübbecke, J.-G. Walter, F. Stahl, T. Scheper; Chem. Eng. Technol. 2011, 34 (12), 2022-2028; DOI: 10.1002/ceat.201000551
2. Aptamer-modified Nanoparticles as Biosensors. Maren Lönne, Guohong Zhu, Frank Stahl, Johanna-Gabriela Walter, Advances in biochemical engineering/biotechnology, 2013, 0724-6145; DOI: 10.1007/10_2013_231
3. Aptamer-based purification of human IgG. G. Zhu, J-G. Walter, F. Stahl, T. Scheper – submitted

Conference contributions (Poster)

1. Investigation of various surfaces and spacers for aptamer microarrays. 2010. G. Zhu, M. Lübbecke, J.-G. Walter, F. Stahl, T. Scheper, University of Hannover, 12th Status Seminar, Chip Technologies, Sequencing and Functional Genomics, 4.-5. February, Frankfurt am Main
2. Detection strategies for protein microarrays based on aptamers. 2010. Miriam Lübbecke, Johanna-Gabriela Walter, Guohong Zhu, Frank Stahl, Thomas Scheper; 28. DECHEMA-Jahrestagung der Biotechnologen, 21.-23. September, Aachen
3. Microarray-based Screening of Aptamers. 2011. Johanna-Gabriela Walter, Miriam Lübbecke, Guohong Zhu, Öznur Kökpınar, Frank Stahl, Thomas Scheper; Functional Genomics – Next Generation Applications and Technologies, 3.-4. Februar, Frankfurt
4. Microarray-basiertes Screening von Aptameren für analytische Methoden. 2010. Johanna-Gabriela Walter, Miriam Lübbecke, Guohong Zhu, E. S. Sinitsyna, Frank Stahl, Thomas Scheper; Chemie Ingenieur Technik, 82(9), 1551

5. Strategien für die Detektion von Proteinen mit aptamer-basierten Microarrays. 2010. Miriam Lübbecke, Johanna-Gabriela Walter, Guohong Zhu, Frank Stahl, Thomas Scheper; Chemie Ingenieur Technik, 82(9), 1546-1547

Prize for best poster:

1. Aptamers as affinity ligands for downstream processing. J.-G. Walter, G. Zhu, Ö. Kökpınar, F. Stahl, T. Scheper, Gottfried-Wilhelm-Leibniz Universität, Hannover/D, Post preis der ProcessNet Fachgruppe Membrantechnik „Membranverfahren in der Biotechnologie“

Patent:

1. Method for isolating fragrance and flavour compounds – pending